

# **WORLD METEOROLOGICAL ORGANIZATION**

## **GLOBAL ATMOSPHERE WATCH**

### **WORLD DATA CENTRE FOR GREENHOUSE GASES**



# **WMO WDCGG DATA SUMMARY**

**WDCGG No. 34**

**GAW DATA**  
**Volume IV-Greenhouse Gases and Other Atmospheric Gases**

**PUBLISHED BY**  
**JAPAN METEOROLOGICAL AGENCY**  
**IN CO-OPERATION WITH**  
**WORLD METEOROLOGICAL ORGANIZATION**

**MARCH 2010**





## Acknowledgements

This issue of *Data Summary* reports the latest status of greenhouse and some reactive gases in the global atmosphere. This *Data Summary* has been prepared by the World Data Centre for Greenhouse Gases (WDCGG), established under the Global Atmosphere Watch (GAW) programme of the World Meteorological Organization (WMO) and operated by the Japan Meteorological Agency (JMA), using data submitted by many contributors worldwide (Appendix: LIST OF CONTRIBUTORS). These contributors include organizations and individuals involved in observations and research at stations and laboratories that measure greenhouse and some reactive gases within the framework of GAW and other cooperative monitoring and research programmes. The WDCGG thanks all of these organizations and individuals, including those from the global air sampling network of the National Oceanic and Atmospheric Administration (NOAA), for their efforts in maintaining the observation programme and continuing to provide observational data. Not all of the contributors may be explicitly acknowledged in this publication, owing to lack of space, but all the organizations and individuals that have submitted data to the WDCGG are nevertheless here acknowledged as invaluable contributors to this latest issue of *Data Summary*.



## CONTENTS

	Page
<b>SUMMARY</b>	<b>1</b>
<b>1. INTRODUCTION</b>	<b>3</b>
<b>2. ANALYSIS</b>	<b>5</b>
<b>3. CARBON DIOXIDE</b>	<b>7</b>
<b>4. METHANE</b>	<b>15</b>
<b>5. NITROUS OXIDE</b>	<b>21</b>
<b>6. HALOCARBONS AND OTHER HALOGENATED SPECIES</b>	<b>25</b>
<b>7. SURFACE OZONE</b>	<b>31</b>
<b>8. CARBON MONOXIDE</b>	<b>35</b>
<b>9. NITROGEN MONOXIDE AND NITROGEN DIOXIDE</b>	<b>41</b>
<b>10. SULPHUR DIOXIDE</b>	<b>45</b>
<b>REFERENCES</b>	<b>49</b>
<b>APPENDICES</b>	<b>53</b>
<b>CALIBRATION AND STANDARD SCALES</b>	<b>54</b>
<b>LIST OF OBSERVATION STATIONS</b>	<b>63</b>
<b>LIST OF CONTRIBUTORS</b>	<b>73</b>
<b>GLOSSARY</b>	<b>91</b>
<b>LIST OF WMO/WDCGG PUBLICATIONS</b>	<b>94</b>



## SUMMARY

This *Data Summary* reports the results of basic analyses of greenhouse and some reactive gas data submitted to the WMO World Data Centre for Greenhouse Gases (WDCGG). This issue covers observations from 1968 through 2008, based on data reported to the WDCGG by November 2009. The *Data Summary* includes analyses of global, hemispheric and latitudinal monthly mean mole fractions of greenhouse and some reactive gases, and provides information on the state of mole fractions of these gases.

Only monthly mean mole fractions are used for the analyses, but the WDCGG greatly appreciate those stations that submit daily and hourly mean mole fractions, which are important for analysing the variations on shorter time scales. All the data submitted to the WDCGG are available on its web site, <http://gaw.kishou.go.jp/wdcgg/wdcgg.html>.

To represent mole fractions, this *Data Summary* uses the units ppm, ppb and ppt, which correspond to the SI units  $\mu\text{mol/mol}$ ,  $\text{nmol/mol}$  and  $\text{pmol/mol}$ , respectively.

Variations in the mole fractions of some gases are presented as a combination of seasonal cycles and deseasonalized long-term trends. Growth rates are presented as time derivatives of the long-term trends. The analytical results are summarized below for each greenhouse and reactive gas.

### Carbon Dioxide ( $\text{CO}_2$ )

The level of carbon dioxide ( $\text{CO}_2$ ), which contributes most to increase of anthropogenic induced radiative forcing, has been increasing since the beginning of the industrial era. The global average mole fraction of  $\text{CO}_2$  in 2008 reached a new high of 385.2 ppm, which is 138% of that in the pre-industrial period. The increase of 2.0 ppm from 2007 to 2008 was larger than the average for the 1990s (about 1.5 ppm/year).

The global growth rate of  $\text{CO}_2$ , with an average of 1.93 ppm/year for the period 1998–2008, has a significant interannual variation. Growth rates higher than 2 ppm/year in 1987/1988, 1997/1998, 2002/2003 and 2005 resulted from warmer conditions caused by El Niño-Southern Oscillation (ENSO) events. The anomalously strong El Niño event in 1997/1998 resulted in worldwide high increases of  $\text{CO}_2$  in 1998. The large growth rates in 2006 may have been related to the global high temperature in the same year. The exceptionally low growth rates in 1992, including negative values in northern high latitudes, may have been due to low global temperatures following the eruption of Mt. Pinatubo in 1991. Variations in  $\text{CO}_2$  mole fraction can be seen both on seasonal and long-term scales. The seasonal amplitudes are large

in northern high and mid-latitudes and small in the Southern Hemisphere. In southern low latitudes, there is no clear annual cycle, but a semiannual cycle can be determined.

### Methane ( $\text{CH}_4$ )

Methane ( $\text{CH}_4$ ) is the second most significant anthropogenic greenhouse gas, whose level has been increasing since the beginning of the industrial era. The annual average mole fraction was 1797 ppb in 2008, an increase of 7 ppb since 2007. The mole fraction is now 257% of that in the pre-industrial period.

The latitudinal gradient of  $\text{CH}_4$  mole fraction is large from the northern mid-latitudes to the Tropics, suggesting that the major sources are located in northern high and mid-latitudes.

The growth rates decreased significantly in some years, including 1992, when negative values were recorded in northern high and mid-latitudes. However, both hemispheres experienced high growth rates in 1998, caused by an exceptionally high global mean temperature. The global growth rates decreased to almost zero in 2000–2001, suggesting that the global  $\text{CH}_4$  budget seemed to be in a steady state. The growth rates increased temporally in 2002 and 2003 with the occurrence of an El Niño event. In 2007 and 2008, the growth rates increased again globally.

The global growth rate averaged over the period 1984–1990 was 11.5 ppb/year, but it decreased markedly in the 1990s. The average global growth rate for the period 1998–2008 was 2.5 ppb/year. Some possible causes of this changing growth rate have been proposed but the issue remains unresolved.

$\text{CH}_4$  mole fractions vary seasonally, with high values in winter and low values in summer. Unlike  $\text{CO}_2$ , the amplitudes of the seasonal cycle of  $\text{CH}_4$  are large, not only in the Northern Hemisphere but also in southern high and mid-latitudes. In southern low latitudes, a distinct secondary maximum in boreal winter overlies the annual cycle.

### Nitrous Oxide ( $\text{N}_2\text{O}$ )

Nitrous oxide ( $\text{N}_2\text{O}$ ) is an important greenhouse gas whose level is increasing on a global scale.  $\text{N}_2\text{O}$  data submitted to the WDCGG show that mole fractions are increasing in both hemispheres. The global mean mole fraction reached a new high of 321.8 ppb in 2008, 0.9 ppb higher than the previous year. This mole fraction corresponds to 119% of that in the pre-industrial period. The mean growth rate of the global mean mole fraction over the period 1998–2008 was 0.78 ppb/year.

## **Halocarbons and Other Halogenated Species**

Halocarbons, most of which are anthropogenic, are potent greenhouse gases and some also act as ozone-depleting compounds. Levels of some halocarbons (e.g. CFCs) increased in the 1970s and 1980s, but the increase has almost ceased by now as a result of the regulation of production and emission under the Montreal Protocol on Substances that Deplete the Ozone Layer and its subsequent Adjustments and Amendments. However, some substances, HFCs and SF<sub>6</sub>, targeted by the Kyoto Protocol but not regulated by the Montreal Protocol are increasing.

The mole fraction of CFC-11 peaked around 1992 and then started decreasing. The growth rate of CFC-12 has declined since around 1990 and is now nearly zero. The mole fraction of CFC-113 stopped increasing in the 1990s, followed by a slight decrease over the last decade. The mole fractions of HCFC-22, HCFC-141b and HCFC-142b, which are industrial replacements of CFCs, are increasing. The mole fractions of Halon-1211 and Halon-1301 are increasing, but their growth rates have decelerated. The mole fraction of CCl<sub>4</sub> was at a maximum around 1991 and has since decreased slowly. The mole fraction of CH<sub>3</sub>CCl<sub>3</sub> peaked around 1992 and decreased thereafter. The mole fractions of HFC-134a, HFC-152a and SF<sub>6</sub> are increasing.

## **Surface Ozone (O<sub>3</sub>)**

Ozone (O<sub>3</sub>) plays important roles in the atmospheric environment through radiative and chemical processes. It absorbs solar UV radiation in the stratosphere, influencing the vertical temperature profile as well as terrestrial IR radiation, contributing to the greenhouse effect as a greenhouse gas. Ozone is also involved in the chemical transformations of the primary air pollutants as its mole fraction in the boundary layer serves as an indicator of air quality.

The mole fraction of O<sub>3</sub> near the surface, so-called surface ozone, reflects various processes. While some of the O<sub>3</sub> in the troposphere comes from the stratosphere, the rest is chemically produced in the troposphere through oxidation of CO or hydrocarbons in the presence of NO<sub>x</sub>.

The mole fraction of surface ozone is measured at many locations in various environments. Due to its uneven geographic distribution, however, it is difficult to identify a global long-term trend of surface O<sub>3</sub>.

## **Carbon Monoxide (CO)**

Carbon monoxide (CO) is not a greenhouse gas itself but influences the mole fractions of greenhouse gases by affecting hydroxyl radicals (OH). Its mole fractions in northern high latitudes have been increasing since the mid-19th century. In 2008, the global mean mole fraction of CO was about 91 ppb.

The mole fraction is high in the Northern Hemisphere and low in the Southern Hemisphere, suggesting substantial anthropogenic emissions in the Northern Hemisphere.

Although the global mole fraction of CO increased until the mid-1980s, this growth ceased or was reversed thereafter (WMO, 1999). There was a large fluctuation in growth rate, however, with high positive rates followed by high negative rates in northern latitudes and southern low latitudes from 1997 to 1999. The growth rates in the Northern Hemisphere increased again in 2002.

The monthly mean mole fractions show seasonal variations, with large amplitudes in the Northern Hemisphere and small amplitudes in the Southern Hemisphere.

## **Nitrogen Monoxide (NO) and Nitrogen Dioxide (NO<sub>2</sub>)**

Nitrogen oxides (NO<sub>x</sub>, i.e., NO and NO<sub>2</sub>) are not greenhouse gases, but influence the mole fractions of important greenhouse gases by affecting OH. In the presence of NO<sub>x</sub>, CO and hydrocarbons are oxidized to produce ozone (O<sub>3</sub>), which affects the Earth's radiative balance as a greenhouse gas and the oxidization capacity of the atmosphere by reproducing OH.

Most of the stations reporting NO<sub>x</sub> data to the WDCGG are located in Europe. NO<sub>x</sub> has a large temporal and geographic variability, and it is difficult to identify its long-term trend.

## **Sulphur Dioxide (SO<sub>2</sub>)**

Sulphur dioxide (SO<sub>2</sub>) is not a greenhouse gas but a precursor of atmospheric sulphate aerosols. Sulphate aerosols are produced by SO<sub>2</sub> oxidation through photochemical gas-to-particle conversion. SO<sub>2</sub> has also been a major source of acid rain and deposition throughout the industrial era.

Most of the stations reporting SO<sub>2</sub> data to the WDCGG are located in Europe. Global analysis can not be performed on this data set.

# 1. INTRODUCTION

Human activities have had major impacts on the global environment. Since the beginning of the industrial era, mankind has increasingly made use of land, water, minerals and other natural resources, and continuous growth of the world human population and economies may further increase our impact on the environment. As the climate, biogeochemical processes and natural ecosystems are closely interlinked, changes in any one of these systems may affect the others and be detrimental to humans and other organisms. Emissions of man-made gaseous and particulate matters alter the energy balance of the atmosphere, and consequently affect the interactions between the atmosphere, hydrosphere and biosphere. Nevertheless, we do not yet have sufficient understanding both the chemical/physical processes in the atmosphere and its interactions with hydrosphere and biosphere. The lack of our understanding of the complete atmospheric system including interactions with other spheres is mainly due to insufficient observations.

The World Meteorological Organization (WMO) launched Global Atmosphere Watch (GAW) in 1989 to promote systematic and reliable observations of the global environment, including greenhouse gases ( $\text{CO}_2$ ,  $\text{CH}_4$ , CFCs,  $\text{N}_2\text{O}$ , etc.) and some reactive gases (e.g.,  $\text{O}_3$ ,  $\text{CO}$ ,  $\text{NO}_x$ , and  $\text{SO}_2$ ) in the atmosphere. In October 1990, WMO designated the Japan Meteorological Agency (JMA) in Tokyo to serve as the World Data Centre for Greenhouse Gases (WDCGG) to collect, archive and provide data for greenhouse and reactive gases in the atmosphere and oceans from a number of observation sites throughout the world participating in GAW and other scientific monitoring programmes (Appendix: LIST OF OBSERVING STATIONS). In August 2002, the WDCGG took over the role of the Data Centre for Surface Ozone from the Norwegian Institute for Air Research (NILU) to take charge of surface ozone data.

With regard to the issue of global warming, the Kyoto Protocol to the United Nations Framework Convention on Climate Change came into force in February 2005. In March 2006, WMO commenced annual publication of the WMO Greenhouse Gas Bulletin, which summarizes the state of greenhouse gases in the atmosphere. The fifth issue of the Bulletin was published in November 2009. The WDCGG contributes to the production of the bulletin through a timely and adequate collection and analysis of data in cooperation with the data contributors.

Since its establishment, the WDCGG has provided its users with data and other information through its regular publications, including the *Data Summary* and *DVD* (Appendix: LIST OF WMO WDCGG PUBLICATIONS). All data and information are also available on the WDCGG web site to improve accessibility of data, information and products in line with the GAW Strategic Plan: (2008–2015) (WMO, 2007a).

The WDCGG published the Data Submission and Dissemination Guide in 2007 (WMO, 2007b), which with its revision in 2009 (WMO, 2009c), is designed to facilitate submission of observational data and access to archived data in the WDCGG.

The GAW Strategic Plan requests that World Data Centres assist data users of atmospheric chemical observations. To this end, the WDCGG provides global and integrated diagnostics on the state of greenhouse and some reactive gases as analytical information in the *Data Summary*. The methods of the WDCGG global analysis are described in a GAW technical report (WMO, 2009a). The contents of the *Data Summary* are revised and improved based on comments from data contributors and scientists. The WDCGG invites comments and suggestions regarding the *Data Summary* or any other publications. We hope the diagnostic information presented here will promote the use of data on greenhouse and reactive gases and will enhance appreciation of the value of the GAW programme.

All users are required to accept the following statement endorsed by the Commission for Atmospheric Sciences (CAS) at its thirteenth session: “For scientific purposes, access to these data is unlimited and provided without charge. By their use you accept that an offer of co-authorship will be made through personal contact with the data providers or owners whenever substantial use is made of their data. In all cases, an acknowledgement must be made to the data providers or owners and to the data centre when these data are used within a publication.” The WDCGG requests data users to make appropriate acknowledgements. The principal investigators and other contact points of the data can be referred to at the WDCGG website, as well as the GAW Station Information System (GAWSIS; <http://gaw.empa.ch/gawsis/>). The information at the WDCGG and GAWSIS is kept updated in cooperation with the data contributors and WMO Secretariat.

Finally, the WDCGG would like to thank all data contributors worldwide, including those involved in on-site measurements, for their efforts to maintain the observational programme and for continuous provision of data.

## Mailing address:

WMO World Data Centre for Greenhouse Gases  
(WDCGG)  
c/o Japan Meteorological Agency  
1-3-4, Otemachi, Chiyoda-ku, Tokyo 100-8122, Japan  
E-mail: [wdcgg@metkishou.go.jp](mailto:wdcgg@metkishou.go.jp)  
Telephone: +81-3-3287-3439  
Facsimile: +81-3-3211-4640  
Web Site: <http://gaw.kishou.go.jp/wdcgg/wdcgg.html>



## 2. ANALYSIS

The WDCGG collects, archives and provides observational data on the mole fractions of greenhouse and some reactive gases, and publishes diagnostic information on these gases based on the reported data.

For CO<sub>2</sub>, CH<sub>4</sub> and CO, long-term trends and seasonal variations in their mole fractions are analyzed for presentation as global and latitudinal means. For N<sub>2</sub>O, only global long-term trends are presented. For surface O<sub>3</sub>, global long-term trends are not analyzed due to an uneven geographical distribution of this compound, substantial spatial gradients which are poorly covered by the stations. For halocarbons, NO<sub>x</sub> and SO<sub>2</sub>, only time series of monthly mean mole fractions are presented due to the small number of reporting sites.

The analyses utilize ppm, ppb, and ppt as units, rather than the SI units of  $\mu\text{mol/mol}$ ,  $\text{nmol/mol}$ , and  $\text{pmol/mol}$ , respectively.

The following sections summarize the methods of analysis for CO<sub>2</sub>, CH<sub>4</sub>, CO and N<sub>2</sub>O. The details of the global analysis methods for CO<sub>2</sub>, CH<sub>4</sub>, and N<sub>2</sub>O are provided in the *Technical Report of Global Analysis Method for Major Greenhouse Gases by the World Data Centre for Greenhouse Gases*, published as a GAW technical report (WMO, 2009a). When deriving a long-term trend of CO<sub>2</sub>, CH<sub>4</sub> and N<sub>2</sub>O, the growth rate at both ends of the period is assumed as a simple linear extension of the adjacent year to avoid end effects. The rate for the rest of the period is approximated by a linear expression for simplicity. These treatments are different from WMO (2009a), especially for CH<sub>4</sub>, in which a quadratic equation was used for the whole period.

### (1) Site selection

For CO<sub>2</sub>, CH<sub>4</sub> and N<sub>2</sub>O, the diagnostic analyses, such as global, hemispheric and zonal means, are based on data from sites that have adopted a standard scale traceable to the Primary Standard designated under GAW. In addition, these analyses utilize data on other standard scales that are convertible to the WMO/GAW scale through a proven equation.

Selection of observation sites for CO<sub>2</sub>, CH<sub>4</sub> and CO, which are sensitive to local sources and sinks, have also been based on their ability to provide data representing a reasonably large geographical area. These sites have been selected objectively using data measured in a reasonably scattered distribution in each latitudinal zone. Only those sites that provide annual mean mole fractions falling within a range of  $\pm 3\sigma$  from a curve fitted to the LOESS model curve (Cleveland *et al.*, 1988) have been selected, by rejecting outliers in an iterated manner. This procedure does not impact the datasets residing in the WDCGG and for other than

global analysis purposes (e.g. sources identification) these data can be extremely useful.

The sites selected according to the above criteria are marked with asterisks in Plate 3.1 for CO<sub>2</sub>, Plate 4.1 for CH<sub>4</sub>, Plate 5.1 for N<sub>2</sub>O and Plate 8.1 for CO.

### (2) Analysis of long-term trends

The mole fractions of greenhouse and reactive gases over time, measured under unpolluted conditions, represent an integration of variations on different time scales. The two major components are seasonal variation and long-term trend. Various attempts have been made to delineate measured data into these two components, including objective curve fitting (Keeling *et al.*, 1989), digital filtering (Thoning *et al.*, 1989; Nakazawa *et al.*, 1991), or both (Conway *et al.*, 1994; Slagkenky *et al.*, 1994).

In this report, seasonal variations derived from components of Fourier harmonics and long-term trends are extracted by low-pass filtering with a cut-off frequency of 0.48 year<sup>-1</sup> for each selected site. Details are described in WDCGG Data Summary No. 22 (WMO, 2000).

### (3) Estimation for missing periods and gaps

The number and distribution of sites used for trend analysis during the analysis period should be kept as constant as possible to avoid the effects of changes in the availability of data over time. However, only a small number of sites provide data throughout the whole analysis period; others may cover shorter periods or have gaps in the measurements due to different reasons. To use as many sites as possible, missing values are estimated for the calculation of zonal means, using interpolation and extrapolation as described below.

For the former, the gaps are interpolated linearly based on the data, by subtracting the seasonal variation calculated from the longest consecutive period of data with Lanczos filters (Duchon, 1979). The subtracted variation is added back to the data to obtain estimated mole fractions in a single sequence.

For the latter, long-term trends calculated from the interpolated series of data are extrapolated based on zonal mean growth rates calculated from other sites in the same latitudinal zone. The seasonal variation is added to the extrapolated long-term trend to obtain estimated mole fractions for the whole analysis period.

Through the mentioned statistical procedures, addition of the new stations in the future would not impact the consistency in the global estimates over time.

#### **(4) Calculation of global, hemispheric and zonal means**

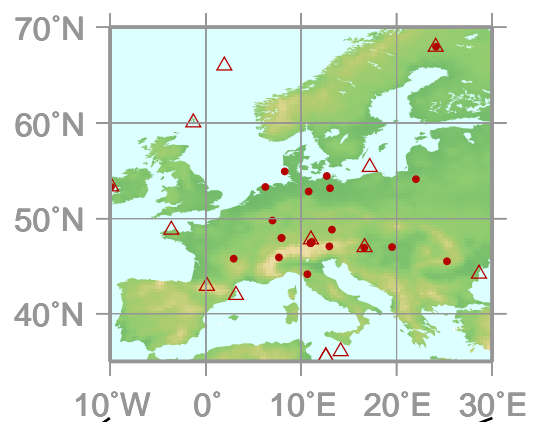
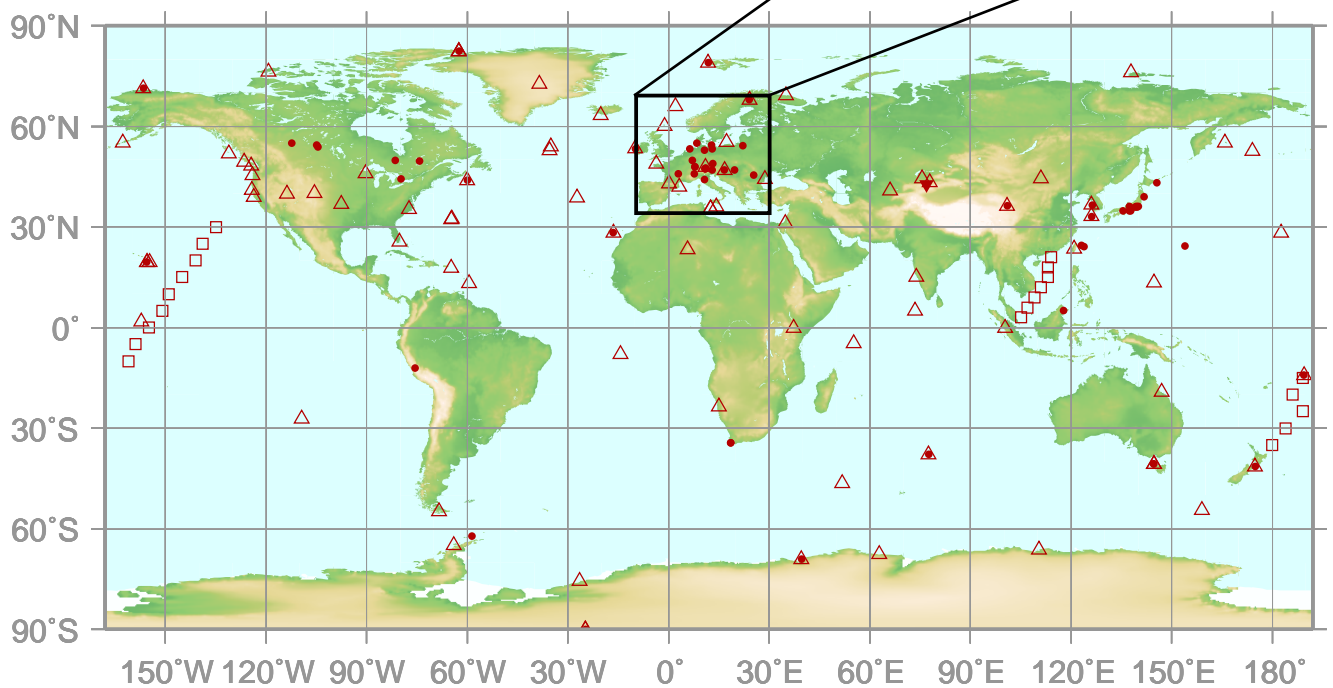
Zonal means are calculated by determining the arithmetic average of the mole fractions in each latitudinal zone, based on consistent datasets derived as above.

Global and hemispheric means are calculated as the weighted averages of the zonal means taking account of the area of each latitudinal zone.

Deseasonalized long-term trends and growth rates for the globe, each hemisphere and each latitudinal zone are calculated from the global, hemispheric and zonal means using the low-pass filter mentioned above.

### 3. CARBON DIOXIDE (CO<sub>2</sub>)

- : CONTINUOUS STATION
- △ : FLASK STATION
- : FLASK MOBILE (SHIP)
- ▼ : REMOTE SENSING STATION



This map shows locations of the stations that have submitted data for monthly mean mole fraction.

# CO<sub>2</sub> Monthly Data

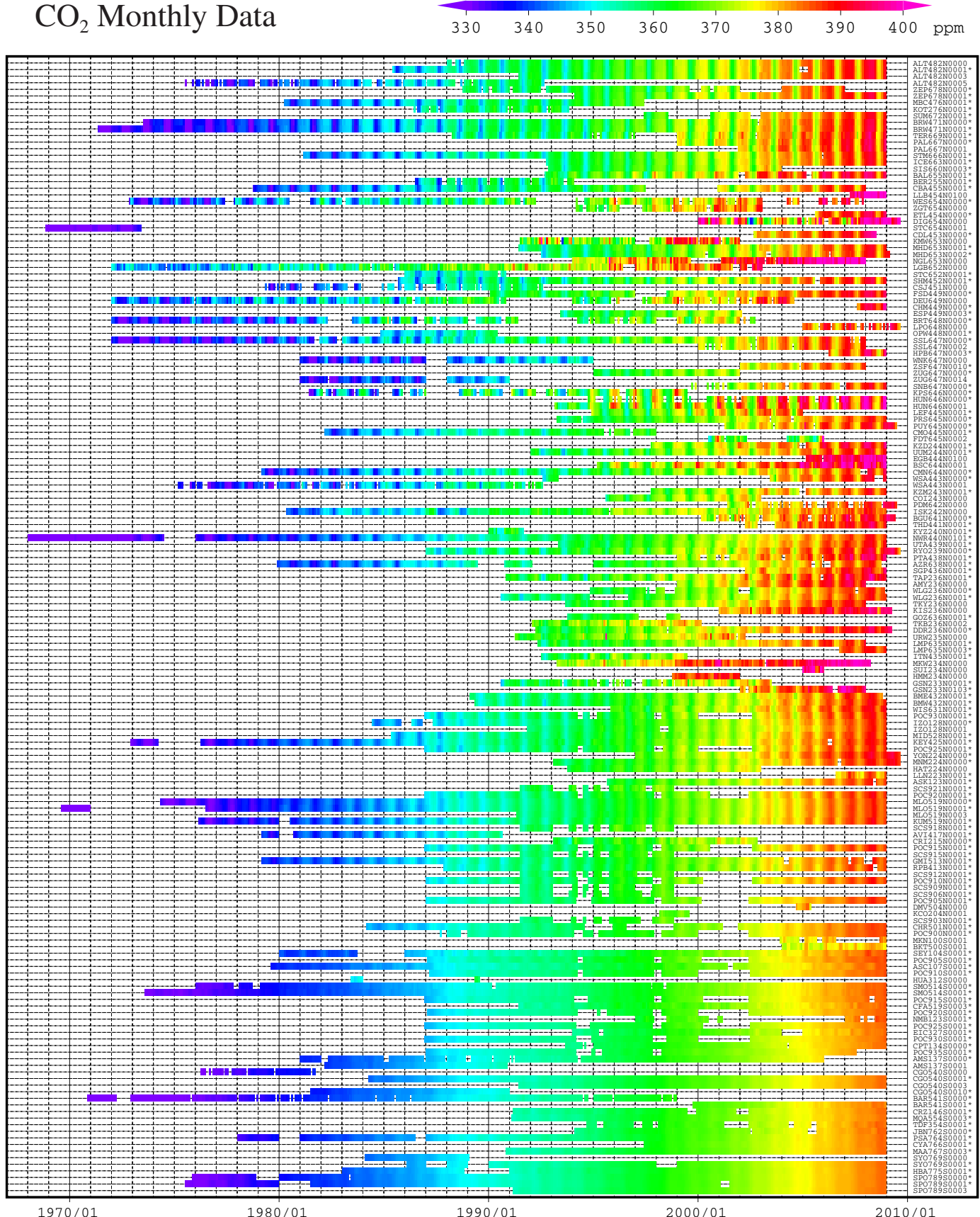
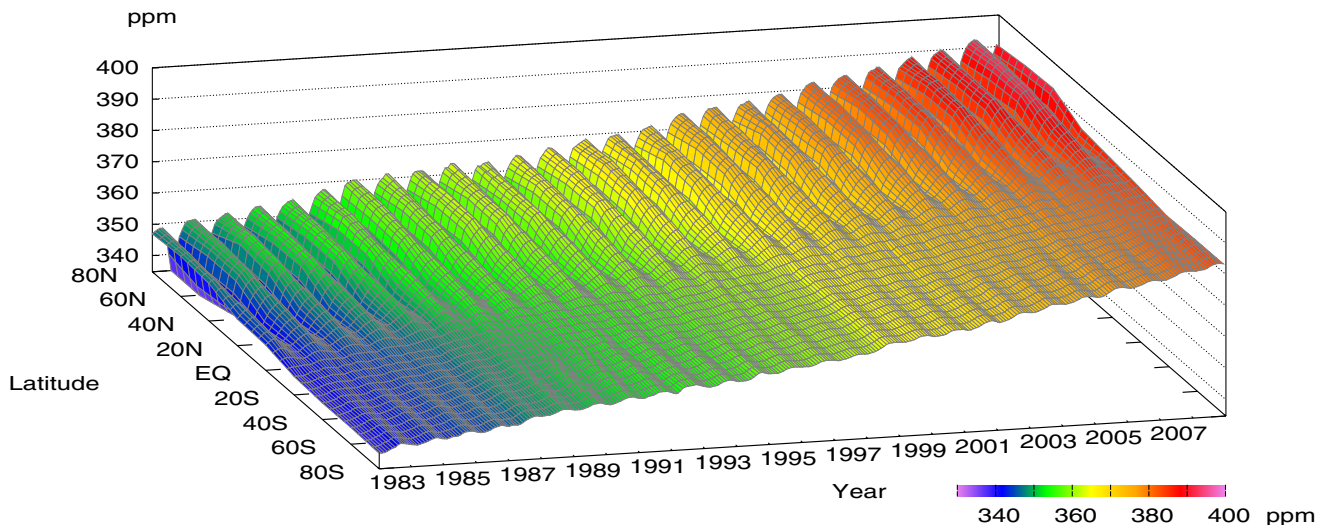
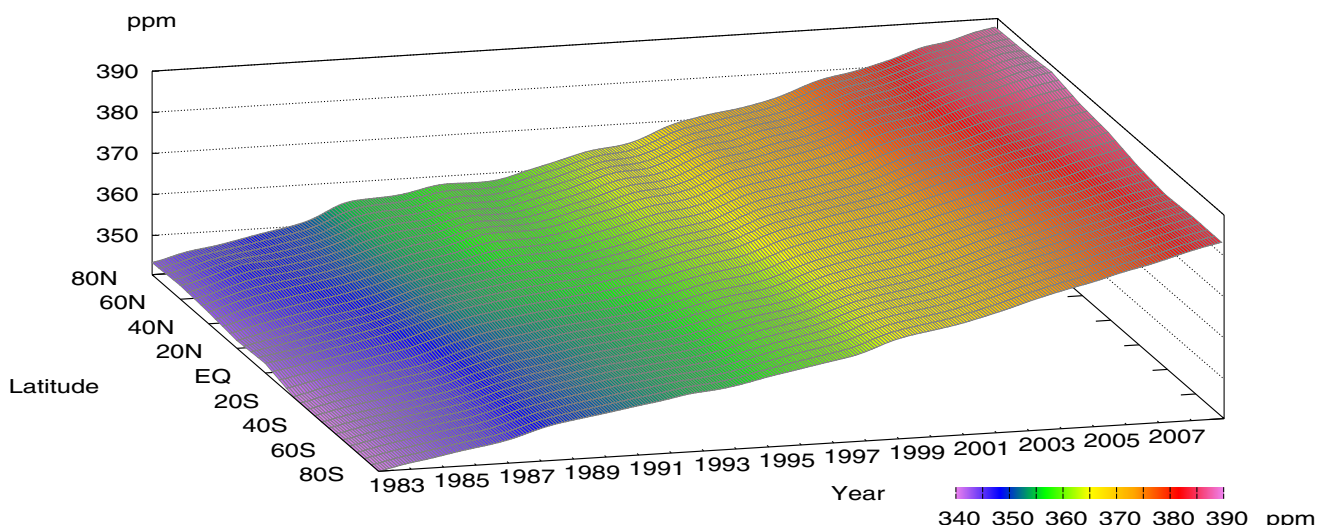


**Plate 3.1** Monthly mean CO<sub>2</sub> mole fractions that have been reported to the WDCGG. The mole fractions are illustrated in different colors. The sites are listed in order from north to south. In the case where data are reported for two or three different altitudes, only the data at the highest altitudes are illustrated. In the case where monthly means are not reported, the WDCGG calculates them from hourly or other mole fractions reported to the WDCGG by simple arithmetic mean. The data from the sites with an asterisk at the end of the station index are used for the analysis shown in Plate 3.2. (see Chapter 2)

### CO<sub>2</sub> mole fraction



### CO<sub>2</sub> deseasonalized mole fraction



### CO<sub>2</sub> growth rate

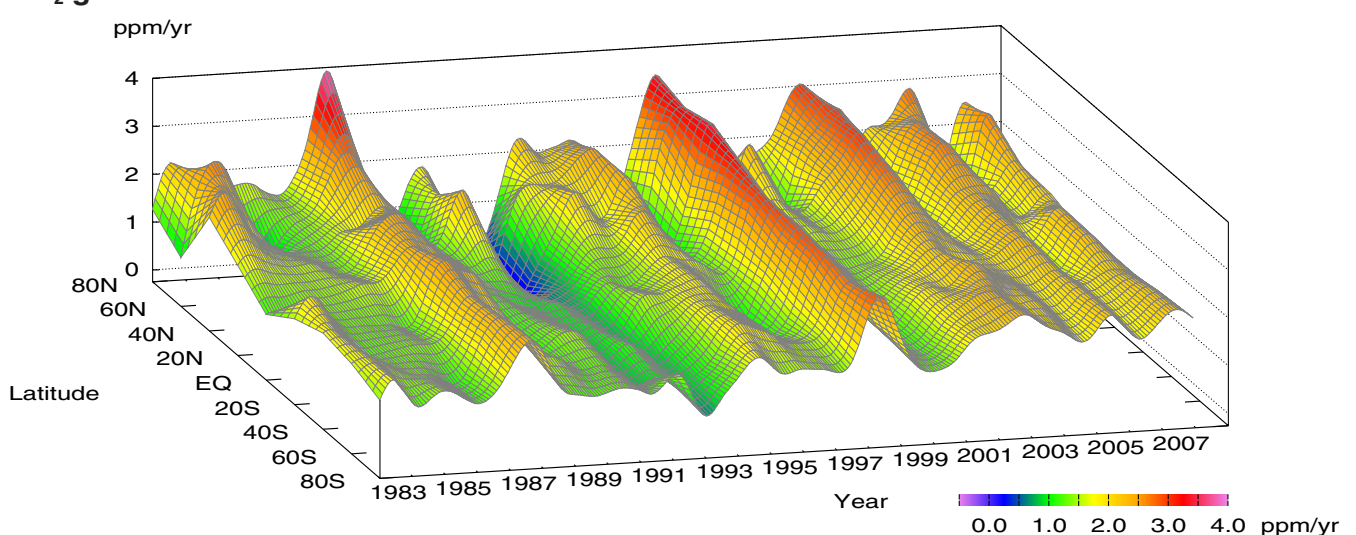


**Plate 3.2** Variation of zonally averaged monthly mean CO<sub>2</sub> mole fractions (top), deseasonalized long-term trends (middle), and growth rates (bottom). The zonally averaged mole fractions are calculated for each 20° zone. The deseasonalized trends and growth rates are derived as described in Chapter 2.

### 3. CARBON DIOXIDE (CO<sub>2</sub>)

#### Basic information on CO<sub>2</sub> with regard to environmental issues

Carbon dioxide (CO<sub>2</sub>) has strong absorption bands in the infrared region and is the biggest anthropogenic contributor to the greenhouse effect. CO<sub>2</sub> accounted for 63.5% of the radiative forcing caused by the increase in well-mixed greenhouse gases from 1750 to 2008 (WMO, 2009b).

The balance between its emission and absorption over the continents and oceans determines the mole fraction of CO<sub>2</sub> in the atmosphere. About 762 gigatonnes of carbon are present in the atmosphere as CO<sub>2</sub> (IPCC, 2007). Carbon in the atmosphere is exchanged with two other large reservoirs, the terrestrial biosphere and the oceans. CO<sub>2</sub> exchanges between the atmosphere and terrestrial biosphere occur mainly through absorption by photosynthesis and emission from the respiration of plants and the decomposition of organic soils. These biogenic activities vary seasonally, resulting in large seasonal variations in the level of CO<sub>2</sub>. CO<sub>2</sub> is transported between the atmosphere and oceans in a direction determined by the relative CO<sub>2</sub> mole fraction, and varying in time and space.

The current mole fractions of atmospheric CO<sub>2</sub> far exceed historic record, dating back 650,000 years (Solomon *et al.*, 2007). Based on the results of ice core studies, the mole fraction of atmospheric CO<sub>2</sub> in pre-industrial times was about 280 ppm (IPCC, 2007). The emission of CO<sub>2</sub> due to human activities has increased since the beginning of the industrial era, and the CO<sub>2</sub> emitted into the atmosphere has been distributed also to the oceans and terrestrial biosphere. The global carbon cycle, which is comprised mainly of CO<sub>2</sub>, is not fully understood. About half of anthropogenic CO<sub>2</sub> emissions have remained in the atmosphere, the rest accounts for the net removal of sinks, including the terrestrial biosphere and oceans, and non-anthropogenic sources. However, the amount of CO<sub>2</sub> removed from the atmosphere varies greatly over time (Figure 3.1).

Carbon isotopic studies have demonstrated the importance of the terrestrial biosphere and oceans as sources and sinks (Francey *et al.*, 1995; Keeling *et al.*, 1995; and Nakazawa *et al.*, 1993, 1997). In contrast, the atmospheric content of O<sub>2</sub> is dependent mainly on its removal by the burning of fossil fuels and on its release from the terrestrial biosphere. Therefore, the uptake of carbon by the terrestrial biosphere and oceans can be estimated from the combination of measurements of O<sub>2</sub> (O<sub>2</sub>/N<sub>2</sub>) and CO<sub>2</sub> (IPCC, 2001). Solomon *et al.*, (2007) showed that the oceans and the terrestrial biosphere absorb about 31% (in the range from 20 to 35%) and 12%, respectively, of the CO<sub>2</sub>

emitted from the anthropogenic sources in 2000–2005, while the remaining 57% contributed to annual increases in CO<sub>2</sub> level in the atmosphere.

Large amounts of CO<sub>2</sub> are exchanged among these reservoirs, and the global carbon cycle is coupled with the climate system on seasonal, yearly and decadal time scales. Accurate understanding of the global carbon cycle is essential for estimating future CO<sub>2</sub> mole fractions in the atmosphere.

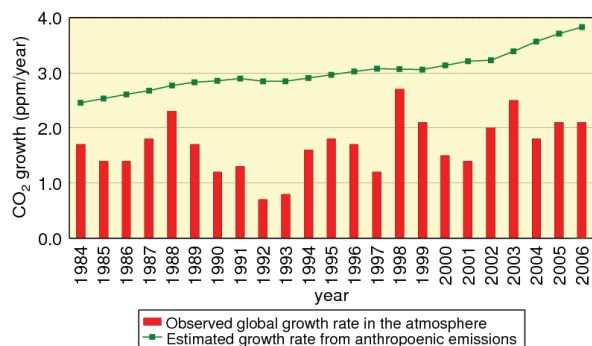


Fig. 3.1. Annual mean growth rates of CO<sub>2</sub> in the atmosphere calculated from observational data (red column) and from data for anthropogenic emissions (green curve). The estimated growth rates were calculated from the CO<sub>2</sub> emission (from CDIAC, Boden *et al.*, 2009) expressed as mole divided by the total mass of gas in the atmosphere (5.2 pettonne) converted into mole based on the mean molar weight of air (about 29), and the observed growth rates were calculated by the WDCGG. The observational CO<sub>2</sub> abundance is expressed as mole fraction with respect to dry air, while the CO<sub>2</sub> amount calculated from anthropogenic emissions is based on the atmosphere including water vapor usually in a mole fraction less than 1%.

Mole fractions of CO<sub>2</sub> are analyzed by using the data from fixed stations and some ships that submitted to the WDCGG. The observation sites where data used for the analysis are shown on the map at the beginning of this chapter. They include *in situ* stations performing continuous measurements as well as flask-sampling stations, including those in the NOAA/ESRL cooperative air sampling network. In addition to such fixed stations, mobile stations on ships and aircraft and other stations observing on an event basis report their data to the WDCGG (see Appendix: LIST OF OBSERVING STATIONS).

## Annual variations of CO<sub>2</sub> mole fraction in the atmosphere

The monthly mean mole fractions of CO<sub>2</sub> used in the analysis are shown in Plate 3.1, with mole fraction levels illustrated in different colours. Global, hemispheric and zonal mean mole fractions were analysed based on data from selected stations under unpolluted conditions (see the caption to Plate 3.1). Latitudinally averaged mole fractions of atmospheric CO<sub>2</sub>, together with their deseasonalized components and growth rates, are shown as three-dimensional representations in Plate 3.2. They indicate that the seasonal variations in mole fraction are large in northern high and mid-latitudes, but are indistinct in the Southern Hemisphere. The increases in the Northern Hemisphere, which precede those in the Southern Hemisphere, propagate to the latter, and the interannual variation in growth rate is large in the Northern Hemisphere.

Figure 3.2 shows global monthly mean mole fractions and their growth rates from 1983 to 2008. The global average mole fraction reached a new high in 2008 at 385.2 ppm, 138% of the pre-industrial level of 280 ppm. The increase from 2007 to 2008 was 2.0 ppm, larger than the average annual increase for the 1990s (about 1.5 ppm/yr).

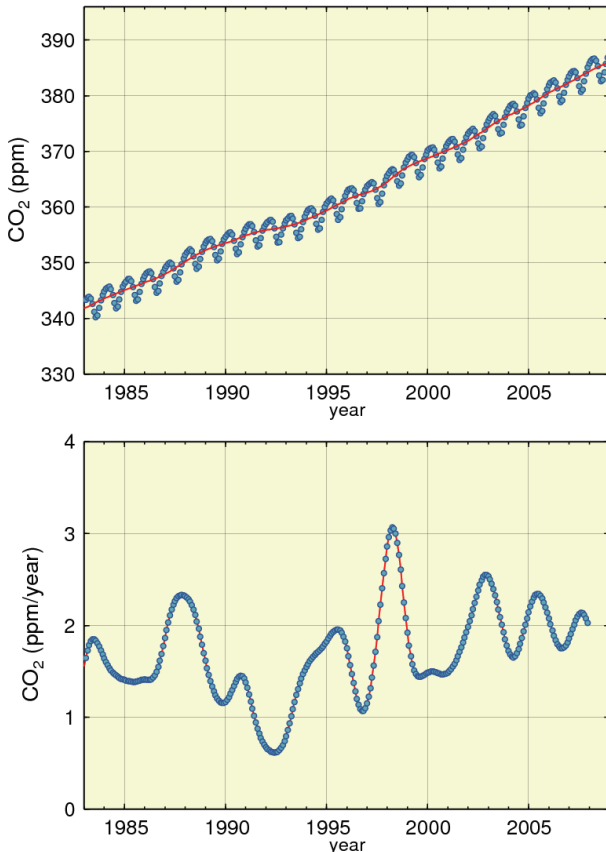


Fig. 3.2 Global monthly mean mole fraction of CO<sub>2</sub> from 1983 to 2008, with deseasonalized long-term trend shown as a red line (top) and its growth rate (bottom).

The average global growth rate for 1998–2008 was 1.93 ppm/year. There were large interannual variations in the growth rate, between the instantaneous maximum of about 3 ppm/year in 1998 and minimum below 1 ppm/year in 1992. These were short periods of high rates in 1987/1988, 1997/1998, 2002/2003, 2005 and 2007.

Figure 3.3 shows monthly mean mole fractions and long-term trends from 1983 to 2008 for each 30° latitudinal zone, indicating clear long-term increases in both hemispheres and seasonal variations in the Northern Hemisphere.

As shown in Figure 3.4, the growth rates for each 30° latitude zone fluctuated between –0.3 and 3.5 ppm/year, with relatively large interannual variability in northern high latitudes. The high growth rates in 1987/1988, 1997/1998, 2002/2003, 2005 and 2007 were observed for all 30° latitude zones, while negative rates were recorded in northern high latitudes in 1992.

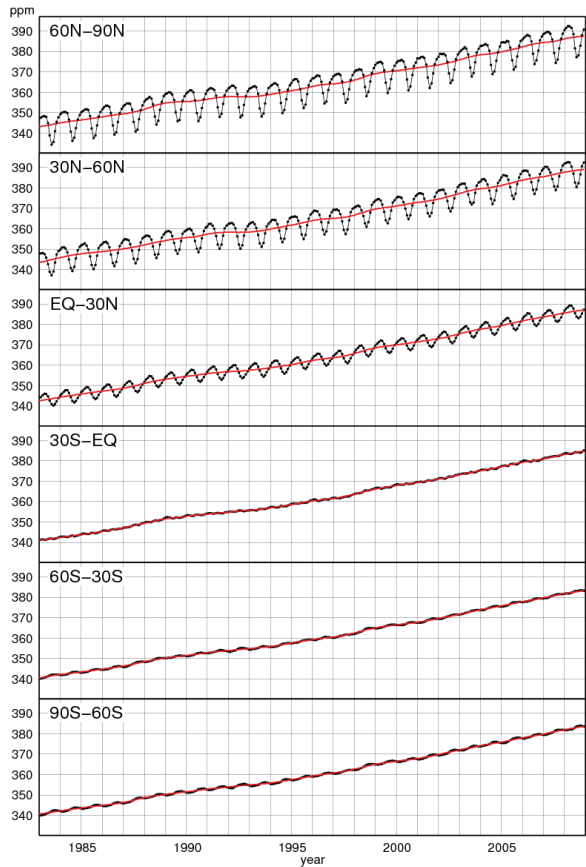


Fig. 3.3 Monthly mean mole fractions of CO<sub>2</sub> from 1983 to 2008 for each 30° latitudinal zone (dots) and their deseasonalized long-term trends (red lines).

Changes in growth rate are partly associated with El Niño-Southern Oscillation (ENSO). The El Niño events in 1982/1983, 1986–1988, 1991/1992, 1997/1998 and 2002/2003 coincided with high growth

rates of CO<sub>2</sub>, with an exception in 1992. The growth rates of CO<sub>2</sub> observed by aircraft at high altitudes (8–13 km) over the Pacific Ocean was also proved to be connected with ENSO (Matsueda *et al.*, 2002).

During El Niño events, the up-welling of CO<sub>2</sub>-rich ocean water in the eastern equatorial Pacific was suppressed, resulting in reduced CO<sub>2</sub> emissions from this area. In contrast, El Niño events induce high temperature anomalies in many areas, particularly in the Tropics, resulting in increased CO<sub>2</sub> emissions from the terrestrial biosphere through the enhanced respiration of plants and activated decomposition of organic matter in soil (Keeling *et al.*, 1995). This effect is enhanced by the suppressed plant photosynthesis in areas of anomalously low precipitation, particularly in the Tropics. These oceanic and terrestrial processes during El Niño events have opposing effects. However, Dettinger and Ghil (1998) suggested that the former was limited to the eastern equatorial Pacific, while the latter was seen more globally.

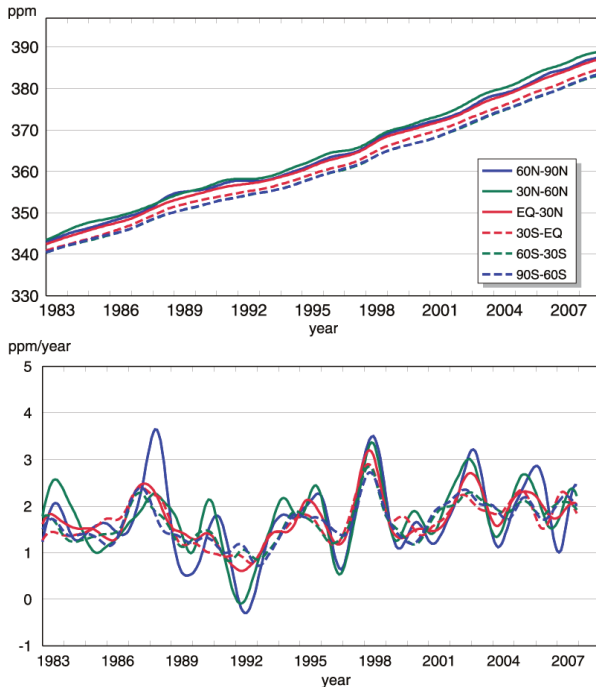


Fig. 3.4 Long-term trends in the mole fraction of CO<sub>2</sub> for each 30° latitudinal zone (top) and their growth rates (bottom).

However, an exceptionally low CO<sub>2</sub> growth rate occurred during the El Niño event in 1991/1992. The injection of 14–20 Mt of SO<sub>2</sub> aerosols into the stratosphere by the Mt. Pinatubo eruption in June 1991 affected the radiation budget and atmospheric circulation (Hansen *et al.*, 1992; Stenchikov *et al.*, 2002), and resulted in a drop in global temperature. Angert *et al.* (2004) suggested that the low CO<sub>2</sub> growth rate observed during this El Niño event was due to reduced CO<sub>2</sub> emissions caused by consequent changes in the respiration of terrestrial vegetation and the

decomposition of organic matter (Conway *et al.*, 1994; Lambert *et al.*, 1995; Rayner *et al.*, 1999), and by enhanced CO<sub>2</sub> absorption due to intensive photosynthesis caused by an increase in diffuse radiation (Gu *et al.*, 2003).

### Seasonal cycle of CO<sub>2</sub> mole fraction in the atmosphere

Figure 3.5 shows average seasonal cycles in the mole fraction of CO<sub>2</sub> for each 30° latitudinal zone. The seasonal cycles are clearly large in amplitude in northern high and mid-latitudes and small in the Southern Hemisphere. Oceanic uptake (Ramonet *et al.*, 1996) and biomass burning (Wittenberg *et al.*, 1998) are thought to influence the seasonal variation. However, these large seasonal cycles in the Northern Hemisphere are characterized by rapid decreases from June to August and large returns from September to December.

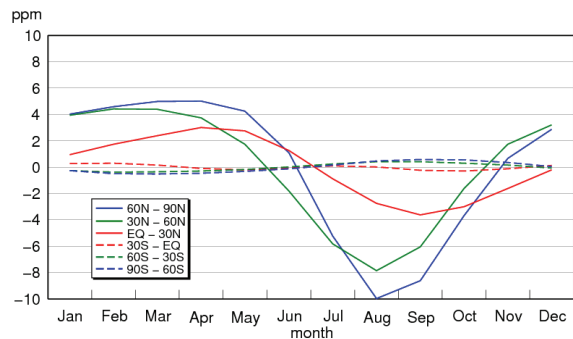


Fig. 3.5 Average seasonal cycles in the mole fraction of CO<sub>2</sub> for each 30° latitudinal zone obtained by subtracting long-term trends from the zonal mean mole fractions .

The mole fractions of CO<sub>2</sub> in northern low latitudes lag behind that in high latitudes by one or two months. The minimum values appear in August in northern high and mid-latitudes and in September in northern low latitudes.

In the Southern Hemisphere, seasonal variations show small amplitudes with a half-year delay due to small amounts of net emission and absorption by the terrestrial biosphere. Seasonal variations in both northern and southern mid-latitudes are apparently superimposed in southern low latitudes (0–30°S). The direct influence of sources and sinks in the Southern Hemisphere may be partially cancelled by the propagation of an antiphase variation from the Northern Hemisphere.

Figure 3.6 shows latitudinal distributions of the mole fractions of CO<sub>2</sub> in January, April, July and October 2008. Data in Figure 3.6 are from the sites that are marked with an asterisk in Plate 3.1. In latitudes north of 30°N, the mole fractions increased towards higher latitudes in January and April, and

decreased towards higher latitudes in July, corresponding to the large seasonal variation in northern high and mid-latitudes, which is connected with activities of the terrestrial biosphere.

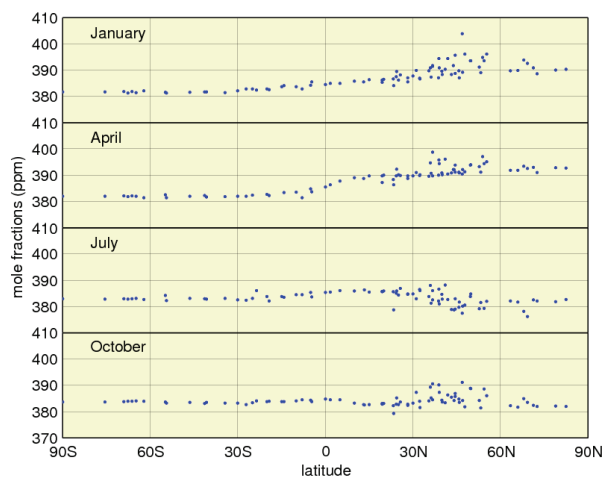


Fig. 3.6 Latitudinal distributions of the monthly mean mole fractions of CO<sub>2</sub> in January, April, July and October 2008.

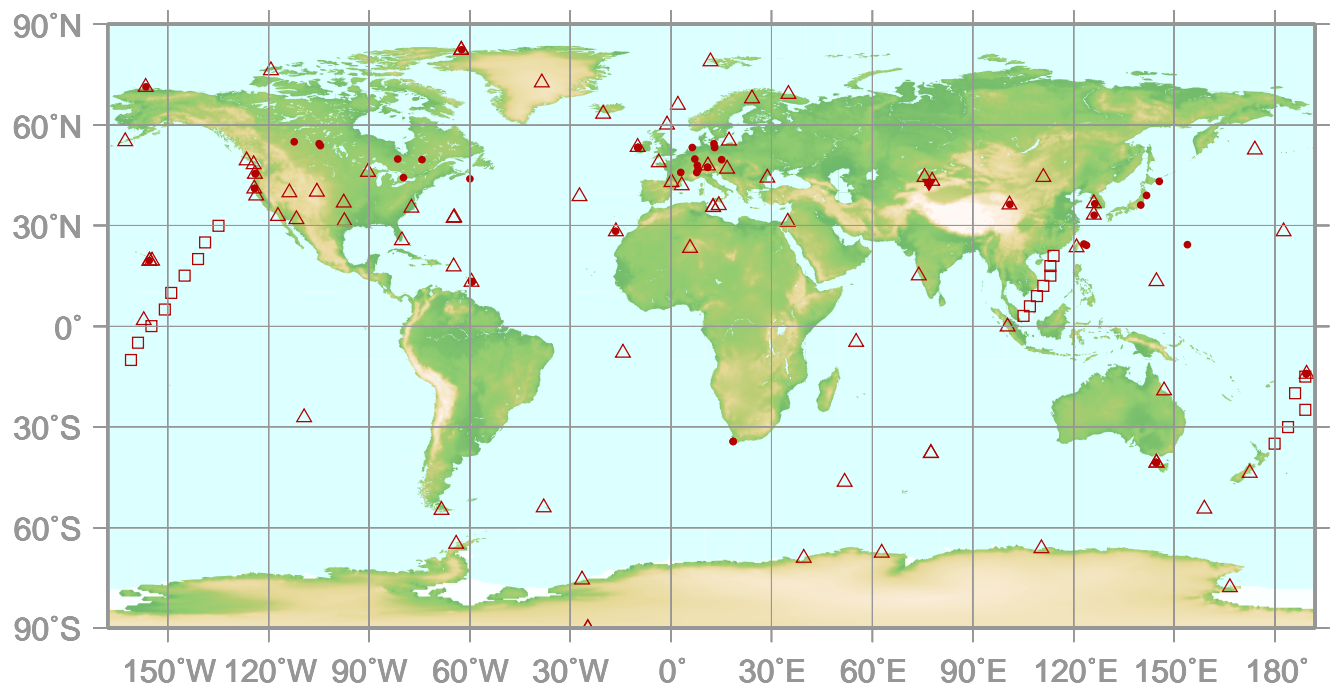


# 4.

## METHANE

### (CH<sub>4</sub>)

- : CONTINUOUS STATION
- △ : FLASK STATION
- : FLASK MOBILE (SHIP)
- ▼ : REMOTE SENSING STATION



This map shows locations of the stations that have submitted data for monthly mean mole fraction.

## CH<sub>4</sub> Monthly Data

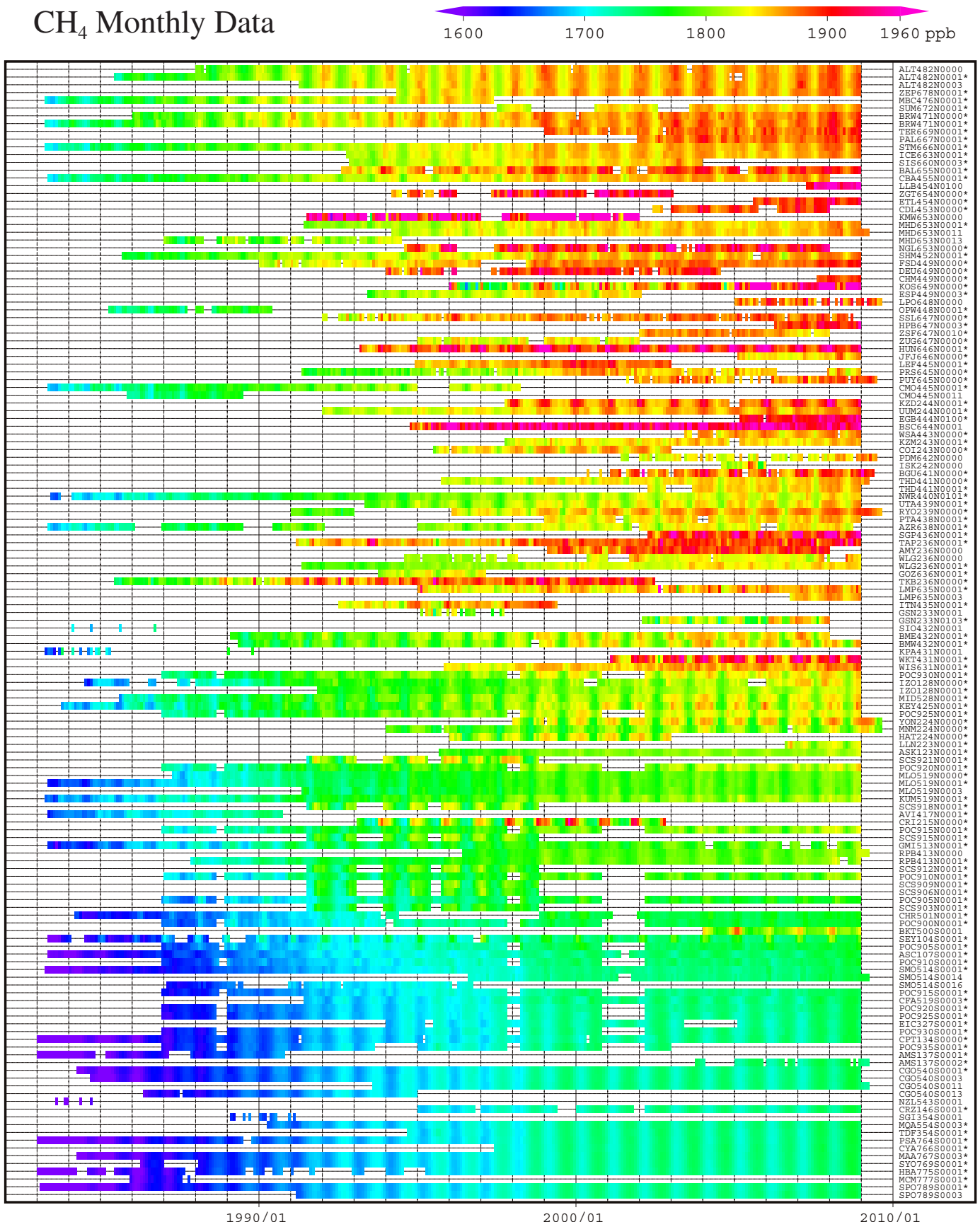
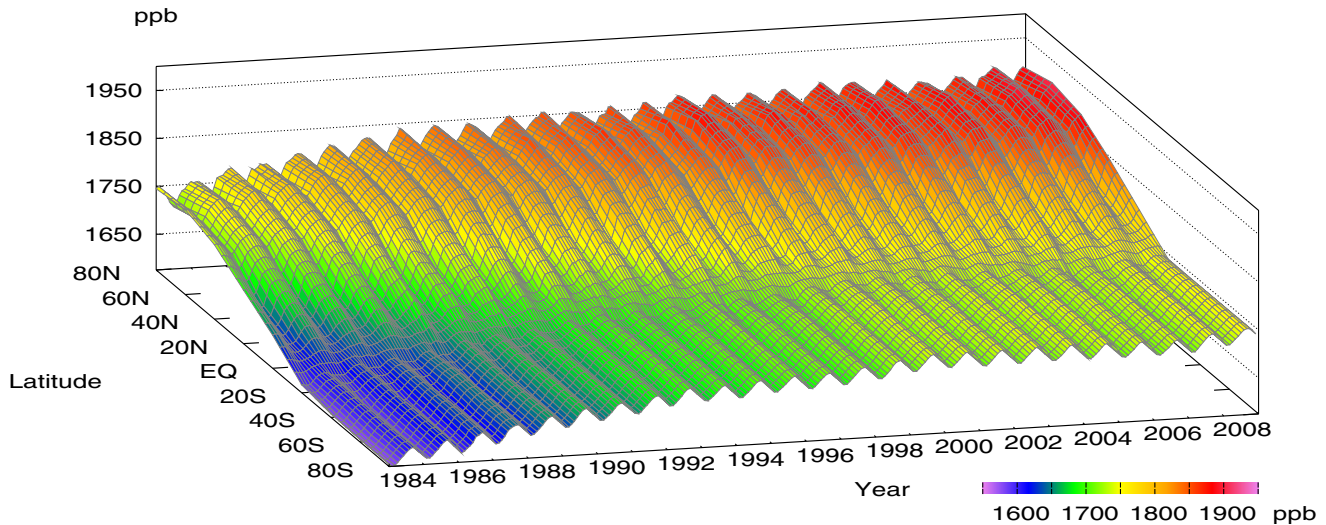
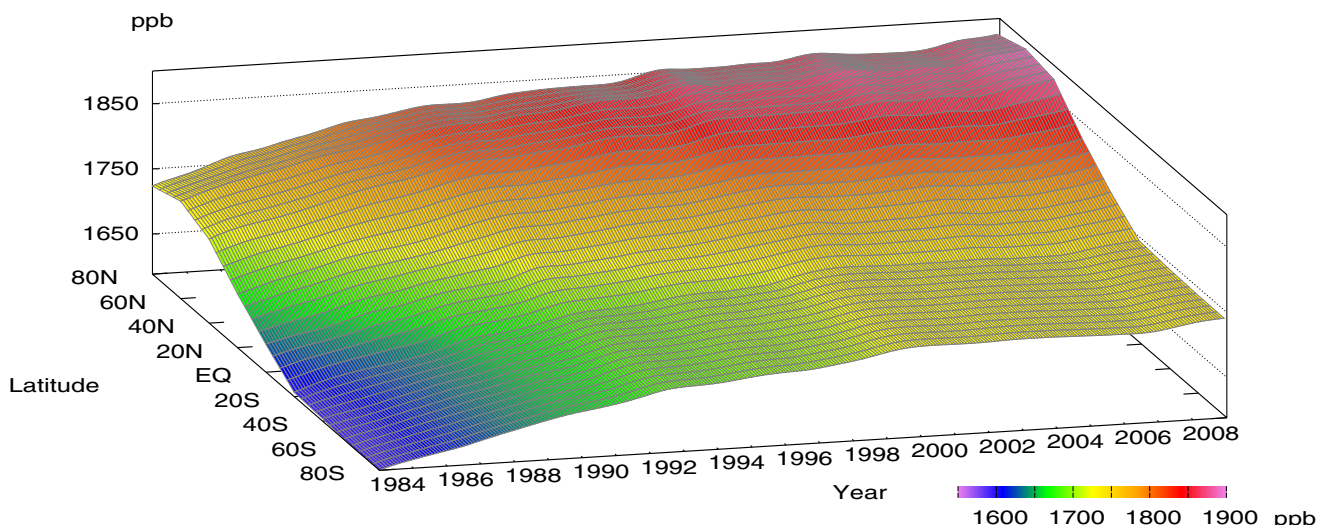


**Plate 4.1** Monthly mean CH<sub>4</sub> mole fractions that have been reported to the WDCGG. The mole fractions are illustrated in different colors. The sites are listed in order from north to south. In the case where data are reported for two or three different altitudes, only the data at the highest altitudes are illustrated. In the case where monthly means are not reported, the WDCGG calculates them from hourly or other mole fractions reported to the WDCGG by simple arithmetic mean. The data from the sites with an asterisk at the end of the station index are used for the analysis shown in Plate 4.2. (see Chapter 2)

### CH<sub>4</sub> mole fraction



### CH<sub>4</sub> deseasonalized mole fraction



### CH<sub>4</sub> growth rate

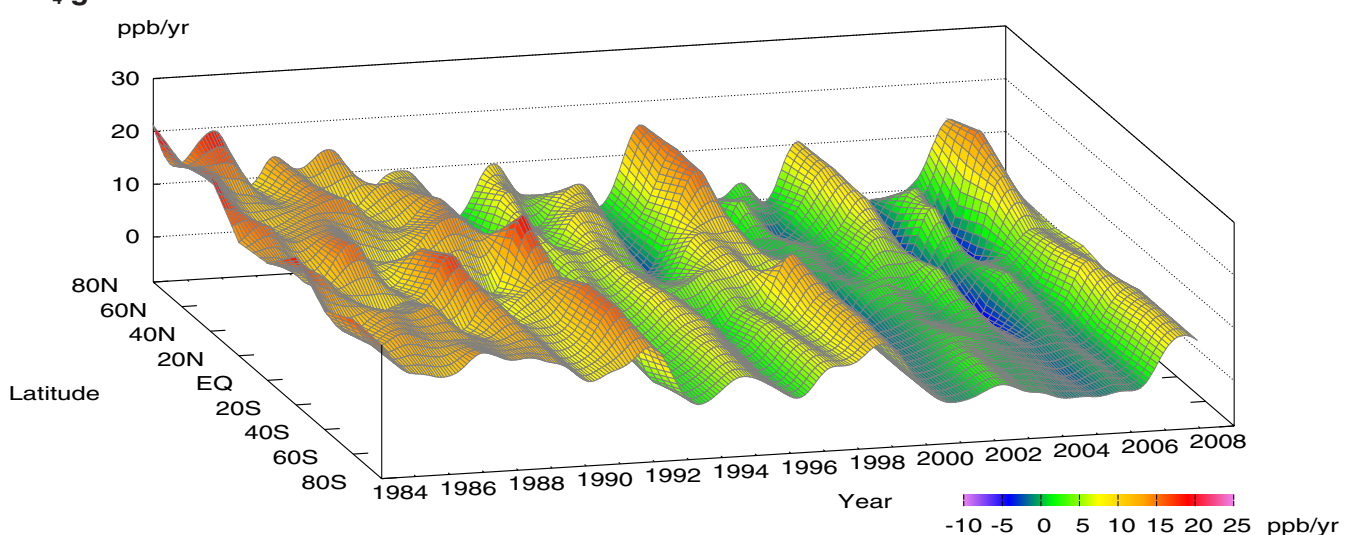


**Plate 4.2** Variation of zonally averaged monthly mean CH<sub>4</sub> mole fractions (top), deseasonalized long-term trends (middle), and growth rates (bottom). The zonally averaged mole fractions are calculated for each 20° zone. The deseasonalized trends and growth rates are derived as described in Chapter 2.

## 4. METHANE ( $\text{CH}_4$ )

### Basic information on $\text{CH}_4$ with regard to environmental issues

Methane ( $\text{CH}_4$ ) is the second most significant anthropogenic greenhouse gas, but has been estimated to have a 25 times greater global warming potential per molecule over a 100 year horizon and 72 times greater over 20 years horizon than  $\text{CO}_2$ . Between 1750 and 2008,  $\text{CH}_4$  accounted for 18.2% of the radiative forcing caused by the increase in well-mixed greenhouse gases (WMO, 2009b).

Analyses of air trapped in ice cores from Antarctica and the Arctic revealed that the current atmospheric  $\text{CH}_4$  mole fraction is the highest over the last 650,000 years (Solomon *et al.*, 2007). The mole fraction of  $\text{CH}_4$  remained steady at 700 ppb from 1000 A.D. until the start of the industrial era (Etheridge *et al.*, 1998), after which it began to increase. Measurements in ice cores from Antarctica and Greenland have shown that the difference in  $\text{CH}_4$  mole fractions between the Northern and Southern Hemispheres ranged from 24 to 58 ppb between 1000 and 1800 A.D. (Etheridge *et al.*, 1998), but is now as high as about 150 ppb (see Fig. 4.3), reflecting more emissions in the Northern Hemisphere, where major anthropogenic sources are situated.

$\text{CH}_4$  is emitted by both natural and anthropogenic sources, including natural wetlands, oceans, landfills, rice paddies, enteric fermentation, fossil fuel production and consumption and biomass burning. Denman *et al.* (2007) estimated the global emission to be 582 teragrams (Tg)  $\text{CH}_4$  per year, with more than 60% related to anthropogenic activities.  $\text{CH}_4$  is destroyed by reaction with hydroxyl radicals ( $\text{OH}$ ) in both the troposphere and stratosphere, and by reaction with chlorine atoms and  $\text{O}(\text{lD})$ , an excited state of oxygen, in the stratosphere.  $\text{CH}_4$  is one of the most important sources of water vapour in the stratosphere and has an atmospheric lifetime of about 10 years. More information regarding sources and sinks of  $\text{CH}_4$  must be collected to better understand the budget of atmospheric  $\text{CH}_4$ .

Mole fractions of  $\text{CH}_4$  are analyzed by using the data from fixed stations and some ships that submitted to the WDCGG. The observational sites where data used for the analysis are shown on the map at the beginning of this chapter.

### Annual variation of $\text{CH}_4$ mole fraction in the atmosphere

The monthly mean mole fractions of  $\text{CH}_4$  used in the analysis are shown in Plate 4.1, with the mole fraction levels illustrated in different colours. Global, hemispheric and zonal mean mole fractions have been analysed based on data from selected stations under

unpolluted conditions (see the caption for Plate 4.1). Latitudinally averaged atmospheric  $\text{CH}_4$  mole fractions, together with their deseasonalized components and growth rates, are shown as three-dimensional representations in Plate 4.2. They indicate that the seasonal variations in mole fraction are larger in the Northern Hemisphere than in the Southern Hemisphere and that the increase in the Northern Hemisphere propagates to the Southern Hemisphere. The growth rates vary on a global scale. These features are similar to those for  $\text{CO}_2$  (see Section 3). A large latitudinal gradient in  $\text{CH}_4$  mole fraction exists from the northern mid-latitudes to the Tropics, suggesting major sources in high and middle northern latitudes and sinks in the Tropics, where the mole fraction of  $\text{OH}$  radicals is higher.

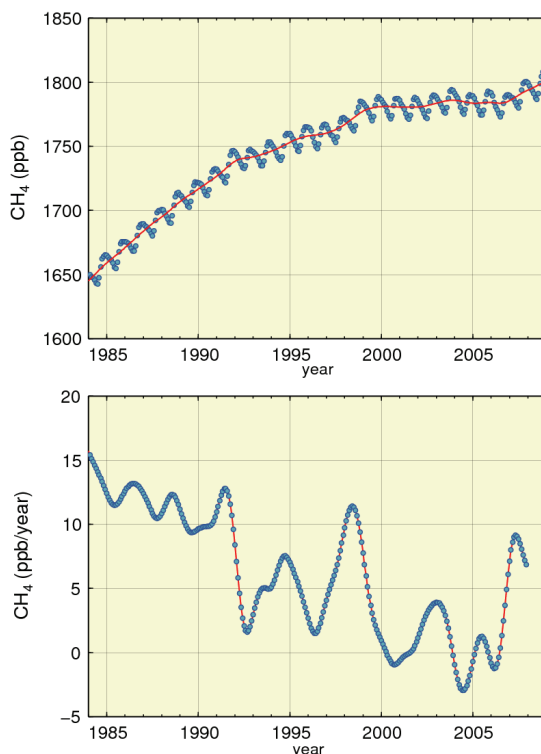


Fig. 4.1 Global monthly mean mole fraction of  $\text{CH}_4$  from 1984 to 2008 with deseasonalized long-term trend in red line (top) and its growth rate (bottom).

Figure 4.1 shows global monthly mean mole fractions and the global growth rate from 1984 to 2008. The mean mole fraction was 1797 ppb in 2008, an increase of 7 ppb since 2007. This increase is as large as in 2007 and the largest since 1998. The average growth rate over the period 1998–2008 was 2.5 ppb/year. The current mole fraction is 257% of its

pre-industrial level, 700 ppb.

Figure 4.2 shows monthly mean mole fractions from 1984 to 2008 for each  $30^{\circ}$  latitudinal zone. The seasonal variation is small in the latitudinal zone between the equator and  $30^{\circ}$ S.

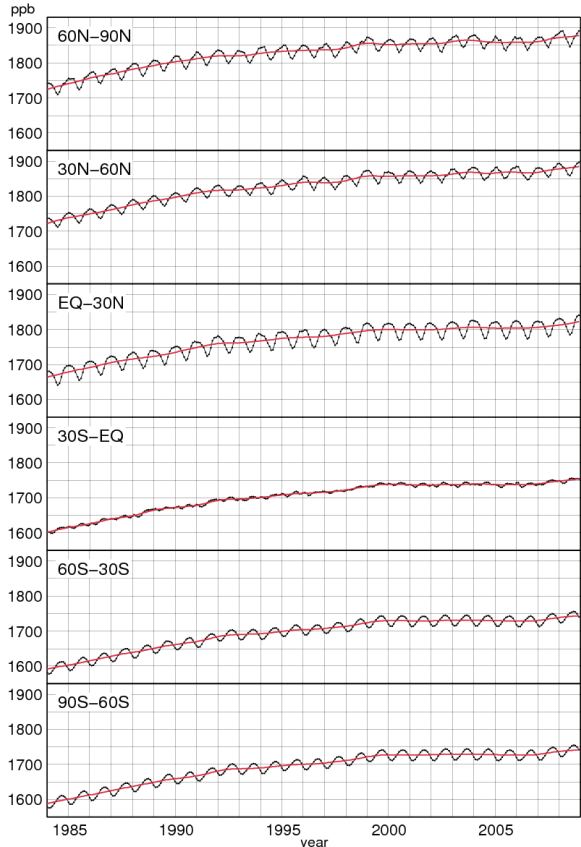


Fig. 4.2 Monthly mean mole fractions of  $\text{CH}_4$  from 1984 to 2008 for each  $30^{\circ}$  latitudinal zone (dots) and their deseasonalized long-term trends (red lines).

Figure 4.3 summarizes deseasonalized long-term trends for each  $30^{\circ}$  latitudinal zone and their growth rates. The deseasonalized long-term trends are characterized by high mole fractions in the northern high and mid-latitudes and low mole fractions in southern latitudes. In the 1990s, the growth rates clearly decreased in all latitudinal zones. Especially, in the second half of 1992 and in 1996, the growth rates were less than 5 ppb/year in all latitudes. In 1998, the global growth rate increased to about 12 ppb/year (Fig. 4.1). Maximum increase occurred in northern high and mid-latitudes, where the growth rates were over 15 ppb/year. In 2000 and 2001, the global growth rate decreased to around  $-1$  ppb/year. Around 2002/2003, the growth rates increased in the Northern Hemisphere, especially in northern high and mid-latitudes where it reached about 10 ppb/year. The global growth rate was  $-3$  ppb/year in 2004 and 1 ppb/year in 2005. Despite the large growth rates in 1998 and 2002/2003, during El Niño events, the global mean mole fraction was

relatively stable between 1999 and 2006. However, the growth rates during 2007 and 2008 increased significantly throughout the entire monitoring network and reached 7 ppb/year (Rigby *et al.*, 2008; Dlugokencky *et al.*, 2009).

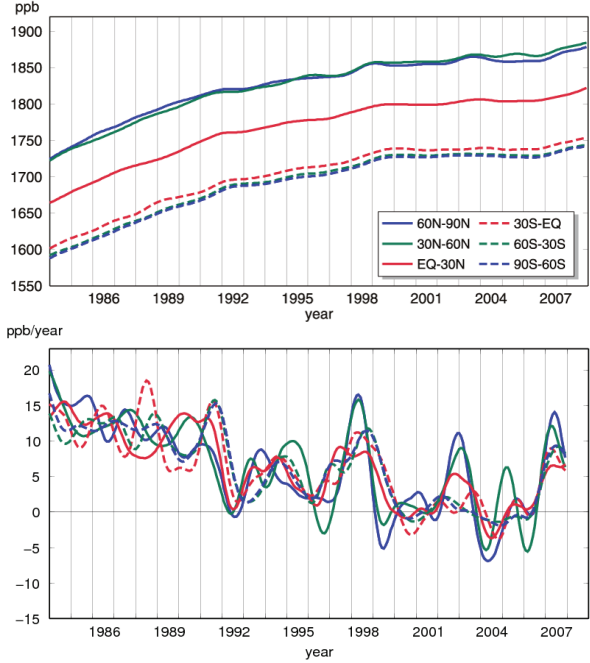


Fig. 4.3 Long-term trends in the mole fraction of  $\text{CH}_4$  for each  $30^{\circ}$  latitudinal zone (top) and their growth rates (bottom).

The large increase in  $\text{CH}_4$  growth rate in 1991 may have been caused by decreased levels of OH radicals due to reduced UV radiation as a result of the eruption of Mt. Pinatubo in 1991 (Dlugokencky *et al.*, 1996) and the subsequent decrease in 1992 may have been attributed to increased OH radicals as a result of the stratospheric ozone depletion following this eruption (Bekki *et al.*, 1994).

In 1998, the growth rates were high in all latitudes, which may have been due to increased emissions in northern high latitudes and tropical wetlands caused by high temperatures and increased precipitation, as well as by biomass burning in boreal forests, mainly in Siberia (Dlugokencky *et al.*, 2001). In contrast, Morimoto *et al.* (2006) estimated from isotope observations that the contribution of biomass burning to the increase in 1998 was about a half that of wetlands. The growth rates decreased afterward, but increased again upon occurrence of the El Niño event of 2002/2003 and after 2007.

The cause of the decreased  $\text{CH}_4$  growth rates from 1991 to 2006 remains unresolved. The growth rates of  $\text{CH}_4$  in 2007 and 2008 were the highest since 1998. But it is not clear if this increase over two years represents the beginning of a new upward trend in  $\text{CH}_4$ .

## Seasonal cycle of CH<sub>4</sub> mole fraction in the atmosphere

Figure 4.4 shows seasonal cycles in the mole fraction of CH<sub>4</sub> for each 30° latitudinal zone. The seasonal cycles are driven mainly by reaction with OH radicals, a major CH<sub>4</sub> sink in the atmosphere. These cycles are also affected by the magnitude and timing of CH<sub>4</sub> emission from sources such as wetlands and biomass burning as well as by its atmospheric transport. The seasonal cycles are large in amplitude in the Northern Hemisphere. Unlike CO<sub>2</sub>, amplitudes were also large in southern high and mid-latitudes. Seasonally, both hemispheres show minima in summer and maxima in winter. The seasonal variation in the mole fraction of CH<sub>4</sub> is almost consistent with that of OH radicals reacting with CH<sub>4</sub>. Southern low latitudes have a distinct antiphase annual component superimposing the annual component of the seasonal cycle arising from southern mid-latitudes. The maximum in the former component occurs in boreal winter due to the interhemisphere transportation of CH<sub>4</sub> from the Northern Hemisphere.

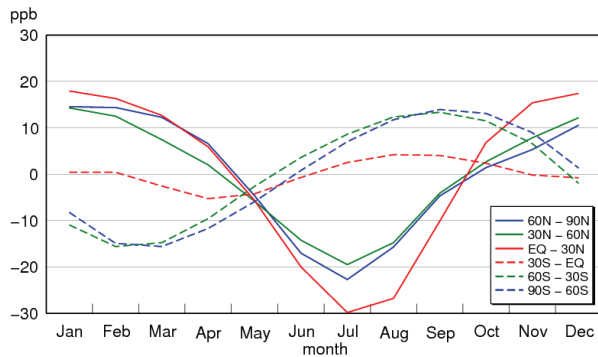


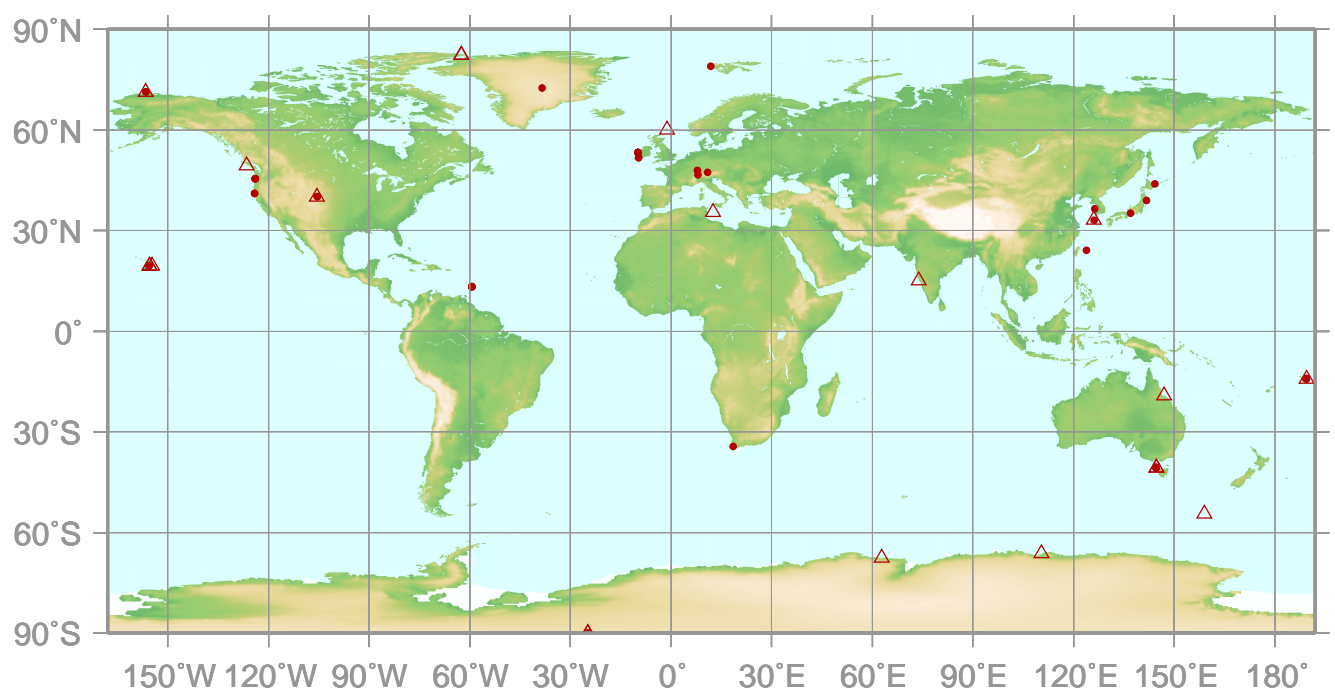
Fig. 4.4 Average seasonal cycles in the mole fraction of CH<sub>4</sub> for each 30° latitudinal zone obtained by subtracting long-term trends from original data sets.

# 5.

## NITROUS OXIDE

### (N<sub>2</sub>O)

- : CONTINUOUS STATION
- △ : FLASK STATION



This map shows locations of the stations that have submitted data for monthly mean mole fraction.

## N<sub>2</sub>O Monthly Data

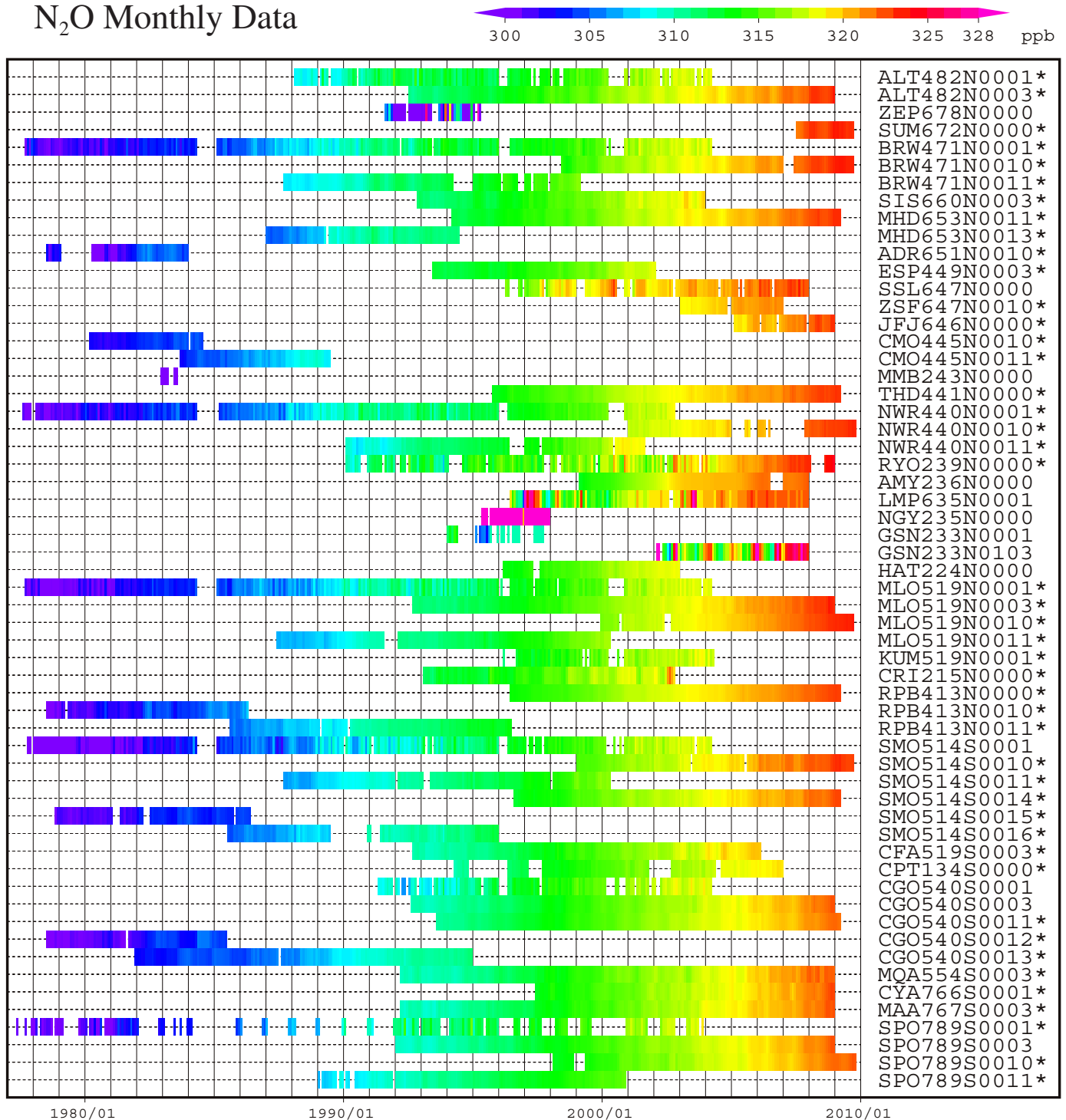


**Plate 5.1** Monthly mean N<sub>2</sub>O mole fractions that have been reported to the WDCGG. The mole fractions are illustrated in different colors. The sites are listed in order from north to south. The data from the sites with an asterisk at the end of the station index are used for the analysis shown in Fig.5.1. (see Chapter 2)

## 5. NITROUS OXIDE ( $\text{N}_2\text{O}$ )

### Basic information on $\text{N}_2\text{O}$ with regard to environmental issues

Nitrous oxide ( $\text{N}_2\text{O}$ ) is a relatively stable greenhouse gas in the troposphere with an “adjustment-time” of 114 years. Radiative forcing due to the increase of  $\text{N}_2\text{O}$  from 1750 to 2005 is estimated at  $0.16 \text{ W/m}^2$ , which is 6.2% of that of all long-lived and globally mixed greenhouse gases (WMO, 2009b). The mole fraction of  $\text{N}_2\text{O}$  in the atmosphere has increased steadily from about 270 ppb in pre-industrial times to a current value, which is 19% higher.

$\text{N}_2\text{O}$  is emitted into the atmosphere from natural and anthropogenic sources, including the oceans, soil, combustion of fuels, biomass burning, use of fertiliser and various industrial processes.  $\text{N}_2\text{O}$  sources to the atmosphere from human activities are approximately equal to  $\text{N}_2\text{O}$  sources from natural systems (oceans, chemical oxidation of ammonia in the atmosphere, and soils). Majority of the anthropogenic  $\text{N}_2\text{O}$  emitted in the atmosphere comes from transformation of fertilizer nitrogen into  $\text{N}_2\text{O}$  and its subsequent emission from agricultural soils.  $\text{N}_2\text{O}$  is removed from the atmosphere mainly by photo-dissociation in the stratosphere.

However, the estimated amounts from sources and sinks have not yet been well defined.

### Annual variation of $\text{N}_2\text{O}$ mole fraction in the atmosphere

Mole fractions of  $\text{N}_2\text{O}$  are analyzed by using the data from fixed stations and some ships that submitted to the WDCGG. The observational sites where data used for the analysis are shown on the map at the beginning of this chapter. The monthly mean mole fractions of  $\text{N}_2\text{O}$  used in the global analysis are shown in Plate 5.1, with the various mole fraction levels illustrated in different colours. The data submitted to the WDCGG show that  $\text{N}_2\text{O}$  mole fractions are increasing at almost all the stations. Figure 5.1 shows global monthly mean mole fraction from 1980 to 2008 and its long-term trend. The global mean mole fraction reached a new high of 321.8 ppb in 2008, an increase of 0.9 ppb over the previous year. This value is 119% of the pre-industrial level of 270 ppb. The mean growth rate of the global mean mole fraction during the period 1998–2008 was 0.78 ppb/year.

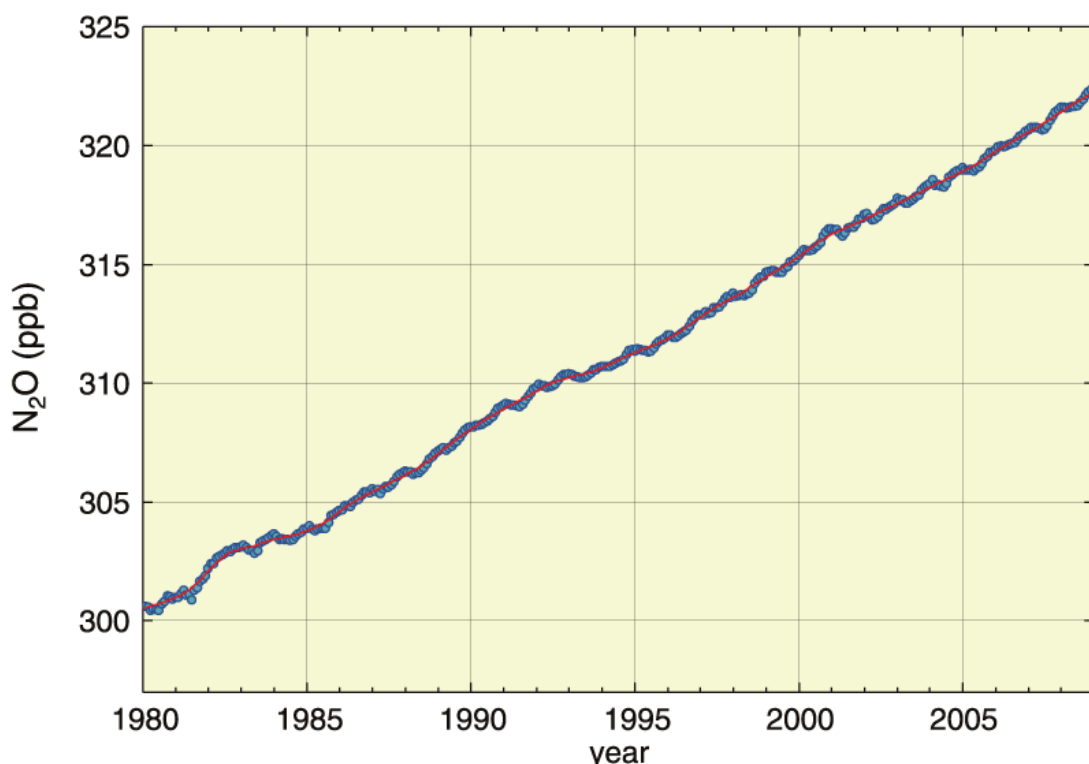
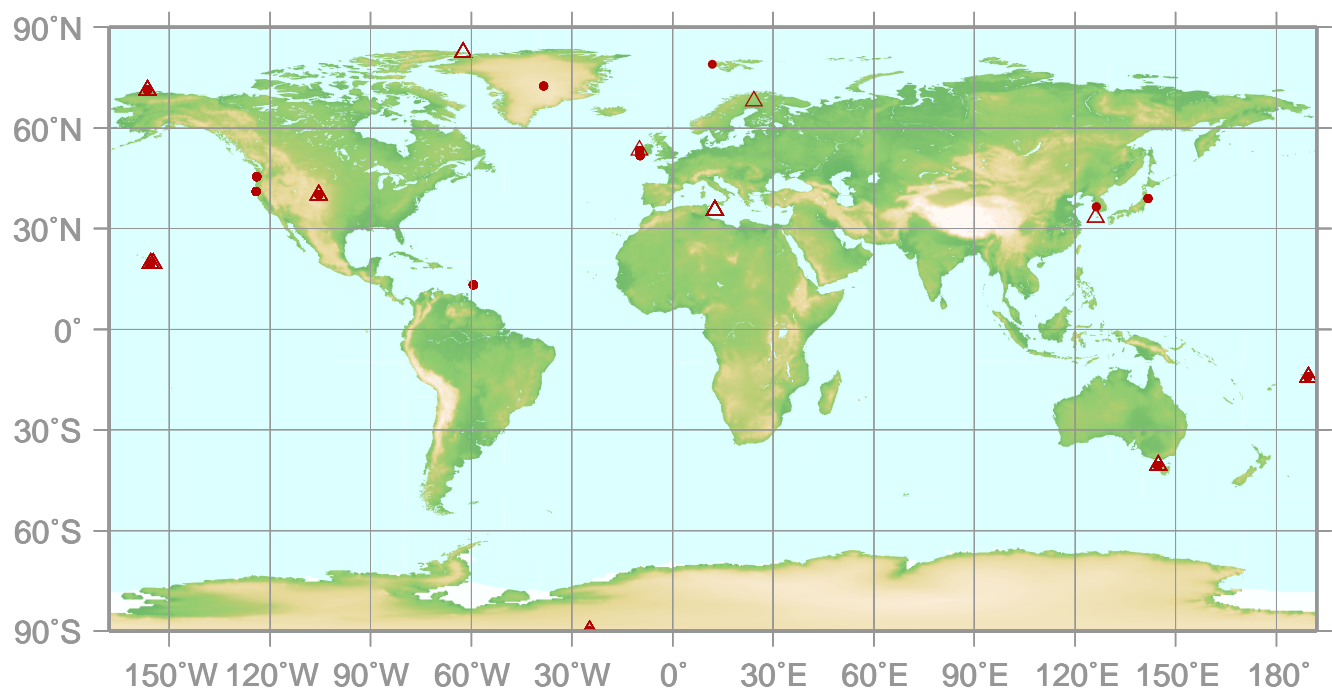


Fig. 5.1 Global monthly mean mole fraction of  $\text{N}_2\text{O}$  from 1980 to 2008 (dots) and its deseasonalized long-term trend (line).



# 6. HALOCARBONS AND OTHER HALOGENATED SPECIES

- : CONTINUOUS STATION
- △ : FLASK STATION



This map shows locations of the stations that have submitted data for monthly mean mole fraction.

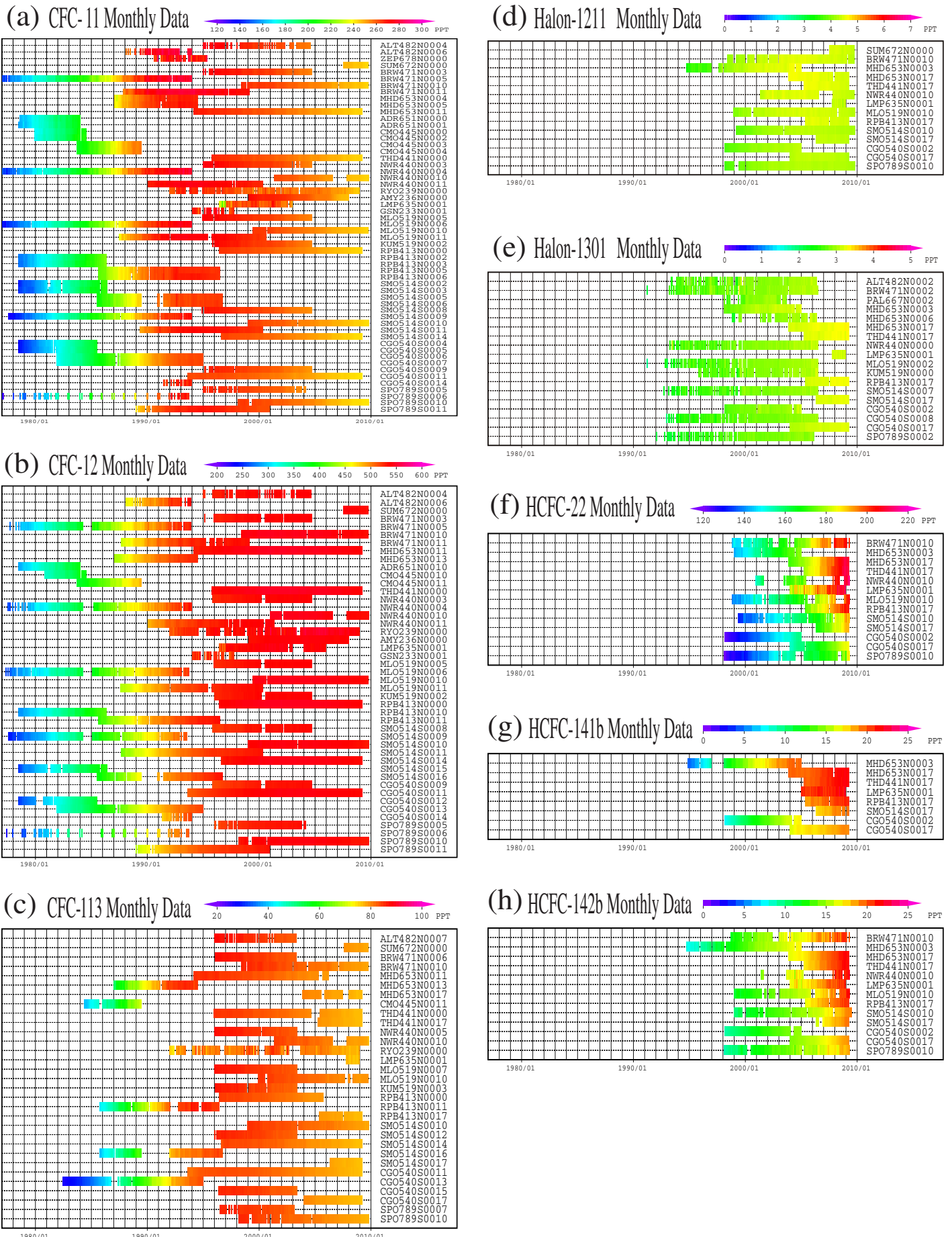


**Plate 6.1** Monthly mean (a) CFC-11, (b) CFC-12, (c) CFC-113, (d) Halon-1211, (e) Halon-1301, (f) HCFC-22, (g) HCFC-141b, (h) HCFC-142b mole fractions that have been reported to the WDCGG. The mole fractions are illustrated in different colors. The sites are listed in order from north to south.

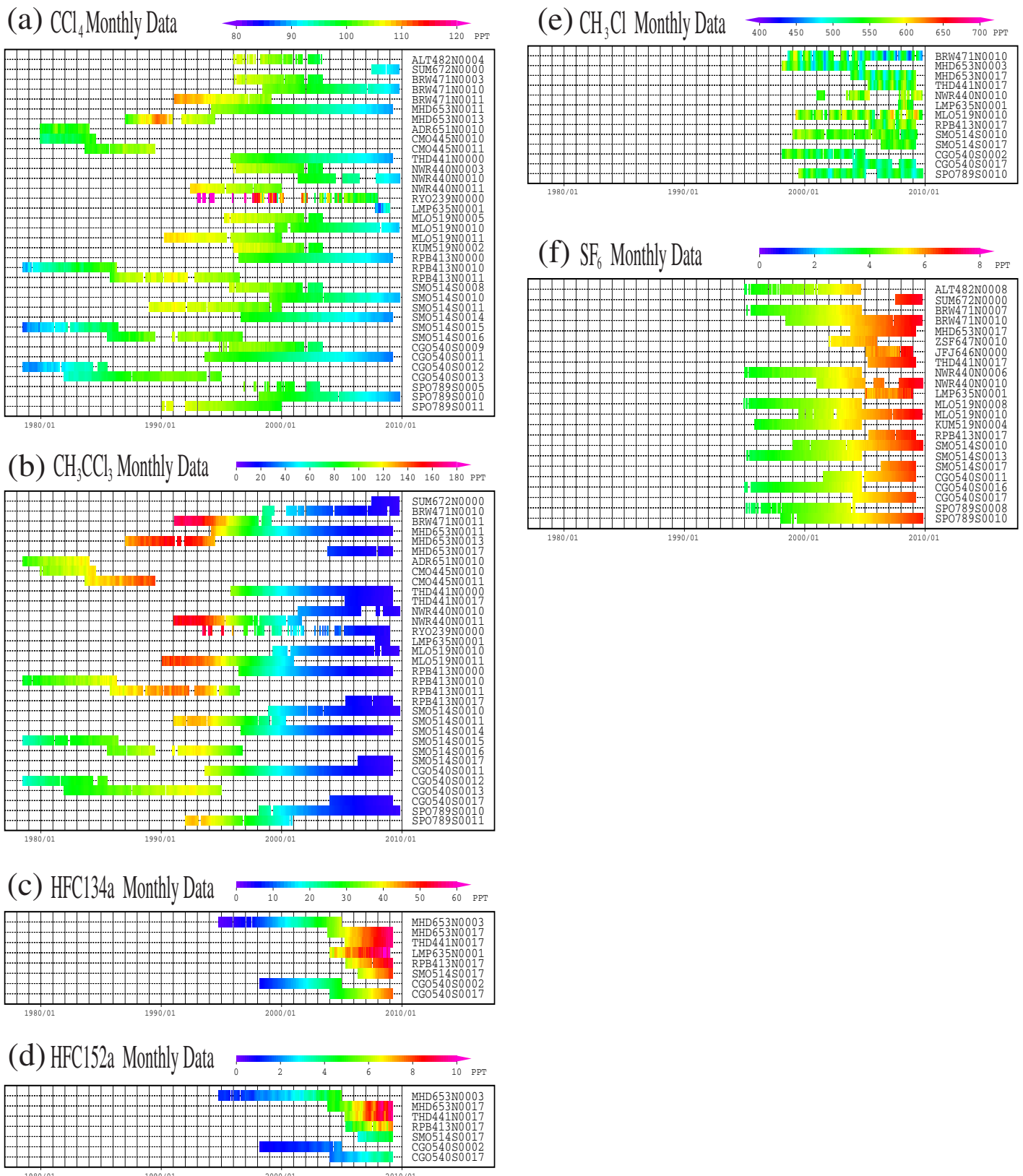


**Plate 6.2** Monthly mean (a) CCl<sub>4</sub>, (b) CH<sub>3</sub>CCl<sub>3</sub>, (c) HFC134a, (d) HFC152a, (e) CH<sub>3</sub>Cl, (f) SF<sub>6</sub> mole fractions that have been reported to the WDCGG. The mole fractions are illustrated in different colors. The sites are listed in order from north to south.

## 6. HALOCARBONS AND OTHER HALOGENATED SPECIES

### Basic information on halocarbons with regard to environmental issues

Halocarbons are carbon compounds containing one or more halogens, *i.e.*, fluorine, chlorine, bromine or iodine, and are mostly industrial products. Chlorofluorocarbons (CFCs) and halons are halocarbons containing fluorine and chlorine, and bromine and other halogen atoms, respectively, while hydrochlorofluorocarbons (HCFCs) contain hydrogen in addition. Perfluorocarbons (PFCs) are carbon compounds in which all hydrogen atoms are substituted by fluorine atoms. Hydrofluorocarbons (HFCs) are halocarbons which contain hydrogen and fluorine but no chlorine. Sulphur hexafluoride ( $SF_6$ ) is not a halocarbon but behaves similarly to halocarbons as a potent long-lived greenhouse gas. Carbon tetrachloride ( $CCl_4$ ) and methyl chloroform ( $CH_3CCl_3$ ) are produced industrially, while methyl chloride ( $CH_3Cl$ ) has natural sources. Although the mole fractions of the halocarbons are relatively low in the atmosphere, they have high global warming potentials. The halocarbons have been shown to account for 12% of the radiative forcing caused by the increased levels of globally mixed long-lived greenhouse gases from 1750 to 2008 (WMO, 2009b).

The halocarbons are colourless, odourless and innocuous substances, which are readily gasified and liquefied and have low surface tension. Thus, they were commonly used as refrigerants, propellants and detergents for semiconductors, resulting in a rapid increase in their mole fractions in the atmosphere until the mid-1980s. Halocarbons containing chlorine and bromine led to the depletion of the ozone layer. Since the mid-1990s, the Montreal Protocol on Substances that Deplete the Ozone Layer and its subsequent Adjustments and Amendments has progressively increased the regulation of the production, consumption and trade of ozone-depleting compounds.

The CFCs are dissociated mainly by ultraviolet radiation in the stratosphere, and their lifetimes are generally long (*e.g.*, about 50 years for CFC-11). However, the HCFCs and  $CH_3CCl_3$ , which contain hydrogen, react with hydroxyl radicals ( $OH$ ) in the troposphere and have relatively short lifetimes (*e.g.*, about 5 years for  $CH_3CCl_3$ ). As the reaction with OH in the troposphere is a major sink for  $CH_3CCl_3$ , global measurements of  $CH_3CCl_3$  provide an accurate estimate of the global mole fraction of OH (Prinn *et al.*, 2001).

The Kyoto Protocol to the United Nations Framework Convention on Climate Change (UNFCCC), which entered into force on 16 February 2005, specifies HFCs, PFCs and  $SF_6$  as targets for quantified emission limitation and reduction

commitments.

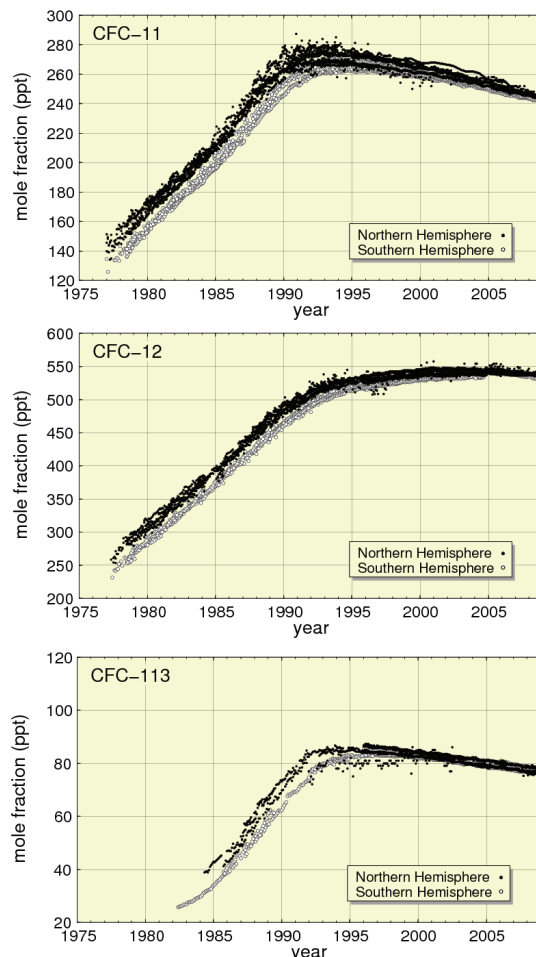


Fig. 6.1 Time series of the monthly mean mole fractions of CFC-11, CFC-12 and CFC-113. Solid circles show mole fractions measured in the Northern Hemisphere and open circles show mole fractions in the Southern Hemisphere. All data reported to the WDCGG are shown.

### Annual changes in the levels of halocarbons in the atmosphere

The map at the beginning of this chapter shows observational sites that have submitted data on halocarbons and other halogenated species to the WDCGG. Plates 6.1 and 6.2 show all the monthly mean mole fractions of these gases submitted to the WDCGG. The figures in this chapter plot all monthly data reported to the WDCGG. There are discrepancies in the absolute mole fractions for several different stations, suggesting that these stations may have adopted different standard scales. Observational data based on identical standard scales revealed that the differences in the mole fractions between the two

hemispheres were large in the 1980s for CFCs,  $\text{CCl}_4$  and  $\text{CH}_3\text{CCl}_3$  but have since narrowed.

Figure 6.1 shows monthly mean mole fractions of CFC-11 ( $\text{CCl}_3\text{F}$ ), CFC-12 ( $\text{CCl}_2\text{F}_2$ ) and CFC-113 ( $\text{CCl}_2\text{FCCl}_2$ ) over time. The mole fractions of CFC-11 were at a maximum around 1992 in the Northern Hemisphere, followed by a maximum about one year later in the Southern Hemisphere. The mole fractions of CFC-113 were at a maximum around 1992 in the Northern Hemisphere and around 1997 in the Southern Hemisphere. The mole fractions of these gases have since been decreasing slowly in both hemispheres. The mole fraction of CFC-12 may have peaked in 2003.

Figure 6.2 shows time series of the monthly mean mole fractions of Halon-1211 ( $\text{CBrClF}_2$ ) and Halon-1301 ( $\text{CBrF}_3$ ). The mole fraction of Halon-1211 has not increased since 2005. The mole fraction of Halon-1301 is increasing.

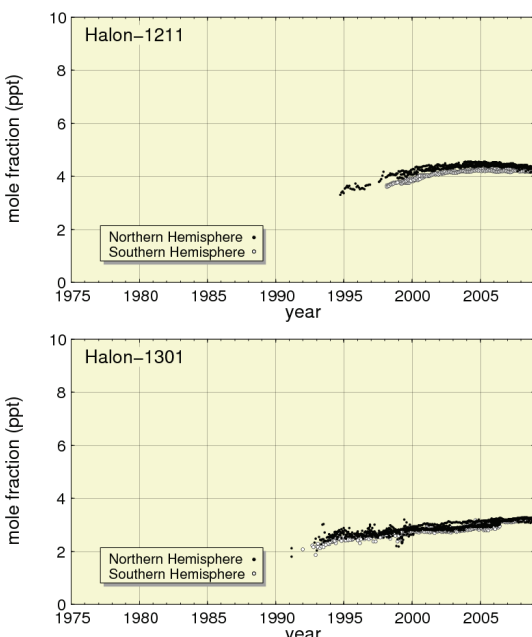


Fig. 6.2 Time series of the monthly mean mole fractions of Halon-1211 and Halon-1301. Solid circles show mole fractions measured in the Northern Hemisphere and open circles show mole fractions in the Southern Hemisphere. All data reported to the WDCGG are shown.

Figure 6.3 shows time series of the mole fractions of HCFC-22 ( $\text{CHClF}_2$ ), HCFC-141b ( $\text{CH}_3\text{CCl}_2\text{F}$ ) and HCFC-142b ( $\text{CH}_3\text{CClF}_2$ ). The mole fractions of these gases increased significantly during the 2000s as a result of continued use as substitutes for CFCs. The HCFCs are increasing rapidly; the mole fractions are 1.4–2.6 times higher than those ten years ago.

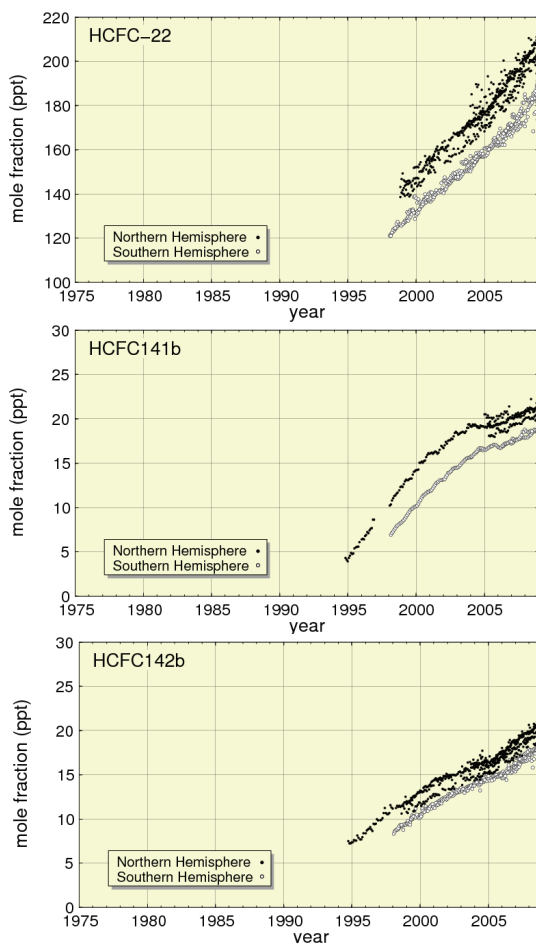


Fig. 6.3 Time series of the monthly mean mole fractions of HCFC-22, HCFC-141b, and HCFC-142b. Solid circles show mole fractions measured in the Northern Hemisphere and open circles show mole fractions in the Southern Hemisphere. All data reported to the WDCGG are shown.

Figure 6.4 shows time series of the mole fractions of  $\text{CCl}_4$  and  $\text{CH}_3\text{CCl}_3$ . The mole fractions of  $\text{CCl}_4$  in both hemispheres were at a maximum around 1991. The mole fractions of  $\text{CH}_3\text{CCl}_3$  were at a maximum around 1992 in the Northern Hemisphere and around 1993 in the Southern Hemisphere. The mole fractions of these gases have since been decreasing.

Figure 6.5 shows time series of the monthly mean mole fractions of HFC-134a ( $\text{CH}_2\text{FCF}_3$ ) and HFC-152a ( $\text{CH}_3\text{CHF}_2$ ). The mole fractions of HFC-134a and HFC-152a have increased by 4–8 times over the last 10 years. The increasing rates of these gases are larger in the Northern Hemisphere, suggesting that predominant sources are located there.

Figure 6.6 shows time series of the monthly mean mole fractions of methyl chloride ( $\text{CH}_3\text{Cl}$ ). The mole fraction of  $\text{CH}_3\text{Cl}$  has remained steady after 1980, although there is large interannual variability.

Figure 6.7 shows time series of the monthly mean mole fractions of  $\text{SF}_6$ . The mole fraction of  $\text{SF}_6$  is

increasing at a rate of about 5%/year.

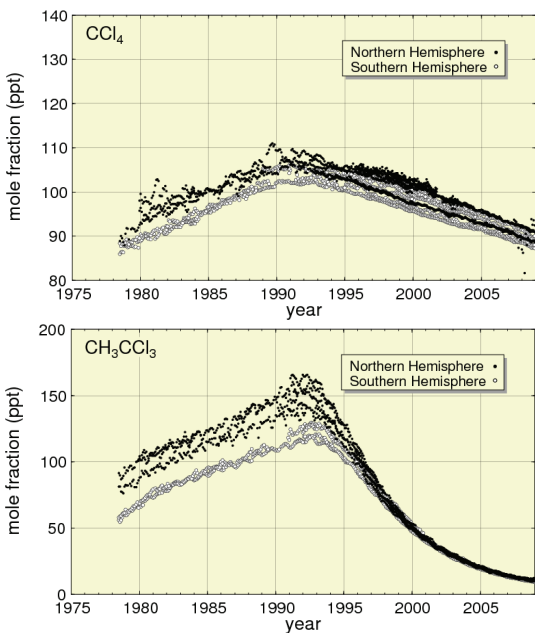


Fig. 6.4 Time series of the monthly mean mole fractions of  $\text{CCl}_4$  and  $\text{CH}_3\text{CCl}_3$ . Solid circles show mole fractions measured in the Northern Hemisphere and open circles show mole fractions in the Southern Hemisphere. All data reported to the WDCGG are shown.

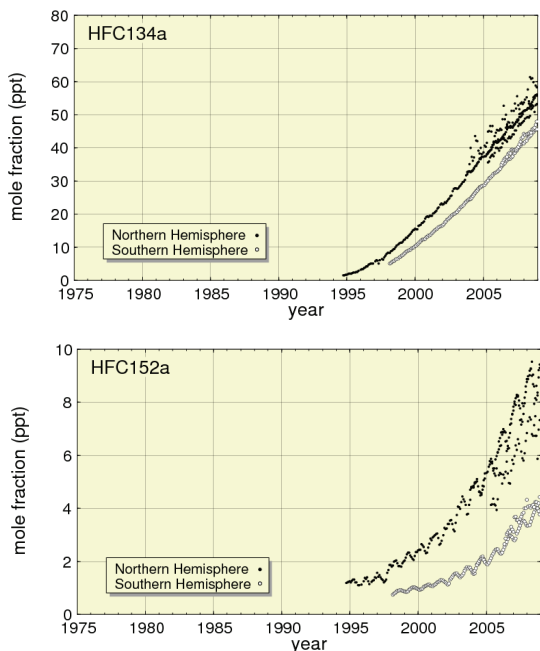


Fig. 6.5 Time series of the monthly mean mole fractions of HFC-134a and HFC-152a. Solid circles show mole fractions measured in the Northern Hemisphere and open circles show mole fractions in the Southern Hemisphere. All data reported to the WDCGG are shown.

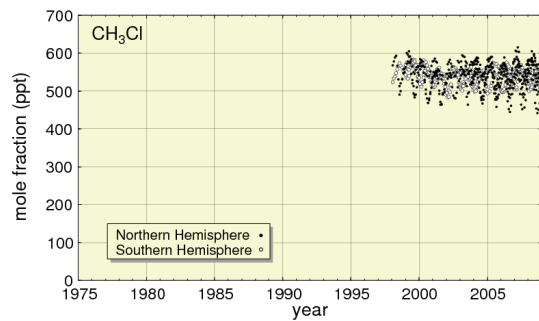


Fig. 6.6 Time series of the monthly mean mole fractions of  $\text{CH}_3\text{Cl}$ . Solid circles show mole fractions measured in the Northern Hemisphere and open circles show mole fractions in the Southern Hemisphere. All data reported to the WDCGG are shown.

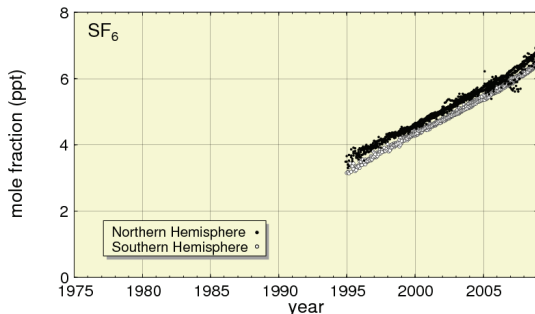


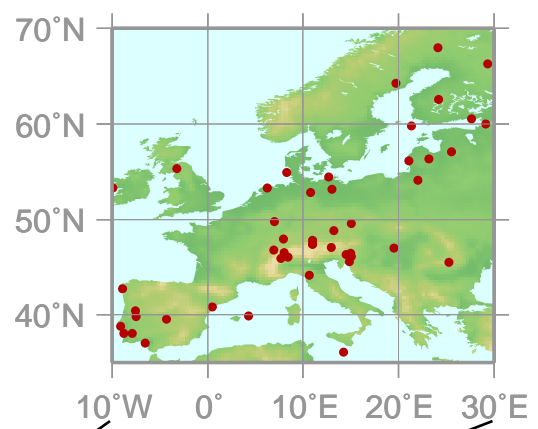
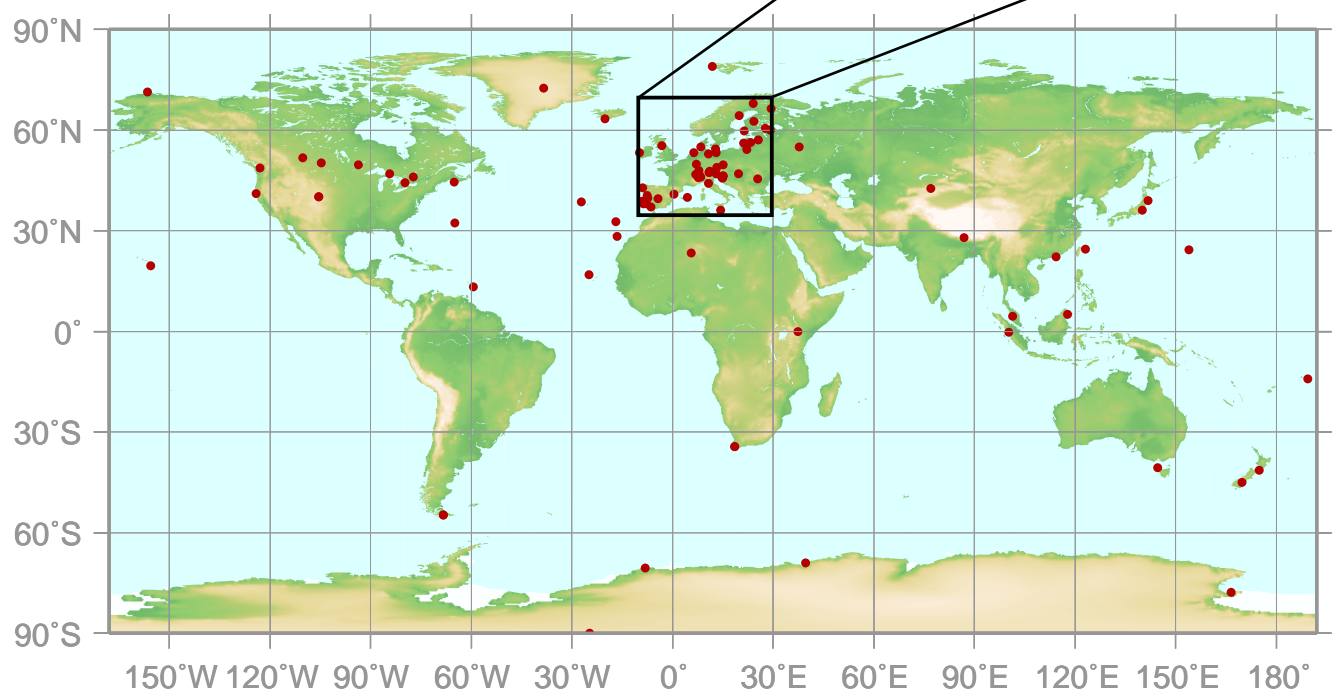
Fig. 6.7 Time series of the monthly mean mole fractions of  $\text{SF}_6$ . Solid circles show mole fractions measured in the Northern Hemisphere and open circles show mole fractions in the Southern Hemisphere. All data reported to the WDCGG are shown.

# 7.

## SURFACE OZONE

### (O<sub>3</sub>)

● : STATION



This map shows locations of the stations that have submitted data for monthly mean mole fraction.

# O<sub>3</sub> Monthly Data

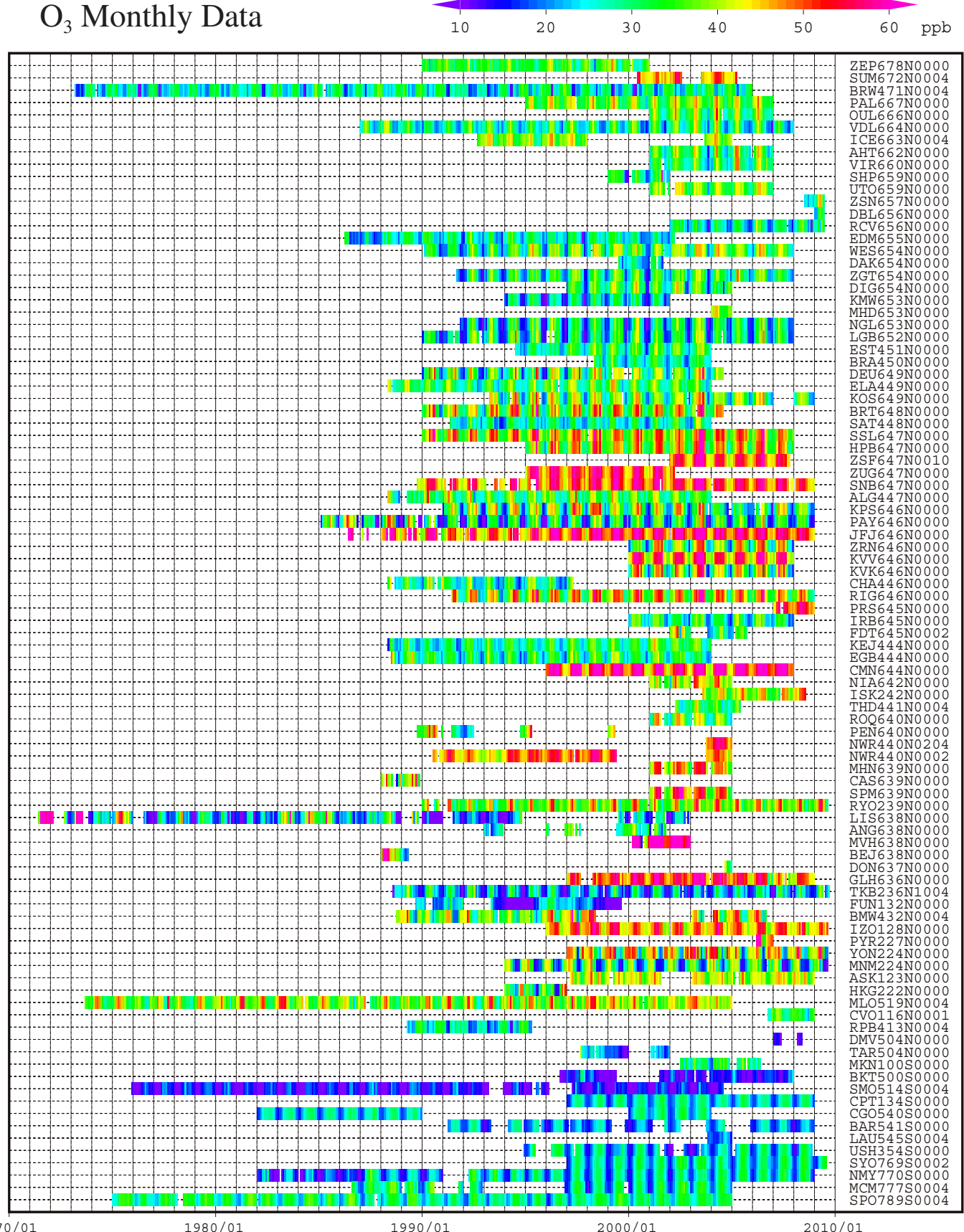


**Plate 7.1** Monthly mean O<sub>3</sub> mole fractions that have been reported to the WDCGG. The mole fractions are illustrated in different colors.

The sites are listed in order from north to south. The stations with a cross incidental (+) at the end of the station index provide data of a single-peak type as shown in Fig 7.1. The other stations provide data of a multi-peak type as shown in Fig 7.2.

## 7. SURFACE OZONE ( $O_3$ )

Basic information on surface ozone ( $O_3$ ) with regard to environmental issues

Ozone ( $O_3$ ) in the atmosphere exists mostly in the stratosphere, with less than 10% in the troposphere. However,  $O_3$  in the troposphere plays an important role in the atmospheric environment through radiative and chemical processes.  $O_3$  absorbs UV radiation in the stratosphere and thus influences the vertical profile of temperature and circulation in the stratosphere. It also absorbs IR radiation as one of the greenhouse gases in the troposphere. The latter effect is more significant in the upper troposphere, and tropospheric  $O_3$  is the third most important anthropogenic greenhouse gas after  $CO_2$  and  $CH_4$  (Denman *et al.*, 2007; IPCC, 2007). Tropospheric  $O_3$  in the northern extratropics was the greatest contributor to global warming during the 20th century, and increases in tropospheric  $O_3$  from industrialization in developing countries was found to contribute to accelerated warming in the Tropics during the latter half of the century (Shindell *et al.*, 2006). Furthermore, through reaction with water vapour under UV radiation,  $O_3$  produces OH radicals, which control atmospheric mole fractions of many greenhouse gases, such as  $CH_4$ , through chemical reactions.

The observational results at high altitudes around 1990, compared with those from the end of the 19th century to the first half of 20th century, show increase in tropospheric ozone in urban areas (Staehelin *et al.*, 1994). However, ozonesonde measurements in the troposphere show stable or decreasing trends in northern mid-latitudes (Oltmans *et al.*, 2006). The consensus on the global trend of tropospheric ozone has not been reached yet. Non uniform and highly variable concentration does not allow estimated of the global trends.

Tropospheric  $O_3$  originates from flux/mixing from the stratosphere and in-situ photochemical production.  $O_3$  is destroyed in various processes including chemical reactions with  $NO$ , the hydroperoxy radical ( $HO_2$ ) and  $OH$ , and deposition at the Earth's surface. The lifetime of tropospheric ozone varies from one or a few days in the boundary layer to a few tens of days or even a few months in the free troposphere.

In the middle troposphere, the mole fractions of  $O_3$  are high in high and mid-latitudes in both hemispheres, and low in the Tropics over the Atlantic (Marencio and Said, 1989) and Pacific (Tsutsumi *et al.*, 2003) Oceans. The localised sources and generally short lifetime of surface  $O_3$  make its distribution spatially non-uniform and time-variant.

### Annual variation of surface $O_3$ mole fraction

The observational sites that have submitted data for

surface  $O_3$  to the WDCGG are shown on the map at the beginning of this chapter. The monthly mean mole fractions of  $O_3$  that have been reported from observational sites around the world are shown in Plate 7.1, with different mole fraction levels illustrated in different colours. Data for the mole fractions of surface  $O_3$  are reported in two different units, *i.e.*, mole fraction (ppb) and weight per volume ( $\mu\text{g}/\text{m}^3$ ) at 25°C. The latter is converted to the former using the formula:

$$X_p [\text{ppb}] = (R \times T / M / P_0) \times 10 \times X_g [\mu\text{g}/\text{m}^3]$$

where  $R$  is the molar gas constant (8.31451 [J/K/mol]),

$T$  is the absolute temperature as reported from the station,

$M$  is the molecular weight of  $O_3$  (47.9982), and

$P_0$  is the standard pressure (1013.25 [hPa]).

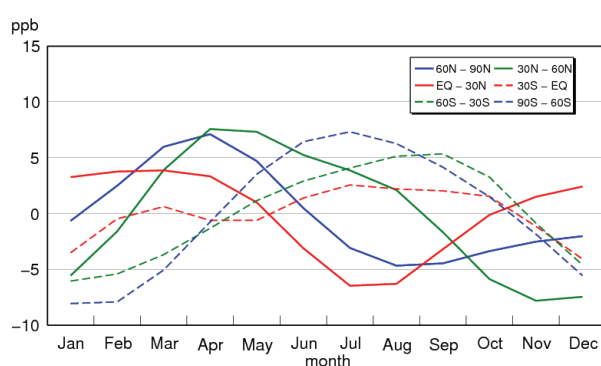


Fig. 7.1 Average seasonal cycles in the mole fraction of  $O_3$  for each 30° latitudinal zone obtained by subtracting long-term trends from latitudinally averaged mole fractions.

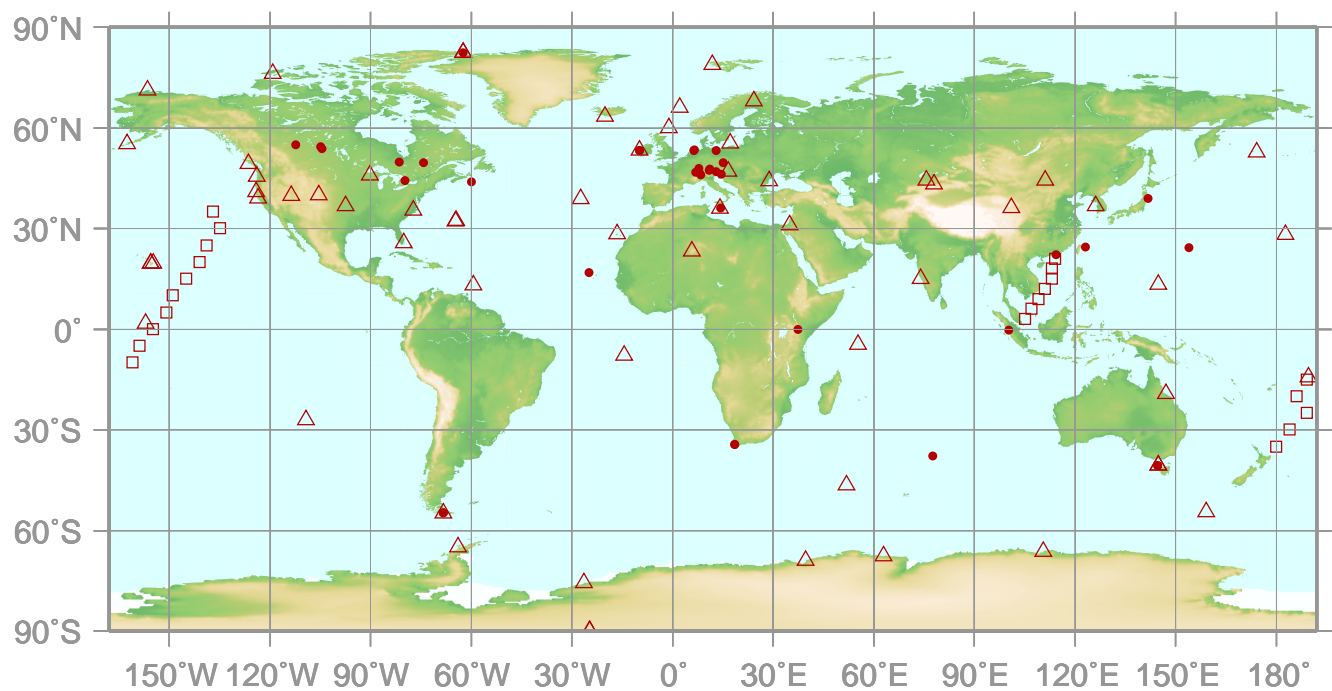
The mole fraction of surface  $O_3$  varies from station to station, though many of these stations are located in Europe. Moreover, the seasonal and interannual variation is relatively large at most stations. Therefore, it is difficult to identify a global long-term trend in the mole fraction of surface  $O_3$ .

As it is done for other species in this Data Summary, seasonal cycles of monthly mean mole fraction of surface ozone averaged for each 30° latitudinal zone are shown in Figure 7.1. The latitudinal mean mole fractions are elevated in spring in most latitudinal zones. However, there are a variety of patterns of seasonal-diurnal cycles at different locations, including a pronounced spring maximum, a spring maximum at night and a summer maximum during the day, a wide spring-summer maximum, and a pronounced winter maximum (Tarasova *et al.*, 2007).



# 8. CARBON MONOXIDE (CO)

- : CONTINUOUS STATION
- △ : FLASK STATION
- : FLASK MOBILE (SHIP)



This map shows locations of the stations that have submitted data for monthly mean mole fraction.

## CO Monthly Data

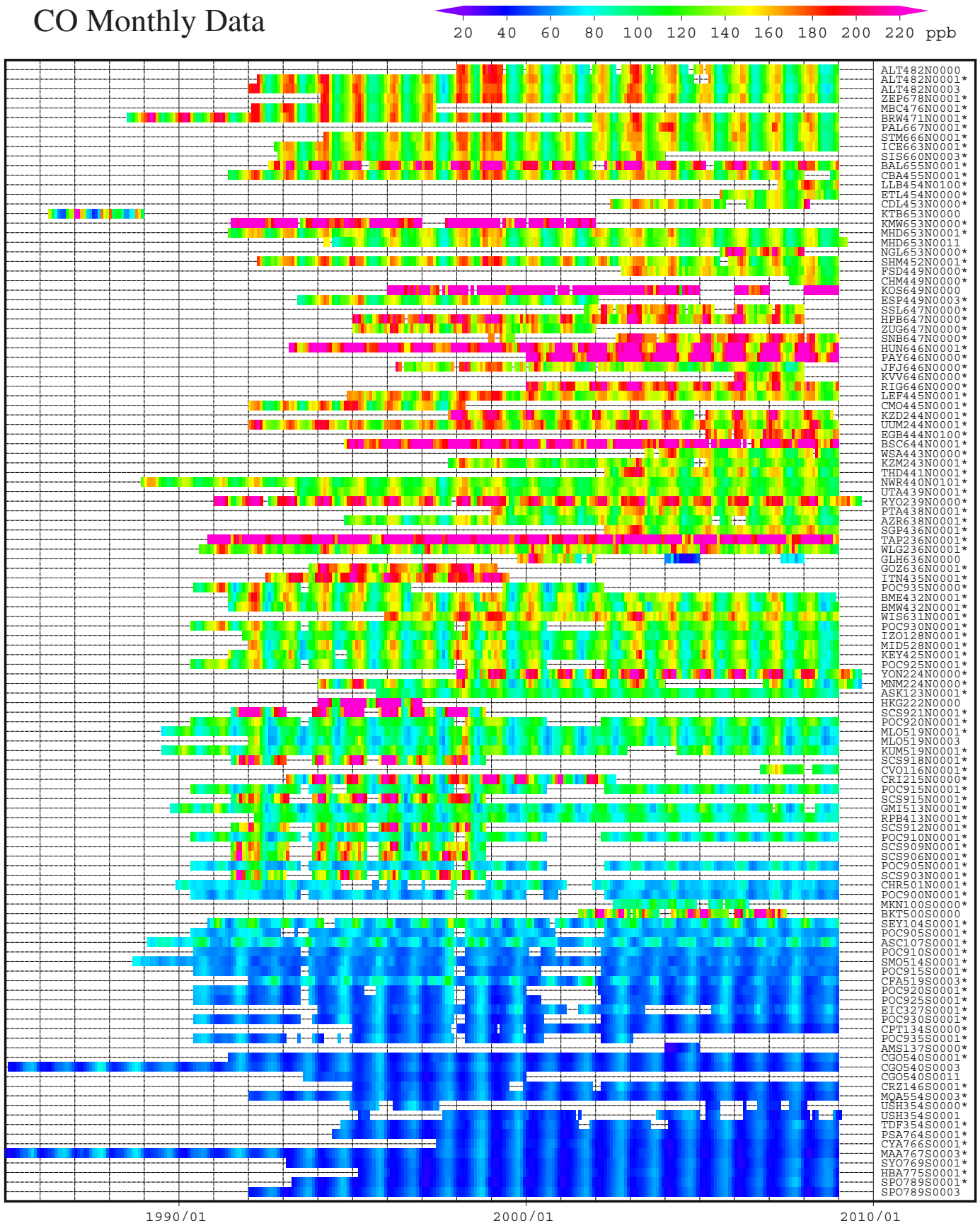
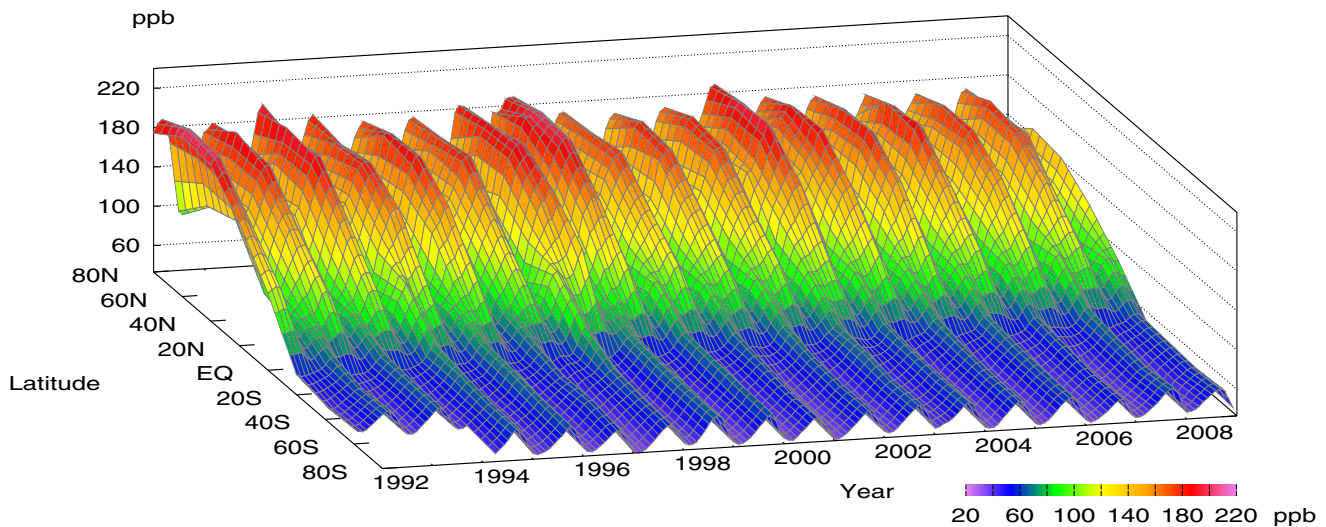
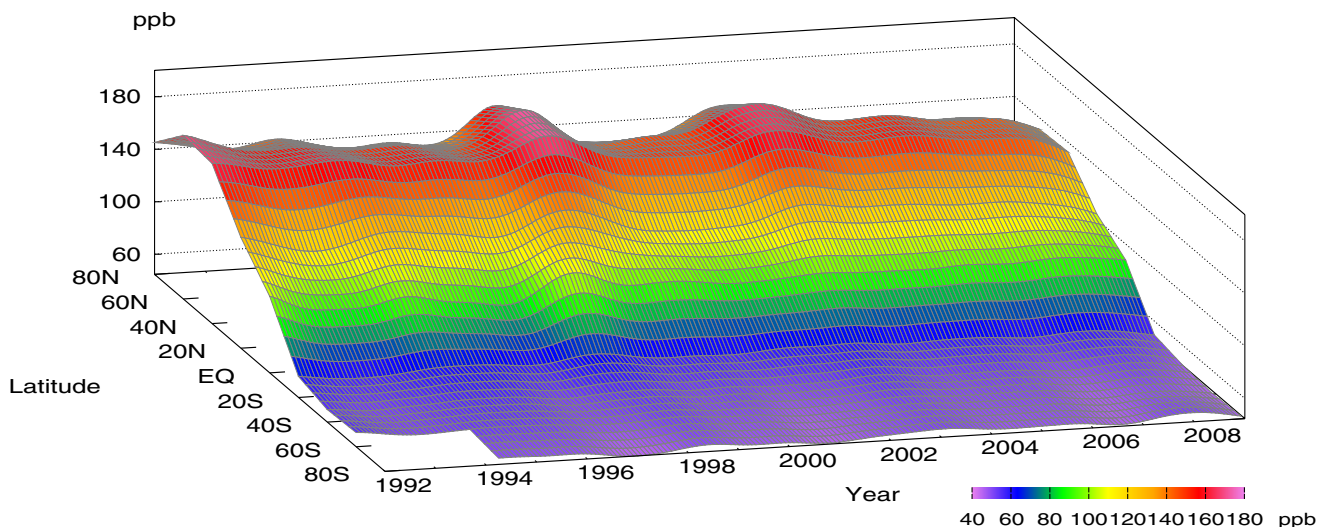


**Plate 8.1** Monthly mean CO mole fractions that have been reported to the WDCGG. The mole fractions are illustrated in different colors. The sites are listed in order from north to south. The data from the sites with an asterisk at the end of the station index are used for the analysis shown in Plate 8.2. (see Chapter 2)

### CO mole fraction



### CO deseasonalized mole fraction



### CO growth rate

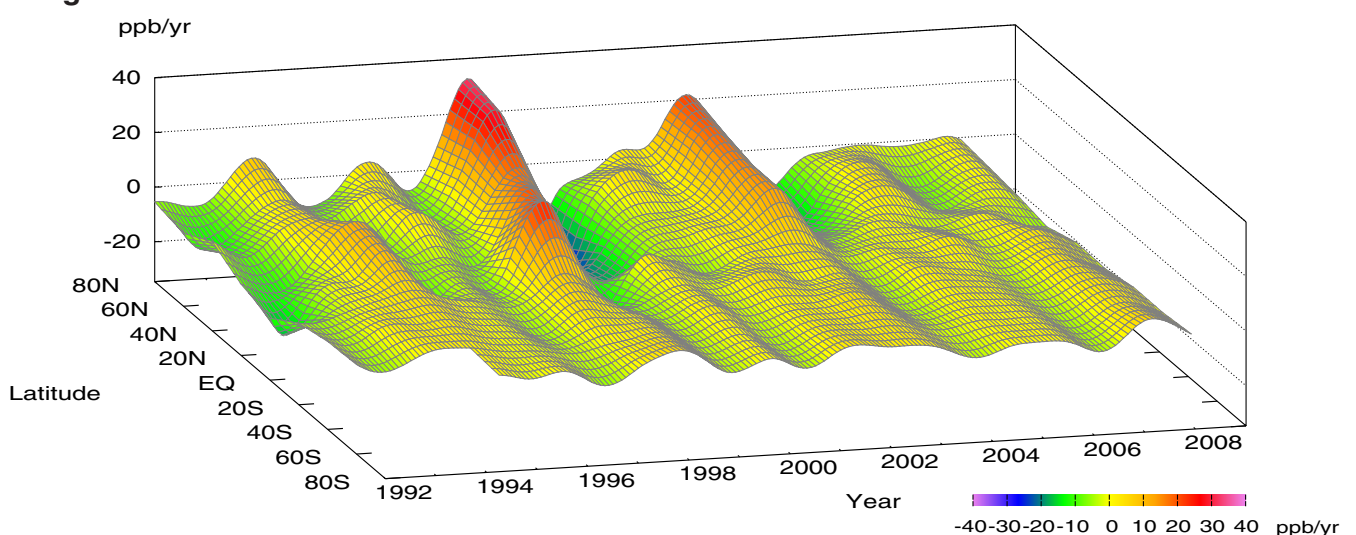


**Plate 8.2** Variation of zonally averaged monthly mean CO mole fractions (top), deseasonalized long-term trends (middle), and growth rates (bottom). The zonally averaged mole fractions are calculated for each  $20^{\circ}$  zone. The deseasonalized trends and growth rates are derived as described in Chapter 2.

## 8. CARBON MONOXIDE (CO)

### Basic information on CO with regard to environmental issues

Carbon monoxide (CO) is not a greenhouse gas; it absorbs hardly any infrared radiation from the Earth. However, CO influences oxidation capacity of the atmosphere through interaction with hydroxyl radicals (OH), which react with methane, halocarbons and tropospheric ozone. CO has been monitored noting its indirect influence on greenhouse gases through such reactions.

Sources of atmospheric CO include fossil fuel combustion and biomass burning, along with the oxidation of natural and anthropogenic methane and non-methane hydrocarbons (NMHC). Major sinks include reactions with OH and surface deposition. CO has a relatively long atmospheric lifetime, ranging from 10 days in summer in the tropics to more than a year over polar regions in winter. So, unlike CO<sub>2</sub>, anthropogenic CO emission does not lead to CO accumulation in the atmosphere. Furthermore, the uneven distribution of sources causes large spatial and temporal variations in the amount of CO.

Measurements of trapped air in ice cores reveal that the CO mole fraction over central Antarctica during the last two millennia was about 50 ppb, increasing to 110 ppb by 1950 in Greenland (Haan and Raynaud, 1998). Beginning in 1950, the CO mole fraction increased at a rate of 1% per year but started to decrease in the late 1980s (WMO, 1999). Between 1991 and 2001, the global average mole fraction of CO decreased at a rate of about 0.5 ppb per year, excluding temporal enhancements from large biomass burning (Novelli *et al.*, 2003).

### Annual variation of CO mole fraction in the atmosphere

The monthly mean mole fractions of CO that have been reported from fixed stations and some ships to the WDCGG are shown in Plate 8.1, in which different mole fraction levels are illustrated in different colours. The observational sites whose data are used for the analysis are shown on the map at the beginning of this chapter.

Latitudinally averaged mole fractions of CO in the atmosphere, together with their deseasonalized mole fractions and growth rates are shown in Plate 8.2 as three-dimensional representations.

Data for the mole fraction of CO are reported in various units, *i.e.*, ppb,  $\mu\text{g}/\text{m}^3$ -25°C,  $\mu\text{g}/\text{m}^3$ -20°C and  $\text{mg}/\text{m}^3$ -25°C. Units other than ppb are converted to ppb using the formulas:

$$X_p [\text{ppb}] = (R \times T / M / P_0) \times 10 \times X_g [\mu\text{g}/\text{m}^3]$$

$$X_p [\text{ppb}] = (R \times T / M / P_0) \times 10^4 \times X_g [\text{mg}/\text{m}^3]$$

where R is the molar gas constant (8.31451 [J/K/mol]),

T is the absolute temperature as reported from the station,

M is the molecular weight of CO (28.0101), and

P<sub>0</sub> is the standard pressure (1013.25 [hPa]).

Plate 8.2 shows that the seasonal variations of CO are large in the Northern Hemisphere and small in the Southern Hemisphere, and that the deseasonalized mole fractions are the highest in northern mid-latitudes and the lowest in the Southern Hemisphere. The latitudinal gradient of CO is large from northern mid-to southern low latitudes, and is small in the Southern Hemisphere. This is due to the presence of numerous CO sources in the northern mid-latitudes, combined with the destruction of CO in the Tropics, where OH radicals are abundant.

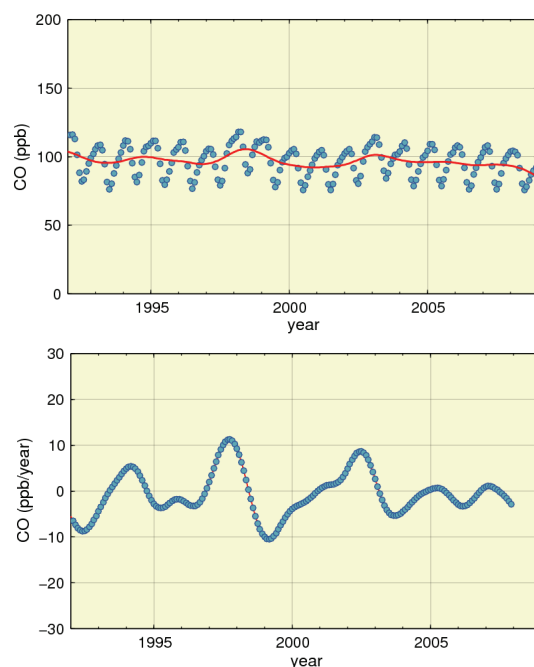


Fig. 8.1 Global monthly mean mole fraction of CO from 1992 to 2008 with deseasonalized long-term trend in red line (top) and its growth rate (bottom).

Figure 8.1 shows global monthly mean CO mole fractions and their growth rates. The growth rate was high in 1993/1994, 1997/1998 and 2002, and low in 1992 and 1998/1999. The global annual mean mole fraction was about 91 ppb in 2008, as calculated without regarding different observation scales, but may

be affected by the latter ones.

Figure 8.2 shows monthly mean mole fractions of CO for each  $30^{\circ}$  latitudinal zone. Seasonal variations are seen in both hemispheres. The mole fractions are higher in winter. Amplitudes of the seasonal cycle are larger in the Northern Hemisphere than in the Southern Hemisphere.

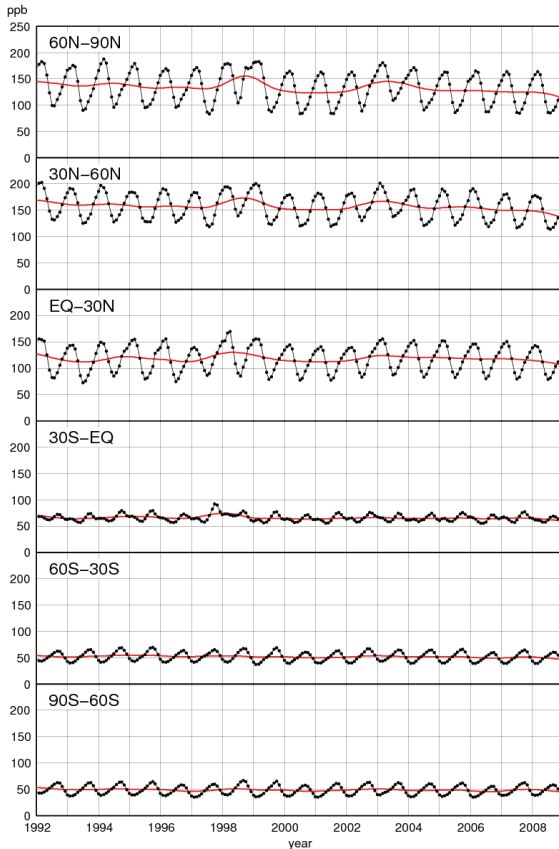


Fig. 8.2 Monthly mean mole fractions of CO from 1992 to 2008 for each  $30^{\circ}$  latitudinal zone (dots) and their deseasonalized long-term trends (red lines).

Figure 8.3 summarizes deseasonalized long-term trends for each  $30^{\circ}$  latitudinal zone and their growth rates. The CO mole fractions are the highest in northern mid-latitudes. There is a decline in CO mole fractions around 1992, which almost coincided with a decrease in the growth rate of  $\text{CH}_4$  mole fraction, most likely due to variations in their common sinks. The enhanced stratospheric ozone depletion due to increased volcanic aerosols following the eruption of Mt. Pinatubo in 1991 may have led to increased OH radicals, which react with both CO and  $\text{CH}_4$  (Dlugokencky *et al.*, 1996).

Increases in CO mole fractions were observed from 1997 to 1998 in northern latitudes and in southern low latitudes. These increases were attributed to large biomass burnings around Indonesia in late 1997 and around Siberia in the summer and autumn of 1998 (Novelli *et al.*, 1998).

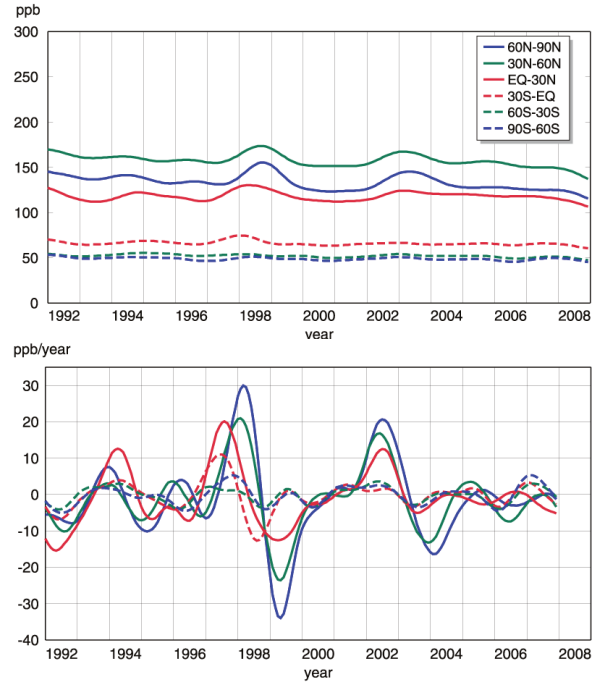


Fig. 8.3 Deseasonalized long-term trends of CO for each  $30^{\circ}$  latitudinal zone (top) and their growth rates (bottom).

The CO mole fractions returned to normal after 1999, but the growth rates in the Northern Hemisphere increased substantially again in 2002. The latter might also be attributed to a large biomass burning. Large-scale boreal forest fires occurred in Siberia and North America from 2002 to 2003.

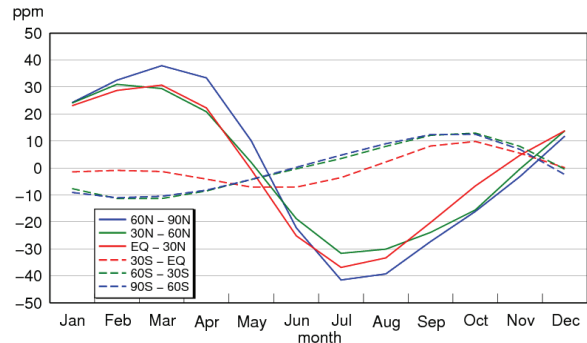


Fig. 8.4 Average seasonal cycles in the mole fraction of CO for each  $30^{\circ}$  latitudinal zone obtained by subtracting long-term trends.

### Seasonal cycle of CO mole fraction in the atmosphere

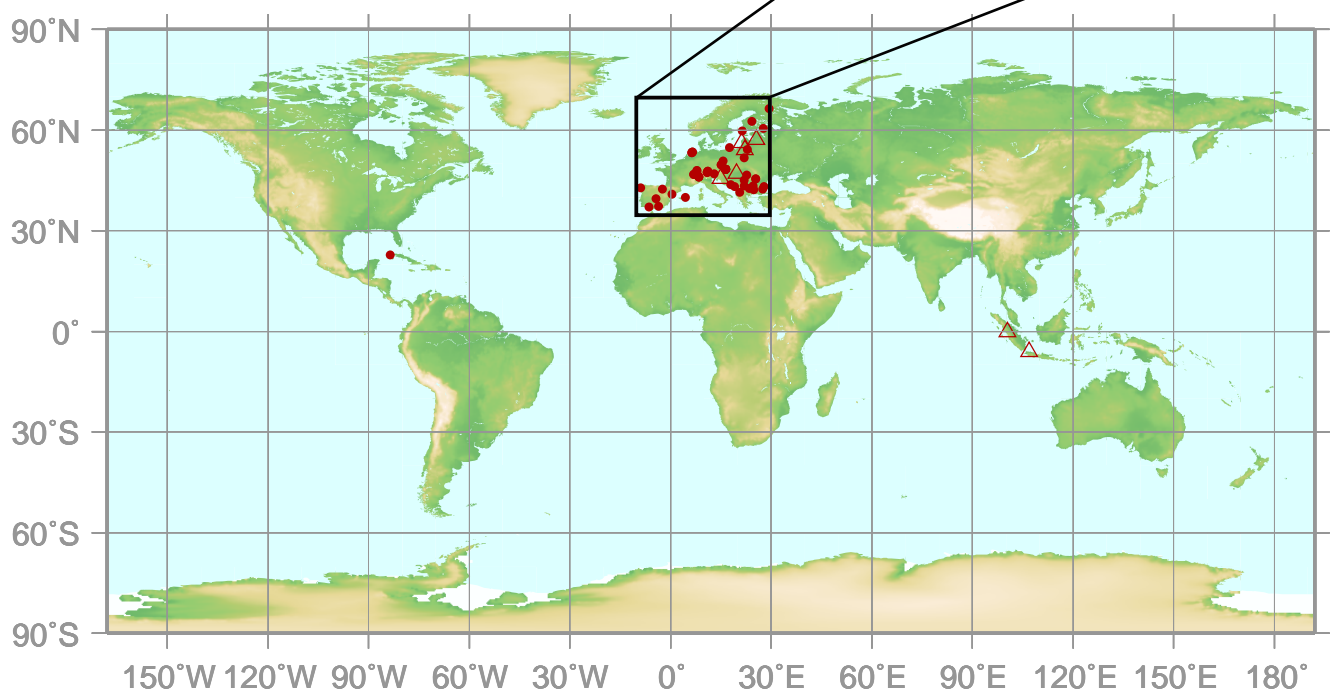
Figure 8.4 shows average seasonal cycles in the mole fraction of CO for each  $30^{\circ}$  latitudinal zone. The seasonal cycle is mainly driven by seasonal variations in OH abundance as a CO sink. Additional factors include emission and oxidation from CO sources and large-scale transport of CO, despite a relatively weak seasonality in emission and oxidation compared with OH abundance. This seasonality and

a short lifetime of about a few months produce a sharp decrease in early summer followed by a relatively slow increase in autumn. Biannual peaks evident in the southern low latitudes may be attributed to the transport of CO from the Northern Hemisphere.

# 9.

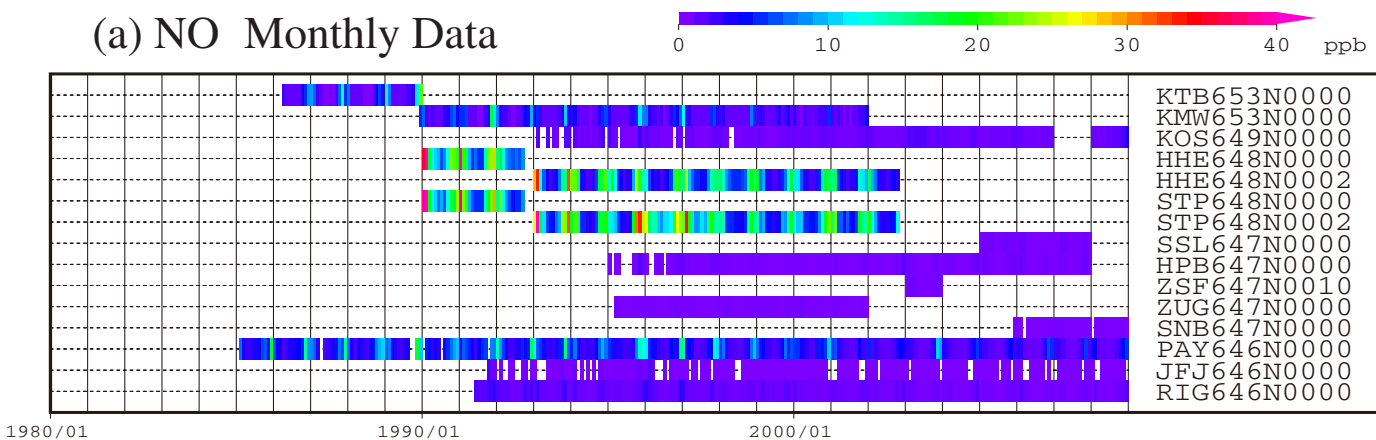
## NITROGEN MONOXIDE (NO) AND NITROGEN DIOXIDE (NO<sub>2</sub>)

- : CONTINUOUS STATION
- △ : FILTER STATION



This map shows locations of the stations that have submitted data for monthly mean mole fraction.

(a) NO Monthly Data



(b) NO<sub>2</sub> Monthly Data

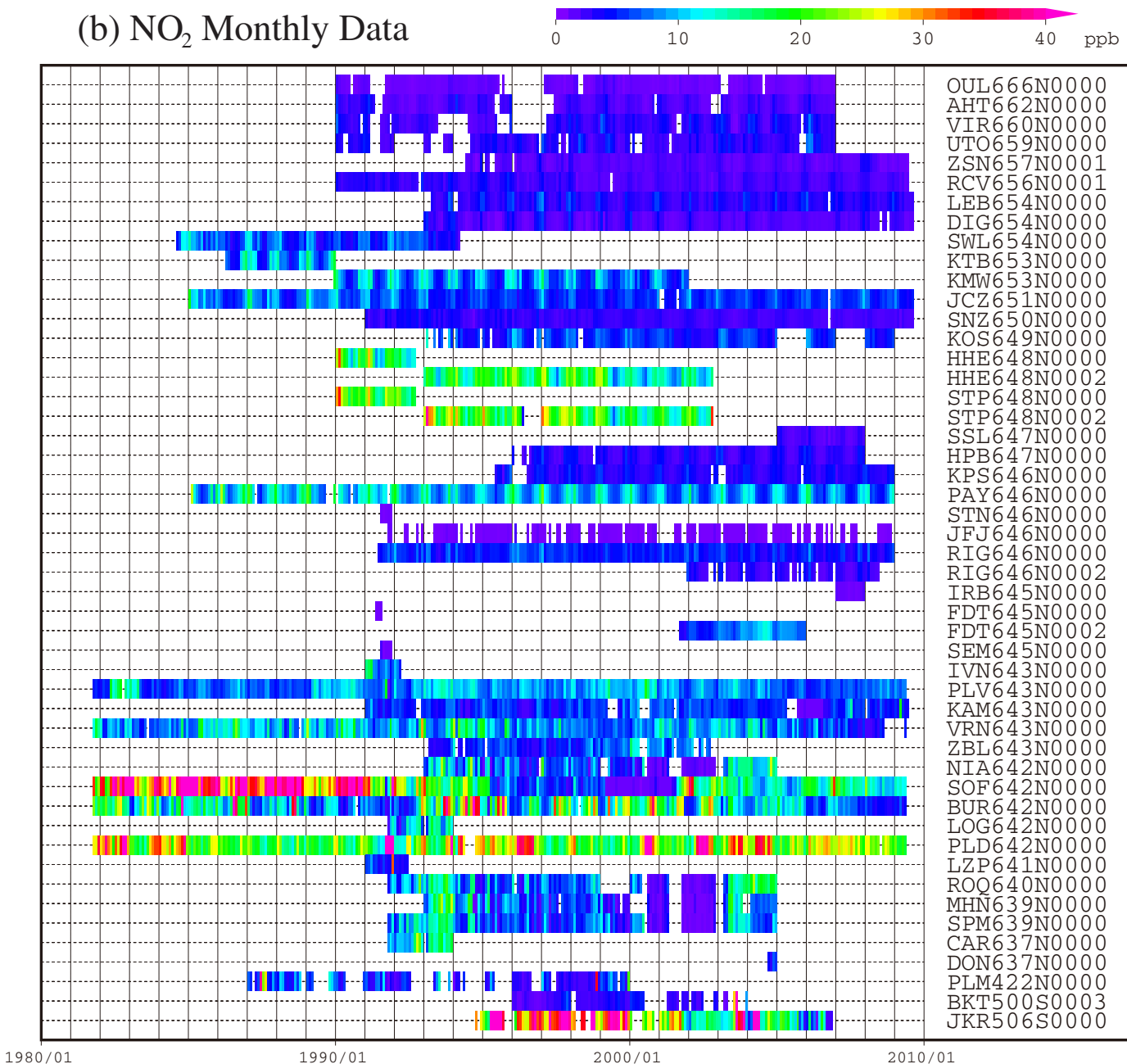


**Plate 9.1** Monthly mean (a) NO and (b) NO<sub>2</sub> mole fractions that have been reported to the WDCGG. The mole fractions are illustrated in different colors. The sites are listed in order from north to south.

## 9. NITROGEN MONOXIDE (NO) AND NITROGEN DIOXIDE (NO<sub>2</sub>)

### Basic information on NO and NO<sub>2</sub> with regard to environmental issues

Nitrogen oxides (NO<sub>x</sub>, *i.e.*, NO and NO<sub>2</sub>) are not greenhouse gases. Nevertheless these compounds have a central regulatory role in the free radical and oxidizing photochemistry of the troposphere. This photochemistry regulates the lifetime of methane and the production of tropospheric ozone and secondary aerosol, all of which have important roles in the natural and anthropogenic greenhouse effect. The ozone produced in the atmosphere as a result of these nitrogen oxides can affect vegetation growth and human health.

Sources of NO<sub>x</sub> include fertilizer use, fossil fuel combustion, biomass burning, lightning and soil (IPCC, 2007). The dominant sink of NO<sub>x</sub> in the atmosphere is its conversion into nitric acid (HNO<sub>3</sub>) and peroxyacetyl nitrate (PAN), which are eventually removed by dry or wet deposition. In some cases, NO<sub>x</sub> is removed from the atmosphere directly by dry deposition. Anthropogenic emission of NO<sub>x</sub> is currently one of the major causes of acid rain and deposition. The NO<sub>x</sub> mole fractions show a large variability in both space and time because of their short lifetimes and uneven source distribution.

### Annual variation of NO and NO<sub>2</sub> mole fractions in the atmosphere

The observational stations that have submitted data for NO and NO<sub>2</sub> to the WDCGG are shown on the map at the beginning of this chapter. Most of these stations are located in Europe.

The monthly mean mole fractions of NO and NO<sub>2</sub> that have been reported to the WDCGG are shown in Plate 9.1, in which different mole fraction levels are illustrated in different colours. Data for NO<sub>x</sub> are reported in various units, *i.e.*, ppb, µg/m<sup>3</sup>-25°C, µg/m<sup>3</sup>-20°C, µgN/m<sup>3</sup>-25°C and mg/m<sup>3</sup>-25°C. Units other than ppb are converted to ppb using the formulas:

$$\begin{aligned} X_p [\text{ppb}] &= (R \times T / M / P_0) \times 10 \times X_g [\mu\text{g}/\text{m}^3] \\ X_p [\text{ppb}] &= (R \times T / M / P_0) \times 10^4 \times X_g [\text{mg}/\text{m}^3] \\ X_p [\text{ppb}] &= (R \times T / M_N / P_0) \times 10 \times X_g [\mu\text{gN}/\text{m}^3] \end{aligned}$$

where R is the molar gas constant (8.31451 [J/K/mol]),

T is the absolute temperature as reported from the station,

M is the molecular weight of NO (30.00614) or NO<sub>2</sub> (46.00554),

M<sub>N</sub> is the atomic weight of N (14.00674), and

P<sub>0</sub> is the standard pressure (1013.25 [hPa]).

The localised sources and short lifetimes of NO and NO<sub>2</sub> make their distributions spatially non-uniform and variable over time. Due to the high temporal variability in the mole fraction of NO<sub>2</sub> at each observation site, it was difficult to identify a long-term trend. A number of stations located in southern Europe showed higher mole fractions, and some stations reported an enhancement of NO<sub>2</sub> in winter.

As there are few observational sites for NO, it is difficult to identify increasing or decreasing trends for NO mole fractions.

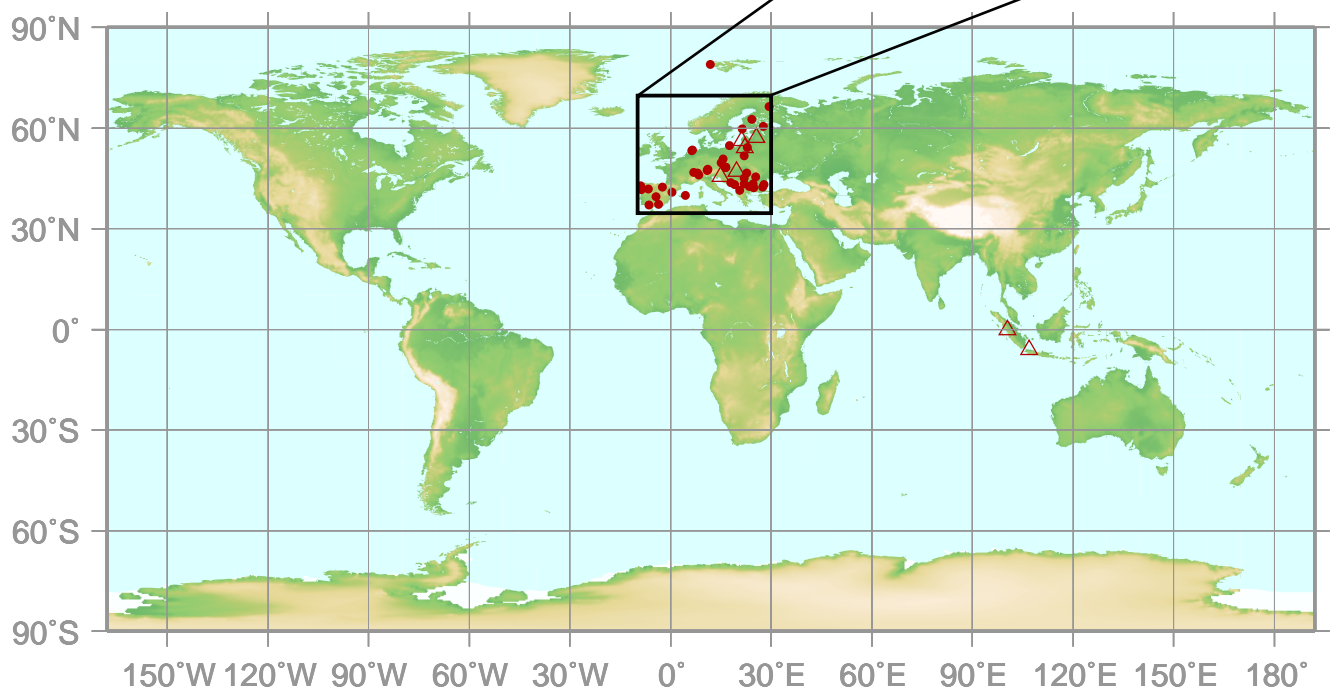


# 10.

## SULPHUR DIOXIDE

### (SO<sub>2</sub>)

- : CONTINUOUS STATION
- △ : FILTER STATION



This map shows locations of the stations that have submitted data for monthly mean mole fraction.

## SO<sub>2</sub> Monthly Data

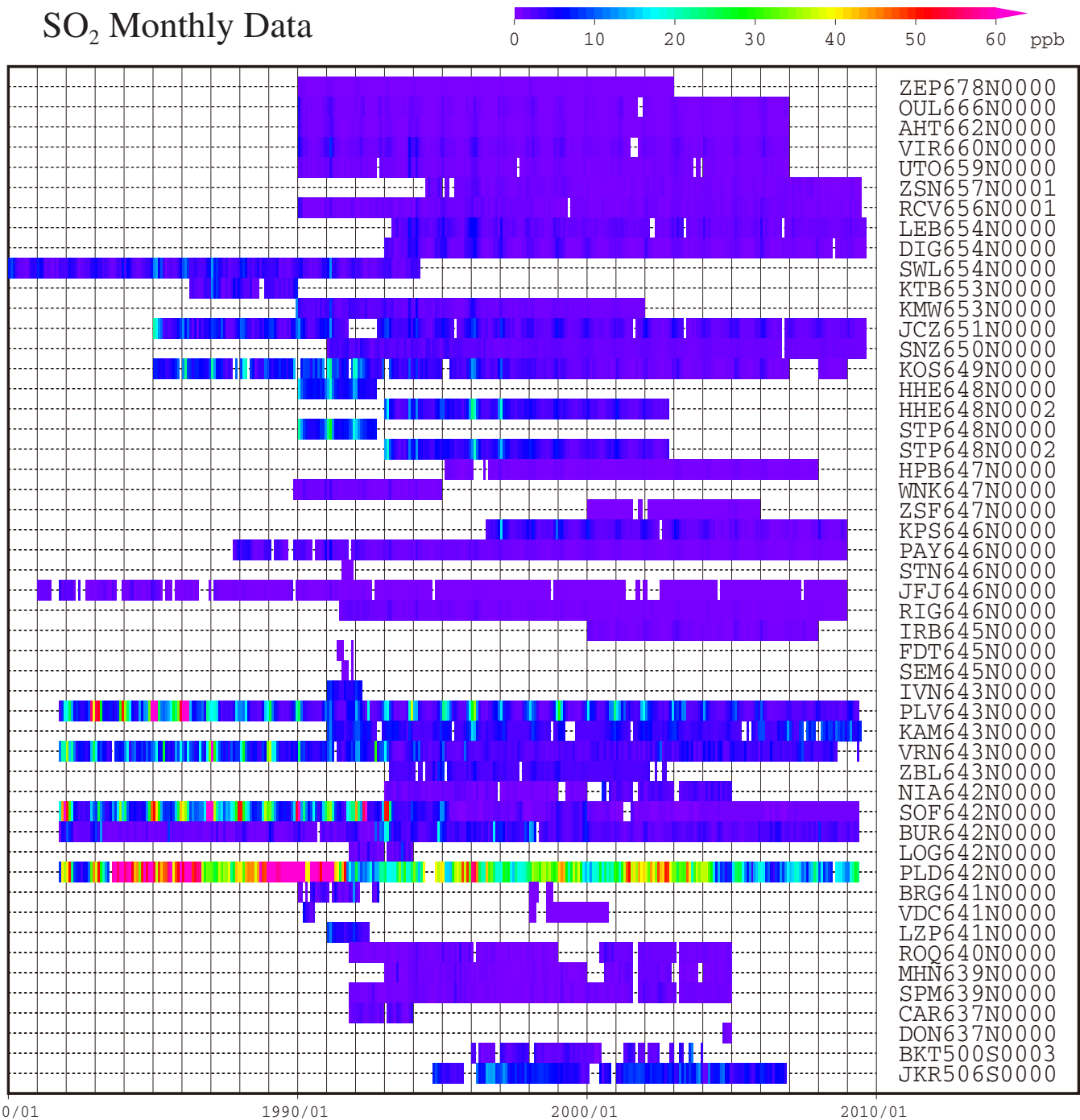


**Plate 10.1** Monthly mean SO<sub>2</sub> mole fractions that have been reported to the WDCGG. The mole fractions are illustrated in different colors. The sites are listed in order from north to south.

## 10. SULPHUR DIOXIDE (SO<sub>2</sub>)

### Basic information on SO<sub>2</sub> with regard to environmental issues

Sulphur dioxide (SO<sub>2</sub>) is not a greenhouse gas, but is a precursor of atmospheric sulphuric acid (H<sub>2</sub>SO<sub>4</sub>) and sulphate aerosol. SO<sub>2</sub> is oxidised by hydroxyl radicals (OH) to form sulphuric acid, which then becomes aerosols through photochemical gas-to-particle conversion. While SO<sub>2</sub> reacts much more slowly with OH than does NO<sub>2</sub>, SO<sub>2</sub> dissolves readily in suspended liquid droplets in the atmosphere. The global sulphur cycle affects atmospheric chemistry, including tropospheric ozone (Berglen *et al.*, 2004).

Sources of SO<sub>2</sub> include fossil fuel combustion by industry, biomass burning, volcanic release and the oxidation of dimethylsulphide (DMS) from the oceans (IPCC, 2007). Major SO<sub>2</sub> sinks are oxidation by OH and deposition onto wet surfaces. Anthropogenic SO<sub>2</sub> has caused acid rain and deposition throughout the industrial era. The mole fractions of SO<sub>2</sub> show large variations in both space and time because of its short lifetime and uneven anthropogenic source distribution.

### Annual variation of SO<sub>2</sub> mole fraction in the atmosphere

The observational sites that have submitted data for SO<sub>2</sub> to the WDCGG are shown on the map at the beginning of this chapter. Most of these stations are located in Europe.

The monthly mean mole fractions of SO<sub>2</sub> that have been reported to the WDCGG are shown in Plate 10.1, with different mole fraction levels illustrated in different colours. Data for SO<sub>2</sub> are reported in various units, *i.e.*, ppb, µg/m<sup>3</sup>, mg/m<sup>3</sup> and µgS/m<sup>3</sup>. Units other than ppb are converted to ppb using the formulas:

$$X_p \text{ [ppb]} = (R \times T / M / P_0) \times 10 \times X_g \text{ [\mu g/m}^3\text{]}$$
$$X_p \text{ [ppb]} = (R \times T / M / P_0) \times 10^4 \times X_g \text{ [mg/m}^3\text{]}$$
$$X_p \text{ [ppb]} = (R \times T / M_S / P_0) \times 10 \times X_g \text{ [\mu gS/m}^3\text{]}$$

where R is the molar gas constant (8.31451 [J/K/mol]),  
T is the absolute temperature as reported from the station,  
M is the molecular weight of SO<sub>2</sub> (64.0648),  
M<sub>S</sub> is the atomic weight of S (32.066), and  
P<sub>0</sub> is the standard pressure (1013.25 [hPa]).

Although some stations in southern Europe have reported higher mole fractions, it has been difficult to identify an increasing or decreasing trend for SO<sub>2</sub>.



# **REFERENCES**

## References

- Angert A., S. Biraud, C. Bonfils, W. Buermann, I. Fung, CO<sub>2</sub> seasonality indicates origins of post-Pinatubo sink, *Geophys. Res. Lett.*, **31**, L11103, doi:10.1029/2004GL019760, 2004.
- Bekki, S., K. S. Law, and J. A. Pyle, Effects of ozone depletion on atmospheric CH<sub>4</sub> and CO concentrations, *Nature*, **371**, 595–597, 1994.
- Berglen, T. F., T. K. Berntsen, I. S. A. Isaksen, and J. K. Sundet, A global model of the coupled sulfur/oxidant chemistry in the troposphere: The sulfur cycle, *J. Geophys. Res.*, **109**, D19310, doi:10.1029/2003JD003948, 2004.
- Boden, T. A., G. Marland, and R. J. Andres, Global, Regional, and National Fossil-Fuel CO<sub>2</sub> Emissions. Carbon Dioxide Information Analysis Center, Oak Ridge National Laboratory, U.S. Department of Energy, Oak Ridge, Tenn., U.S.A., doi: 10.3334/CDIAC/00001, 2009.
- Cleveland, W. S., S. J. Devlin, Locally weighted regression: an approach to regression analysis by local fitting, *J. Amer. Statist. Assn.*, **83**, 596–610, 1988.
- Conway, T. J., P. P. Tans, L. S. Waterman, K. W. Thoning, D. R. Kitzis, K. A. Masarie, and N. Zhang, Evidence for interannual variability of the carbon cycle from the National Oceanic and Atmospheric Administration/Climate Monitoring and Diagnostics Laboratory global air sampling network, *J. Geophys. Res.*, **99**, 22831–22855, 1994.
- Denman, K. L., G. Brasseur, A. Chidthaisong, P. Ciais, P. M. Cox, R. E. Dickinson, D. Hauglustaine, C. Heinze, E. Holland, D. Jacob, U. Lohmann, S. Ramachandran, P. L. da Silva Dias, S. C. Wofsy and X. Zhang, 2007: Couplings Between Changes in the Climate System and Biogeochemistry. In: Climate Change 2007: The Physical Science Basis. Contribution of Working Group I to the Fourth Assessment Report of the Intergovernmental Panel on Climate Change [Solomon, S., D. Qin, M. Manning, Z. Chen, M. Marquis, K. B. Averyt, M. Tignor and H. L. Miller (eds.)]. Cambridge University Press, Cambridge, United Kingdom and New York, NY, USA.
- Dettinger, M. D. and M. Ghill, Seasonal and interannual variations of atmospheric CO<sub>2</sub> and climate, *Tellus*, **50B**, 1–24, 1998.
- Dlugokencky, E. J., L. P. Steele, P. M. Lang, and K. A. Masarie, The growth rate and distribution of atmospheric methane, *J. Geophys. Res.*, **99**, 17021–17043, 1994.
- Dlugokencky, E. J., E. G. Dutton, P. C. Novelli, P. P. Tans, K. A. Masarie, K. O. Lantz, and S. Mardronich, Changes in CH<sub>4</sub> and CO growth rates after the eruption of Mt. Pinatubo and their link with changes in tropical tropospheric UV flux, *Geophys. Res. Lett.*, **23**, 2761–2764, 1996.
- Dlugokencky, E. J., B. P. Walter, K. A. Masarie, P. M. Lang and E. S. Kasischke, Measurements of an anomalous global methane increase during 1998, *Geophys. Res. Lett.*, **28**, 499–502, 2001.
- Dlugokencky, E. J., L. Bruhwiler, J. W. C. White, L. K. Emmons, P. C. Novelli, S. A. Montzka, K. A. Masarie, P. M. Lang, A. M. Crotwell, J. B. Miller, and L. V. Gatti Observational constraints on recent increases in the atmospheric CH<sub>4</sub> burden, *Geophys. Res. Lett.*, **36**, L18803, 2009.
- Duchon, C. E., Lanczos filtering in one and two dimensions, *J. Appl. Meteor.*, **18**, 1016–1022, 1979.
- Etheridge, D. M., L. P. Steele, R. J. Francey, and R. L. Langenfelds, Atmospheric methane between 1000 A.D. and present: Evidence of anthropogenic emissions and climatic variability, *J. Geophys. Res.*, **103**, 15979–15993, 1998.
- Francey, R. J., P. P. Tans, C. E. Allison, I. G. Enting, J. W. C. White, and M. Trolier, Changes in oceanic and terrestrial carbon uptake since 1982, *Nature*, **373**, 326–330, 1995.
- Gu, L., D. D. Baldocchi, S. C. Wofsy, J. W. Munger, J. J. Michalsky, S. P. Urbanski, and T. A. Bonden, Response of a deciduous forest to the Mount Pinatubo eruption enhanced photosynthesis, *Science*, **299**, 2035–2038, 2003.
- Haan, D. and D. Raynaud, Ice core record of CO variations during the last two millennia: atmospheric implications and chemical interactions within the Greenland ice, *Tellus*, **50B**, 253–262, 1998.
- Hansen, J., A. Lacis, R. Ruedy, and M. Sato, Potential Clim. Impact of Mount-Pinatubo Eruption, *Geophys. Res. Lett.*, **19(2)**, 215–218, 1992.
- IPCC, Climate Change 2001: The Science Basis, Contribution of Working Group I to the Third Assessment Report of the Intergovernmental Panel on Climate Change, Cambridge University Press, Cambridge, United Kingdom and New York, NY, USA, 881pp, 2001.
- IPCC, Climate Change 2007: The Physical Science Basis. Contribution of Working Group I to the Fourth Assessment Report of the Intergovernmental Panel on Climate Change [Solomon, S., D. Qin, M. Manning, Z. Chen, M. Marquis, K. B. Averyt, M. Tignor and H. L. Miller(eds.)]. Cambridge University Press, Cambridge, United Kingdom and New York, NY, USA, 2007.
- Keeling, C. D., R. B. Bacastow, A. F. Carter, S. C. Piper, T. P. Whorf, M. Heimann, W. G. Mook, and H. Roeloffzen, A three-dimensional model of atmospheric CO<sub>2</sub> transport based on observed

- winds: 1. Analysis of observational data, in aspects of climate variability in the Pacific and the Western Americas, edited by D. H. Peterson, *Geophysical Monograph* **55**, 165–236, American Geophysical Union, Washington, D.C, 1989.
- Keeling, C. D., T. P. Whorf, M. Wahlen, and J. van der Plicht, Interannual extremes in the rate of rise of atmospheric carbon dioxide since 1980, *Nature*, **375**, 666–670, 1995.
- Lambert, G., P. Monfray, B. Ardouin, G. Bonsang, A. Gaudry, V. Kazan and G. Polian, Year-to-year changes in atmospheric CO<sub>2</sub>, *Tellus*, **47B**, 35–55, 1995.
- Marenco, A., and F. Said: Meridional and vertical ozone distribution in the background troposphere from Scientific aircraft measurements during the STRATOZ III experiment. *Atmos. Env.*, **23**, 201–214, 1989.
- Matsueda, H., S. Taguchi, H.Y. Inoue, and M. Ishii, A large impact of tropical biomass burning on CO and CO<sub>2</sub> in the upper troposphere. *Science in China (Series C)*, **45**, 116–125, 2002.
- Morimoto, S., S. Aoki, T. Nakazawa, and T. Yamanouchi, Temporal variations of the carbon isotopic ratio of atmospheric methane observed at Ny Alesund, Svalbard from 1996 to 2004, *Geophys. Res. Lett.*, **33**, L01807, doi:10.1029/2005GL024648, 2006.
- Nakazawa, T., K. Miyashita, S. Aoki, and M. Tanaka, Temporal and spatial variations of upper tropospheric and lower stratospheric carbon dioxide, *Tellus*, **43B**, 106–117, 1991.
- Nakazawa, T., S. Morimoto, S. Aoki and M. Tanaka, Time and space variations of the carbon isotopic ratio of tropospheric carbon dioxide over Japan, *Tellus*, **45B**, 258–274, 1993.
- Nakazawa, T., S. Morimoto, S. Aoki and M. Tanaka, Temporal and spatial variations of the carbon isotopic ratio of atmospheric carbon dioxide in the western Pacific region, *J. Geophys. Res.*, **102**, 1271–1285, 1997.
- Novelli, P. C., K. A. Masarie, and P. M. Lang, Distributions and recent changes of carbon monoxide in the lower troposphere, *J. Geophys. Res.*, **103**, 19015–19033, 1998.
- Novelli, P. C., K. A. Masarie, P. M. Lang, B. D. Hall, R. C. Myers, and J. W. Elkins, Reanalysis of tropospheric CO trends: Effects of the 1997–1998 wildfires. *J. Geophys. Res.*, **108(D15)**, 4464, doi:10.1029/2002JD003031, 2003.
- Oltmans et al., Long-term changes in tropospheric ozone, *Atmos. Env.*, **40**, 3156–3173, 2006.
- Onogi, J. K., Tsutsui, H. Koide, M. Sakamoto, S. Kobayashi, H. Hatsushika, T. Matsumoto, N. Yamazaki, H. Kamahori, K. Takahashi, S. Kadokura, K. Wada, K. Kato, R. Oyama, T. Ose, N. Manojoji, and R. Taira, The JRA-25 Reanalysis, *Journal of the Meteorological Society of Japan*, **85**, No.3, 369–432, 2007.
- Prinn, R. G., J. Huang, R. F. Weiss, D. M. Cunnold, P. J. Fraser, P. G. Simmonds, A. McCulloch, C. Harth, P. Salameh, S. O'Doherty, R. H. J. Wang, L. Porter and B. R. Miller, Evidence for substantial variations of atmospheric hydroxyl radicals in the past two decades, *Science*, **292**, 1882–1888, 2001.
- Rayner, P. J., I. G. Enting, R. J. Francey and R. Langenfelds, Reconstructing the recent carbon cycle from atmospheric CO<sub>2</sub>, δ<sup>13</sup>C and O<sub>2</sub>/N<sub>2</sub> observations, *Tellus*, **51B**, 213–232, 1999.
- Ramonet, M. and P. Monfray, CO<sub>2</sub> baseline concept in 3-D atmospheric transport models, *Tellus*, **48B**, 502–520, 1996.
- Rigby, M., R. G. Prinn, P. J. Fraser, P. G. Simmonds, R. L. Langenfelds, J. Huang, D. M. Cunnold, L. P. Steele, P. B. Krummel, R. F. Weiss, S. O'Doherty, P. K. Salameh, H. J. Wang, C. M. Harth, J. Mühlé, and L. W. Porter, Renewed growth of atmospheric methane, *Geophys. Res. Lett.*, **35**, L22805, doi:10.1029/2008GL036037, 2008.
- Shindell, D., G. Faluvegi, A. Lacis, J. Hansen, R. Ruedy, and E. Aguilar, Role of tropospheric ozone increases in 20th-century climate change, *J. Geophys. Res.*, **111**, D08302, doi:10.1029/2005JD006348, 2006.
- Solomon, S., D. Qin, M. Manning, R.B. Alley, T. Berntsen, N.L. Bindoff, Z. Chen, A. Chidthaisong, J.M. Gregory, G.C. Hegerl, M. Heimann, B. Hewitson, B.J. Hoskins, F. Joos, J. Jouzel, V. Kattsov, U. Lohmann, T. Matsuno, M. Molina, N. Nicholls, J. Overpeck, G. Raga, V. Ramaswamy, J. Ren, M. Rusticucci, R. Somerville, T.F. Stocker, P. Whetton, R.A. Wood and D. Wratt, Technical Summary. In: Climate Change 2007: The Physical Science Basis. Contribution of Working Group I to the Fourth Assessment Report of the Intergovernmental Panel on Climate Change [Solomon, S., D. Qin, M. Manning, Z. Chen, M. Marquis, K.B. Averyt, M. Tignor and H.L. Miller (eds.)]. Cambridge University Press, Cambridge, United Kingdom and New York, NY, USA., 2007.
- Staehelin, J., J. Thudium, R. Buehler, A. Voltz-Thomas, and W. Graber, Trends in surface ozone concentrations at Arosa (Switzerland), *Atmos. Env.*, **28**, 75–87, 1994.
- Stenchikov, G., A. Robock, V. Ramaswamy, M. D. Schwarzkopf, K. Hamilton, and S. Ramachandran, Arctic Oscillation response to the 1991 Mount Pinatubo eruption: Effects of volcanic aerosols and ozone depletion, *J. Geophys. Res.*, **107(D24)**, 4803, doi:10.1029/2002JD002090., 2002.
- Tarasova, O. A., C.A. M. Brenninkmeijer, P. Jöckel, A. M. Zvyagintsev, and G.I. Kuznetsov: A climatology of surface ozone in the extra tropics: cluster analysis of observations and model results. *Atmos.*

- Chem. Phys.*, **7**, 6099–6117, 2007.
- Tsutsumi, Y., Y. Makino, and J. B. Jensen: Vertical and latitudinal distributions of tropospheric ozone over the western Pacific: Case studies from the PACE aircraft missions. *J. Geophys. Res.*, **108(D8)**, 4251, doi:10.1029/2001JD001374, 2003.
- Thoning, K. W., P. P. Tans, and W. D. Komhyr, Atmospheric carbon dioxide at Mauna Loa observatory, 2. Analysis of the NOAA GMCC data, 1974–1985, *J. Geophys. Res.*, **94**, 8549–8565, 1989.
- Wittenberg, U., M. Heimann, G. Esser, A.D. McGuire, and W. Sauf, On the influence of biomass burning on the seasonal CO<sub>2</sub> signal as observed at monitoring stations, *Global Biogeochem. Cycles*, **12**, 531–544, 1998.
- WMO, Scientific assessment of ozone depletion: 1998. WMO global ozone research and monitoring project—Report No. 44, World Meteorological Organization, Geneva, 1999.
- WMO, World Data Centre for Greenhouse Gases (WDCGG) Data Summary, WDCGG No. 22, 84pp, 2000.
- WMO, Global Atmospheric Watch (GAW) Strategic Plan: 2008–2015, GAW Report No. 172, WMO TD No. 1384, 2007a.
- WMO, World Data Centre for Greenhouse Gases Data Submission and Dissemination Guide, GAW Report No. 174, WMO TD No. 1416, 2007b.
- WMO, Technical Report of Global Analysis Method for Major Greenhouse Gases by the World Data Center for Greenhouse Gases, GAW Report No. 184, WMO/TD - No. 1473, 2009a.
- WMO, WMO Greenhouse Gas Bulletin No.5, 2009b.  
([http://www.wmo.int/pages/prog/arep/gaw/ghg/GH\\_Gbulletin.html](http://www.wmo.int/pages/prog/arep/gaw/ghg/GH_Gbulletin.html), accessed 12 Feb. 2010)
- WMO, Revision of the World Data Centre for Greenhouse Gases Data Submission and Dissemination Guide, GAW Report No. 188, 2009c.  
([http://www.wmo.int/pages/prog/arep/gaw/documents/GAW\\_188\\_web\\_20100128.pdf](http://www.wmo.int/pages/prog/arep/gaw/documents/GAW_188_web_20100128.pdf), accessed 1 Mar. 2010)

# **APPENDICES**

# CALIBRATION AND STANDARD SCALES

## 1. Calibration System in the GAW programme

Under the Global Atmosphere Watch (GAW) programme, the World Calibration Centres (WCCs) are responsible for maintaining calibration standards for certain compounds, establishing instrument calibrations and providing training to the stations. A Reference Standard is designated for each variable to be used for all GAW measurements of that variable at

the Central Calibration Laboratories. Table 1 lists the organizations that serve as WCCs and CCLs for GAW [WMO, 2007]. For CFCs and SO<sub>2</sub>, no central facilities or quality control systems have so far been established within the GAW programme, while central facilities for NO<sub>x</sub> have only recently been formulated.

**Table 1. Overview of the GAW Central Calibration Laboratories (GAW-CCL, Reference Standard) and World Calibration Centres for greenhouse and other related gases. The World Calibration Centres have assumed global responsibilities, except where indicated (Am, Americas; E/A, Europe and Africa; A/O, Asia and the South-West Pacific)**

Compounds	Central Calibration Laboratory (Host of Primary Standard)	World Calibration Centre
Carbon Dioxide (CO <sub>2</sub> )	NOAA/GMD	NOAA/GMD
Methane (CH <sub>4</sub> )	NOAA/GMD	EMPA (Am, E/A) JMA (A/O)
Nitrous Oxide (N <sub>2</sub> O)	NOAA/GMD	IMK-IFU
Chlorofluorocarbons (CFCs)		
Surface Ozone (O <sub>3</sub> )	NIST	EMPA
Carbon Monoxide (CO)	NOAA/GMD	EMPA
Volatile Organic Compounds (VOCs)		IMK-IFU
Sulphur Dioxide (SO <sub>2</sub> )		
Nitrogen Oxides (NO <sub>x</sub> )		

## 2. Carbon Dioxide (CO<sub>2</sub>)

In 1995, the Global Monitoring Division of the National Oceanic and Atmospheric Administration's Earth System Research Laboratory (NOAA/GMD, formerly CMDL) in Boulder, Colorado, USA took over the role of the Central Calibration Laboratory (CCL) from the Scripps Institution of Oceanography (SIO) in San Diego, California, USA. Since then, NOAA/GMD has served as the CCL responsible for the maintenance of the GAW Primary Standard for CO<sub>2</sub>. As the World Calibration Centre (WCC) for CO<sub>2</sub>, NOAA/GMD maintains a high-precision manometric system for absolute calibration of CO<sub>2</sub> as the reference for GAW measurements throughout the world [Zhao *et al.*, 1997]. It is recommended that the standards of the GAW measurement laboratories be calibrated every two years at the CCL (WMO, 2003).

Under the WMO calibration system, there have been several calibration scales for CO<sub>2</sub>, *e.g.*, SIO-based X74, X85, X87, X93 and X2002 scales and the NOAA/GMD-based WMO Mole Fraction Scale

partially based on previous SIO scales. The NOAA/GMD and SIO are working to resolve the possible small differences between their scales. The CCL adopted the WMO X2005 scale, reflecting historical manometric calibrations of the CCL's set of cylinders and the possible small differences between SIO and NOAA/GMD calibrations. The most current WMO Mole Fraction Scale is the WMO-X2007 scale.

To assess the differences in standard scales among measuring laboratories, NOAA/GMD organizes intercomparisons or Round Robin experiments endorsed by WMO every few years. Many laboratories participated in the experiments organized in 1991–1992, 1995–1997, 1999–2000, and 2002–2006. Table 2 shows the results of the experiments performed in 2002–2006, in which the mole fractions measured by various laboratories are compared with the mole fractions measured by NOAA/GMD [Zhou *et al.*, 2009]. In addition, many laboratories compare their standards bilaterally or multilaterally.

Table 3 lists laboratories and sites used in the present issue of the *Data Summary* with standard scales of

reported data and history of participation in WMO intercomparison experiments.

**Table 2. Round robin results for the mole fraction of carbon dioxide. Differences between the mole fractions measured by various laboratories and the mole fractions measured by NOAA (Laboratory minus NOAA, ppm).**

Laboratory	Analysis Date	Mole fraction Difference (ppm)		
		Low 340–350 ppm	Medium 350–360 ppm	High 370–380 ppm
Tohoku Univ.	Jan-03	-0.11	-0.19	-0.29
NIES	Apr-03	-0.10	-0.15	-0.14
MRI	Jul-03	-0.16	-0.16	-0.08
AIST	Sep/Dec-03	-0.11	-0.22	-0.29
JMA	Jan-04	0.13	0.00	-0.02
KMA	Mar/Jun-04	-0.44	-0.12	-0.08
CMA (WLG)	Jul-04	-0.05	-0.19	-0.10
CMA (BJ)	Aug-04	-0.03	-0.20	0.02
Scripps (CMM)	Jun-05	0.23	0.17	0.20
Scripps (ECM II)		0.10	0.02	0.02
LSCE	Oct/Nov-05	-0.05	-0.11	-0.09
Monte Cimone	Oct-02	0.08	0.02	-0.03
Lampedusa	Nov-02	0.05	-0.15	-0.26
Plateau Rosa	Dec-02	-0.02	0.00	-0.05
HMS	Feb-03	0.06	-0.21	-0.06
MSC	May-05	0.06	-0.05	-0.06
Penn State Univ.	Sep-05	0.09	-0.07	-0.05
Univ. Heidelberg	Sep/Oct-02	-0.01	-0.06	-0.06
UBA	Oct-02	0.05	-0.11	-0.21
LSCE	Nov/Dec-02	0.10	0.03	0.05
FMI	Jan-03	-0.02	-0.04	-0.14
Univ. Groningen	Oct/Nov-03	0.01	0.02	0.04
MPI-BGC	Nov/Dec-03	0.04	0.02	-0.02
HMS	Mar-04	-0.19	-0.36	-0.59
NIWA	May-05	-0.08	-0.08	-0.09
CSIRO	Sep/Oct-05	-0.01	-0.03	-0.08
Cape Point	Dec-05	-0.02	-0.09	-0.18
NCAR	May/Jun-06	0.07	-0.04	-0.04

**Table 3. Status of standard scales and calibration/intercomparison for CO<sub>2</sub> at laboratories.**

Laboratory	WDCGG Filename Code	Calibration Scale	WMO Inter-comparison
AEMET	IZO128N0000	WMO	91/92, 96/97, 99/00
Aichi	MKW234N0000	WMO	
AIST	TKY236N0000	NIRE	96/97, 99/00, 02/06

BoM & CSIRO	CGO540S0010,CGO540S0000	WMO	
CMA	WLG236N0000	WMO	96/97, 99/00, 02/06
CNR-ICES ITALY DNA-IAA ARGENTINE	JBN762S0000	WMO	
CSIRO	ALT482N0003,CFA519S0003,CGO540S0003, CRI215N0000, CYA766S0001, ESP449N0003, MAA767S0003, MLO519N0003, MQA554S0003,SIS660N0003,SPO789S0003	WMO	91/92, 96/97, 99/00, 02/06
EC	ALT482N0000 ,ALT482N0005, CDL453N0000 ,HM449N0000 ,CSJ451N0000, EGB444N0100 ,ETL454N0000 ,FSD449N0000, LLB454N0100 ,WSA443N0000 ,WSA443N0001	WMO	91/92, 96/97, 99/00, 02/06
ENEA	LMP635N0001	WMO	91/92, 96/97, 99/00, 02/06
ERSE S.P.A.	PRS645N0000	WMO	99/00, 02/06
FMI	PAL667N0000	WMO	02/06
GERC	GSN233N0103	WMO	
HMS	KPS646N0000,HUN646N0000	WMO	91/92, 96/97, 99/00, 02/06
IAFMS	CMN644N0000	WMO	91/92, 96/97, 02/06
IGP	HUA312S0000	WMO	
IMK-IFU	WNK647N0000,ZUG647N0014	WMO	99/00
INMH	FDT645N0002		
IOEP	DIG654N0000		
ITM	ZEP678N0000	WMO	96/97, 99/00
JMA	MNM224N0000,RYO239N0000,YON224N0000	WMO	91/92, 96/97, 99/00, 02/06
KMA	AMY236N0000		02/06
KSNU	ISK242N0000		
LSCE	AMS137S0000, BGU641N0000 , LPO648N0000, MHD653N0002,PDM642N0000, PUY645N0000	WMO	91/92, 96/97, 99/00, 02/06
METRI	GSN233N0000	WMO	96/97
MGO	BER255N0001,KOT276N0001,KYZ240N0001,STC652N0001, TER669N0001	WMO	
MMD	DMV504N0000	WMO	
MRI	TKB236N0002	MRI	91/92, 96/97, 99/00, 02/06
NIES	COI243N0000,HAT224N0000	NIES	96/97, 99/00, 02/06
NIPR&Tohoku Univ.	SYO769S0000		Tohoku Univ.:91/92, 96/97, 99/00, 02/06
NIWA	BAR541S0000	WMO	91/92, 96/97, 99/00, 02/06
NOAA/GMD	BRW471N0000,MLO519N0000,SMO514S0000,SPO789S0000, NOAA/GMD flask network*	WMO	91/92, 96/97, 99/00, 02/06
Osaka Univ.	SUI234N0000		

RIVM	KMW653N0000	NIST	
Saitama	DDR236N0000,KIS236N0000,URW235N0000	WMO	
SAWS	CPT134S0000	WMO	99/00, 02/06
Shizuoka Univ.	HMM234N0000		
UBA	BRT648N0000,DEU649N0000,LGB652N0000,NGL653N0000 SNB647N0000,SSL647N0000,SSL647N0002,WES654N0000, ZGT654N0000,ZSF647N0010,ZUG647N0000	WMO	91/92, 96/97, 99/00, 02/06

\* NOAA/GMD flask network:

ALT482N0001,AMS137S0101,ASC107S0001,ASK123N0101,AVI417N0001,AZR638N0001,BAL655N0001,BAR541S0001,BKT500S0001,  
BME432N0001,BMW432N0001,BRW471N0001,BSC644N0001,CBA455N0001,CGO540S0001,CHR501N0001,CMO445N0001,CRZ146S0001,  
EIC329S0001,GMI513N0001,GOZ636N0001,HBA775S0001,HPB647N0003,HUN646N0101,ICE663N0001,ITN435N0001,IZO128N0001,  
KCO204N0001,KEY425N0001,KUM519N0001,KZD244N0001,KZM243N0001,LEF445N0001,LLN223N0001,LMP635N0003,MBC476N0001,  
MHD653N0001,MID528N0001,MKN100S0001,MLO519N0001,NMB123S0001,NWR440N0101,OPW448N0001,PAL667N0001,POC900N0001,  
POC905N0001,POC905S0001,POC910N0001,POC910S0001,POC915N0001,POC915S0001,POC920N0001,POC920S0001,POC925N0001,  
POC925S0001,POC930N0001,POC930S0001,POC935S0001,PSA764S0001,PTA438N0001,RPB413N0001,SCS903N0001,SCS906N0001,  
SCS909N0001,SCS912N0001,SCS915N0001,SCS918N0001,SCS921N0001,SEY104S0001,SGP436N0001,SHM452N0001,SMO514S0001,  
SPO789S0001,STC654N0001,STM666N0001,SUM672N0001,SYO769S0001,TAP236N0001,TDF354S0001,TRH441N0001,UTA439N0001,  
UUM244N0001,WIS631N0001,WLG236N0001,ZEP678N0001

### 3. Methane ( $\text{CH}_4$ )

The GAW programmes have established two WCCs for  $\text{CH}_4$ : the Swiss Federal Laboratory for Materials Testing and Research (EMPA), Dübendorf, Switzerland; and the Japan Meteorological Agency (JMA), Tokyo, Japan [WMO, 2007]. In addition, the Central Calibration Laboratory for  $\text{CH}_4$  has been established in NOAA/GMD [Dlugokencky, et. al., 2005; WMO, 2007].

The NOAA04 scale has been designated as the Primary Standard of the GAW programme. This scale results in  $\text{CH}_4$  mole fractions that are a factor of 1.0124 higher than the previous NOAA scale [Dlugokencky et al., 2005].

Table 4 summarizes the methane standard scales used by laboratories contributing to the WDCGG and lists tentative multiplying conversion factors applied

for analysis in this issue of the *Data Summary*. The standard is the NOAA04 scale, and conversion factors were calculated from the results of comparisons with other laboratories performed bilaterally or multilaterally before the establishment of the GAW Standard.

The former CMDL scale is lower than an absolute gravimetric scale [Aoki et al., 1992] by ~1.5% [Dlugokencky et al., 1994] and lower than the AES (currently MSC) scale by a factor of 1.0151 [Worthy et al., 1998]. The former CMDL scale can be converted to the Tohoku University standard by multiplying by 1.0121 [Dlugokencky et al., 2005]. The conversion factors  $1.0124 / 1.0151 = 0.9973$  and  $1.0124 / 1.0121 = 1.0003$  have been adopted for comparisons with the NOAA04 scale.

Table 4. Status of the standard scales of  $\text{CH}_4$  at laboratories with conversion factors.

Laboratory	WDCGG Filename Code	Calibration Scale	Conversion Factor
AEMET	IZO128N0000	NOAA04	1
AGAGE	CGO540S0011,CGO540S0013,CMO445N0011, MHD653N0011,MHD653N0013,RPB413N0000, RPB413N0011,SMO514S0014,SMO514S0016, THD441N0000	Tohoku Univ.	1.0003
CHMI	KOS649N0000	CHMI	0.9973
CMA	WLG236N0000	NOAA04	1
CSIRO	ALT482N0003,CFA519S0003,CGO540S0003, CRI215N0000,CYA766S0000,ESP449N0003, MAA767S0003,MLO519N0003,MQA554S0003, SIS660N0003,SPO789S0003	NOAA04	1
EC	ALT482N0000,CDL453N0000,CHM449N0000, EGB444N0100,ETL454N0000,FSD449N0000, LLB454N0100,WSA443N0000	NOAA04	1
EMPA	JFJ646N0000	NOAA04	1
ENEA	LMP635N0000	NOAA04	1

ERSE S.P.A.	PRS645N0000	NOAA04	1
JMA	MNM224N0000,RYO239N0000,YON224N0000	NOAA04	1
KMA	AMY236N0000	KRISS	
KSNU	ISK242N0000		
LSCE	AMS137S0002, BGU641N0000, LPO648N0000, PDM642N0000, PUY645N0000		1.0124
METRI	GSN233N0000	SIO X97	
MGO	TER669N0001	NOAA04	1
MRI	TKB236N0000	MRI	0.9973
NIES	COI243N0000,HAT224N0000	NIES	0.9973
RIVM	KMW653N0000	NIST	0.9973
SAWS	CPT134S0000	NOAA04	1
UBA	DEU649N0000,NGL653N0000,SSL647N0000, ZGT654N0000,ZSF647N0010,ZUG647N0000	NOAA04	1
NOAA/GMD	BRW471N0000,MLO519N0000, NOAA/GMD flask network*	NOAA04	1
	KPA432N0001,LEF445N0001,MCM777S0001, NZL543S0001,POC935S0001,SGI354S0001, SIO432N0001	NOAA/CMDL	1.0124

\* NOAA/GMD flask network:

ALT482N0001,AMS137S0001,ASC107S0001,ASK123N0001,AVI417N0001,AZR638N0001,BAL655N0001,BKT500S0001,BME432N0001,  
BMW432N0001,BRW471N0001,BSC644N0001,CBA455N0001,CGO540S0001,CHR501N0001,CMO445N0001,CRZ146S0001,EIC329S0001,  
GM1513N0001,GOZ636N0001,HBA775S0001,HPB647N0003,HUN646N0101,ICE663N0001,ITN435N0001,IZO128N0001,KEY425N0001,  
KUM519N0001,KZD244N0001,KZM243N0001,LLN223N0001,LMP635N0003,MBC476N0001,MHD653N0001,MID528N0001,MLO519N0001,  
NWR440N0101,OPW448N0001,PAL667N0001,POC90000001,POC905N0001,POC905S0001,POC910N0001,POC910S0001,POC915N0001,  
POC915S0001,POC920N0001,POC920S0001,POC925N0001,POC925S0001,POC930N0001,POC930S0001,PSA764S0001,PTA438N0001,  
RPB413N0001,SCS903N0001,SCS906N0001,SCS909N0001,SCS912N0001,SCS915N0001,SCS918N0001,SCS921N0001,SEY104S0001,  
SGP436N0000,SHM452N0001,SMO514S0001,SPO789S0001,STM666N0001,SUM672N0001,SYO769S0001,TAP236N0001,TDF354S0001,  
THD441N0001,UTA439N0001,UUM244N0001,WIS631N0001,WKT431N0001,WLG236N0001,ZEP678N0001

#### 4. Nitrous Oxide (N<sub>2</sub>O)

The Halocarbons and other Atmospheric Trace Species (HATS) Group of NOAA/GMD maintains a set of standards for N<sub>2</sub>O [Hall *et al.*, 2001]. The NOAA-2006 N<sub>2</sub>O scale [Hall *et al.*, 2007] has been designated as the Primary Standard of the GAW programme. This group analyses the standards of laboratories, including the Meteorological Service of Canada (MSC) and the Australian Commonwealth Scientific and Industrial Research Organisation (CSIRO). The Fraunhofer Institut für Atmosphärische Umweltforschung (IFU) in

Garmisch-Partenkirchen, Germany, serves as the GAW WCC.

The SIO-98 scale is essentially equivalent to the NOAA-2006 scale, with an average difference of 0.01% over the range of 299–319 ppb, and the NOAA-2000 scale can be converted to the 2006 scale by using the factor 0.99402 [Hall *et al.*, 2007]. A constant ratio of 1.0017 between CSIRO and AGAGE data was used by Huang *et al.* (2008), and a factor of 1 / 1.0017 = 0.9983 has been used in this report to convert CSIRO scale to the NOAA-2006 scale.

Table 5. Status of the standard scales of N<sub>2</sub>O at laboratories.

Submitter	WDCGG Filename Code	Calibration Scale	Conversion Factor
AGAGE	ADR652N0010,CGO540S0011,CGO540S0012, CGO540S0013,CMO445N0010,CMO445N0011, MHD653N0011,MHD653N0003,RPB413N0000, RPB413N0010,RPB413N0011,SMO514S0014, SMO514S0015,SMO514S0016,THD441N0000	SIO 1998	1
CSIRO	ALT482N0003,CFA519S0003,CGO540S0003, CRI215N0000,CYA766S0000,EPC449N0003, MAA767S0003,MLO519N0003,MQA554S0003, SIS660N0003,SPO789S0003	CSIRO	0.9983

EMPA	JFJ646N0000	SIO 1998	1
ENEA	LMP635N0001	NOAA/CMDL	0.999402
GERC	GSN233N0103	NOAA-2006	1
JMA	RYO239N0000	NOAA-2006	1
KMA	AMY236N0000	KRISS	
METRI	GSN233N0001		
MRI	MMB243N0000	MRI	
Nagoya Univ.	NGY235N0000		
NIES	HAT224N0000	NIES	
NILU	ZEP678N0000		
NOAA/GMD	ALT482N0001,BRW471N0001,BRW471N0011, CGO540S0001,KUM519N0001,MLO519N0001, MLO519N0011,NWR440N0001, NWR440N0011, SMO514S0001, SMO514S0011,SPO789S0001, SPO789S0011	NOAA/CMDL	0.999402
	BRW471N0010, MLO519N0010, NWR440N0010, SMO514S0010, SPO789S0010,SUM672N0000	NOAA-2006	1
SAWS	CPT134S0000	NOAA/CMDL	0.999402
UBA	SSL647N0000,ZSF647N0010	SIO 1998	1

## 5. Surface Ozone ( $O_3$ )

The National Institute of Standards and Technology (NIST) has developed and deployed Standard Reference Photometers (SRPs) in the USA and other countries. The GAW has designated SRP #2 maintained by NIST as the Primary Standard for the GAW programme, making NIST the CCL for  $O_3$ . The Swiss Federal Laboratory for Materials Testing and Research (EMPA) maintains NIST SRP #15 as the reference and is the GAW WCC for surface ozone

[Hofer et al., 1998]. The traceability and uncertainty of  $O_3$  within the GAW network were reported by Klausen et al., (2003). Regional Calibration Centres have been established at the Solar and Ozone Observatory, Hradec Kralove, Czech Republic, and Observatorio Central Buenos Aires, Argentina [WMO, 2007]. The former maintains SRP #17 directly purchased from NIST.

**Table 6. Status of surface ozone standard scales at laboratories**

Laboratory	WDCGG Filename Code	Calibration Scale	Audit EMPA-WCC
AEMET	IZO128N0000	WMO (NIST & EMPA)	96, 98, 00, 04
AQRB	ALG447N0000,BRA450N0000,CHA446N0000, EGB444N0000,EST451N0000,ELA449N0000, KEJ444N0000,SAT448N0000		
AWI	NMY770S0000		
BMG EMPA	BKT500S0000	WMO (NIST & EMPA)	99,01,04,07,08
BoM & CSIRO	CGO540S0000	WMO (NIST & EMPA)	02
CHMI	KOS649N0000		
DEFRA	EDM655N0000		
DWD	HPB647N0000	WMO (NIST & EMPA)	97,06

EARS	IRB645N0000,KVV646N0000,KVK646N0000, ZRN646N0000	WMO (NIST & EMPA)	
EMPA	JFJ646N0000,MKN100S0000,PAY646N0000, RIG647N0000	WMO (NIST & EMPA)	Jungfraujoch: 99, 06
ERSE S.P.A.	PRS645N0000		
FMI	AHT662N0000,OUL666N0000,PAL667N0000, UTO659N0000,VIR660N0000		Pallas-Sammaltunturi: 97, 03, 07
HMS	KPS646N0000		
IM	ANG638N0000,BEJ638N0000,CAS639N0000, FUN132N0000,LIS638N0000,MVH638N0000, PEN640N0000		
INM	DON637N0000,MHN639N0000,NIA642N0000, ROQ640N0000,SPM639N0000	NPL (U. K.)	
INMH	FDT645N0002		
IOEP	DIG654N0000	WMO (NIST & EMPA)	
ISAC	CMN644N0000,PYR227N0000		
IVL	VDL664N0000	Stockholm Univ. (Sweden)	
JMA	MNM224N0000,RYO239N0000,SYO769S0002, YON224N0000	WMO (NIST & EMPA)	Ryori: 05
	TKB236N1003		
KSNU	ISK242N0000		
LEGMA	DBL656N0000,RCV656N0000,ZSN657N0000	WMO (NIST & EMPA)	
MMD	TAR504N0000		
NILU	ZEP678N0000	WMO (NIST & EMPA)	97, 01, 05
NIWA	BAR541S0000	WMO (NIST & EMPA)	
NOAA/GMD	BMW432N0004,BRW471N0004,ICE663N0004, LAU545S0004, MCM777S0104,MLO519N40, NWR440N0002,NWR440N0204,RPB413N0004, SMO514S0004,SPO789S0004,SUM672N0004, THD441N0004	NOAA/GMD	Mauna Loa: 03 Barrow: 08
NUI	MHD653N0000	WMO (NIST & EMPA)	96, 98, 02, 05
ONM	ASK123N0000		03, 07
PolyU	HKG222N0000		
RIVM	KMW653N0000		
Roshydromet	DAK654N0000, SHP659N0000		
SAWS	CPT134S0000	WMO (NIST & EMPA)	97, 98, 02, 06
SMN	USI354S0000,USH354S0001	WMO (NIST & EMPA)	98, 03

UBA	BRT648N0000,DEU649N0000,LGB652N0000, NGL653N0000,SNB647N0000,SSL647N0000, WES654N0000,ZGT654N0000,ZSF647N0010, ZUG647N0000	WMO (NIST & EMPA)	Zugspitze: 96, 97, 01 Sonnblick: 98 Zugspitze/Schneefern erhaus: 06
UM	GLH636N0000		
UY	CVO116N0001		

## 6. Carbon Monoxide (CO)

The Swiss Federal Laboratory for Materials Testing and Research (EMPA) serves as the WCC under GAW based on its secondary standards calibrated against the

standard at NOAA/GMD designated as the Primary Standard for GAW.

Table 7. Status of carbon monoxide standard scales at laboratories

Laboratory	WDCGG Filename Code	Calibration Scale	Audit EMPA-WCC
AGAGE	CGR540S0011,MCH653N0011	SIO 1998	
BMG EMPA	BKT500S0000	WMO 2000 (NOAA/GMD & EMPA)	
CHMI	KOS649N0000	CHMI	
CSIRO	ALT482N0003,CFA519S0003,CGO540S0003, CRI215N0000,CYA766S0000,ESP449N0003, MAA767S0003,MLO519N0003,MQA554S0003, SIS660N0003,SPO789S0003	CSIRO	Cape Grim: 02
DWD	HPB647N0000	WMO (NOAA/GMD & EMPA)	06
EARS	KVV646N0000		
EMPA	JFJ646N0000,MKN100S0000,PAY646N0000, RIG646N0000	WMO 2000 (NOAA/GMD & EMPA)	Jungfraujoch: 99,06
JMA	RYO239N0000, MNM224N0000, YON224N0000	WMO 2000 (NOAA/GMD)	Ryori:05
NOAA/GMD	NOAA/GMD flask network*	WMO (NOAA/GMD & EMPA)	Mauna Loa: 03 Barrow: 08
PolyU	HKG222N0000		
RIVM	KMW653N0000,KTB653N0000	National	
SAWS	CPT134S0000	WMO (NOAA/CMDL)	98, 02, 06
SMN	USI354S0000 ,USH354S0001	WMO (NOAA/GMD & EMPA)	98, 03
UBA	NGL653N0000,SNB647N0000,SSL647N0000, ZUG647N0000	WMO (NOAA/CMDL)	Zugspitze: 01 Sonnblick: 98
UM	GLH636N0000		
UY	CVO116N0001	WMO 2000 (NOAA/GMD & EMPA)	

NOAA/GMD flask network:

ALT482N0001,ASC107S0001,ASK123N0101,AZR638N0001,BAL655N0001,BME432N0001,BMW432N0001,BRW471N0001,BSC644N0001,  
CBA45N0001,CGO540S0001,CHR501N0001,CMO445N0001,CRZ146S0001,EIC329S0001,GM1513N0001,GOZ636N0001,HBA775S0001,  
HUN646N0101,ICE663N0001,ITN435N0001,IZO128N0001,KEY425N0001,KUM519N0001,KZD244N0001,KZM243N0001,LEF445N0001,  
MBC476N0001,MHD653N0001,MID528N0001,MLO519N0001,NWR440N0001,PAL667N0001,POC90000001,POC905N0001,POC905S0001,  
POC910N0001,POC910S0001,POC915S0001,POC920N0001,POC925N0001,POC930N0001,  
POC930S0001,POC935N0001,POC935S0001,PSA764S0001,PTA438N0001,RPB413N0001,SCS903N0001,SCS906N0001,SCS909N0001,  
SCS912N0001,SCS915N0001,SCS918N0001,SCS921N0001,SEY104S0001,SGP436N0000,SHM452N0001,SMO514S0001,SPO789S0001,  
STM666N0001,SYO769S0001,TAP236N0001,TDF354S0001,THD441N0000,UTA439N0001,UUM244N0001,WIS631N0001,WLG236N0001,  
ZEP678N0101

## References

- Aoki, S., T. Nakazawa, S. Murayama and S. Kawaguchi, Measurements of atmospheric methane at the Japanese Antarctic station, Syowa, *Tellus, Ser. B*, **44**, 273–281, 1992.
- CMDL, Climate Monitoring and Diagnostics Laboratory Summary Report No.26 2000-2001, 2002.
- Cunnold, D. M., L. P. Steele, P. J. Fraser, P. G. Simmonds, R. G. Prinn, R. F. Weiss, L. W. Porter, S. O'Doherty, R. L. Langenfelds, P. B. Krummel, H. J. Wang, L. Emmons, X. X. Tie, and E. J. Dlugokencky, In situ measurements of atmospheric methane at GAGE/AGAGE sites during 1985–2000 and resulting source inferences, *J. Geophys. Res.*, **107(D14)**, 10.1029/2001JD001226, 2002.
- Dlugokencky, E. J., L. P. Steele, P. M. Lang, and K. A. Masarie, The growth rate and distribution of atmospheric methane, *J. Geophys. Res.*, **99**, 17021–17043, 1994.
- Dlugokencky, E. J., R. C. Myers, P. M. Lang, K. A. Masarie, A. M. Crotwell, K. W. Thoning, B. D. Hall, J. W. Elkins, and L. P. Steele, Conversion of NOAA atmospheric dry air CH<sub>4</sub> mole fractions to a gravimetrically prepared standard scale, *J. Geophys. Res.*, **110**, D18306, doi: 10.1029/2005JD006035, 2005.
- Hall, B. D. (ed.), J. W. Elkins, J. H. Butler, S. A. Montzka, T. M. Thompson, L. Del Negro, G. S. Dutton, D. F. Hurst, D. B. King, E. S. Kline, L. Lock, D. Mactaggart, D. Mondeel, F. L. Moore, J. D. Nance, E. A. Ray, and P. A. Romashkin, Halocarbons and Other Atmospheric Gases, Section 5 in Climate Monitoring and Diagnostics Laboratory, Summary Report N. 25, 1998–1999, R. S. Schnell, D. B. King, R. M. Rosson (eds.), NOAA-CMDL, Boulder, CO., USA, 2001.
- Hall, B. D., G. S. Dutton, and J. W. Elkins, The NOAA nitrous oxide standard scale for atmospheric observations, *J. Geophys. Res.*, **112**, D09305, doi:10.1029/2006JD007954, 2007.
- Hofer, P., B. Buchmann and A. Herzog, Traceability, Uncertainty and Assessment Criteria of Surface Ozone Measurements, *EMPA-WCC Report 98/5*, 20 pp, 1998.
- Huang, J., A. Golombek, R. Prinn, R. Weiss, P. Fraser, P. Simmonds, E. J. Dlugokencky, B. Hall, J. Elkins, P. Steele, R. Langenfelds, P. Krummel, G. Dutton, and L. Porter, Estimation of regional emissions of nitrous oxide from 1997 to 2005 using multinetowrk measurements, a chemical transport model, and an inverse method, *J. Geophys. Res.*, **113**, D17313, doi:10.1029/2007JD009381, 2008.
- Klausen, J., C. Zellweger, B. Buchmann, and P. Hofer, Uncertainty and bias of surface ozone measurements at selected Global Atmosphere Watch sites, *J. Geophys. Res.*, **108(D19)**, 4622, doi:10.1029/2003JD003710, 2003.
- WMO, Report of the Eleventh WMO/IAEA Meeting of Experts on Carbon Dioxide Concentration and Related Tracer Measurement Techniques, Global Atmosphere Watch Report Series No.148, 2003.
- WMO, WMO Global Atmosphere Watch (GAW) Strategic Plan: 2008–2015, WMO/GAW Report No. 172, 104pp, 2007.
- Worthy, D. E. J., I. Levin, N. B. A. Trivett, A. J. Kuhlmann, J. F. Hopper and M. K. Ernst, Seven years of continuous methane observations at a remote boreal site in Ontario, Canada, *J. Geophys. Res.*, **103**, 15995–16007, 1998.
- Zhao, C. L., P. P. Tans, and K. W. Thoning, A high precision manometric system for absolute calibrations of CO<sub>2</sub> in dry air, *J. Geophys. Res.*, **102**, 5885–5894, 1997.
- Zhou, L. X., D. Kitzis, P. P. Tans, “Report of the Fourth WMO Round-Robin Reference Gas Intercomparison, 2002–2007” in the report of the 14th WMO/IAEA Meeting of Experts on Carbon Dioxide, Other Greenhouse Gases and Related Tracers Measurement Techniques, Helsinki, Finland, 10–13 September 2007, edited by T. Laurila, WMO/GAW Report No. 186, 2009

# LIST OF OBSERVING STATIONS

Station	Country/Territory	Index Number	Location Latitude (°')	Longitude (°')	Altitude (m)	Parameter
<b>REGION I (Africa)</b>						
Amsterdam Island	France	AMS137S00	37 47 S	77 31 E	55	CH <sub>4</sub> , CO, CO <sub>2</sub> , O <sub>3</sub> , VOCs
Amsterdam Island	France	AMS137S00	37 47 S	77 31 E	55	CH <sub>4</sub> , CO <sub>2</sub>
Ascension Island	United Kingdom of Great Britain and Northern Ireland	ASC107S00	7 55 S	14 25 W	54	<sup>13</sup> CO <sub>2</sub> , C <sup>18</sup> O <sub>2</sub> , CH <sub>4</sub> , CO, CO <sub>2</sub> , H <sub>2</sub>
Assekrem	Algeria	ASK123N00	23 16 N	5 37 E	2710	<sup>13</sup> CO <sub>2</sub> , C <sup>18</sup> O <sub>2</sub> , CH <sub>4</sub> , CO, CO <sub>2</sub> , H <sub>2</sub>
Assekrem	Algeria	ASK123N00	23 16 N	5 37 E	2710	O <sub>3</sub>
Cape Point	South Africa	CPT134S00	34 21 S	18 28 E	230	CH <sub>4</sub> , CO, CO <sub>2</sub> , N <sub>2</sub> O, O <sub>3</sub>
Cape Verde Observatory	Cape Verde	CVO116N00	16 50 N	24 52 W	10	CO, NO <sub>x</sub> , O <sub>3</sub> , VOCs
Crozet	France	CRZ146S00	46 27 S	51 51 E	120	<sup>13</sup> CO <sub>2</sub> , C <sup>18</sup> O <sub>2</sub> , CH <sub>4</sub> , CO, CO <sub>2</sub> , H <sub>2</sub>
Funchal	Portugal	FUN132N00	32 38 N	16 52 W	58	O <sub>3</sub>
Gobabeb	Namibia	NMB123S00	23 34 S	15 01 E	461	<sup>13</sup> CO <sub>2</sub> , C <sup>18</sup> O <sub>2</sub> , CH <sub>4</sub> , CO <sub>2</sub>
Izaña (Tenerife)	Spain	IZO128N00	28 18 N	16 30 W	2367	<sup>13</sup> CO <sub>2</sub> , C <sup>18</sup> O <sub>2</sub> , CH <sub>4</sub> , CO, CO <sub>2</sub> , H <sub>2</sub>
Izaña (Tenerife)	Spain	IZO128N00	28 18 N	16 30 W	2367	CH <sub>4</sub> , CO <sub>2</sub> , O <sub>3</sub>
Mahe Island	Seychelles	SEY104S00	4 40 S	55 10 E	7	<sup>13</sup> CO <sub>2</sub> , C <sup>18</sup> O <sub>2</sub> , CH <sub>4</sub> , CO, CO <sub>2</sub> , H <sub>2</sub>
Mt. Kenya	Kenya	MKN100S00	0 03 S	37 17 E	3678	<sup>13</sup> CO <sub>2</sub> , C <sup>18</sup> O <sub>2</sub> , CH <sub>4</sub> , CO <sub>2</sub>
Mt. Kenya	Kenya	MKN100S00	0 03 S	37 17 E	3678	CO, O <sub>3</sub>
<b>REGION II (Asia)</b>						
Anmyeon-do	Republic of Korea	AMY236N00	36 31 N	126 19 E	47	CFCs, CH <sub>4</sub> , CO <sub>2</sub> , N <sub>2</sub> O
Bering Island	Russian Federation	BER255N00	55 12 N	165 58 E	13	CO <sub>2</sub>
Cape Ochi-ishi	Japan	COI243N00	43 08 N	145 30 E	45	CH <sub>4</sub> , CO <sub>2</sub>
Cape Rama	India	CRI215N00	15 04 N	73 49 E	60	<sup>13</sup> CO <sub>2</sub> , CH <sub>4</sub> , CO, CO <sub>2</sub> , H <sub>2</sub> , N <sub>2</sub> O
Everest - Pyramid	Nepal	PYR227N00	27 57 N	86 48 E	5079	O <sub>3</sub>
Gosan	Republic of Korea	GSN233N00	33 16 N	126 10 E	72	CFCs, CH <sub>4</sub> , CO <sub>2</sub> , N <sub>2</sub> O
Gosan	Republic of Korea	GSN233N01	33 08 N	126 07 E	72	CFCs, CH <sub>4</sub> , CO <sub>2</sub> , N <sub>2</sub> O
Hamamatsu	Japan	HMM234N00	34 43 N	137 43 E	35	CO <sub>2</sub>
Hateruma	Japan	HAT224N00	24 03 N	123 47 E	10	CH <sub>4</sub> , CO <sub>2</sub> , N <sub>2</sub> O
Hok Tsui	Hong Kong, China	HKG222N00	22 13 N	114 15 E	60	CO, O <sub>3</sub>
Issyk-Kul	Kyrgyzstan	ISK242N00	42 37 N	76 58 E	1640	CH <sub>4</sub> , CO <sub>2</sub> , O <sub>3</sub>
Kaashidhoo	Maldives	KCO204N00	4 58 N	73 28 E	1	<sup>13</sup> CO <sub>2</sub> , CH <sub>4</sub> , CO <sub>2</sub>
Kisai	Japan	KIS236N00	36 04 N	139 33 E	13	CO <sub>2</sub>
Kotelny Island	Russian Federation	KOT276N00	76 00 N	137 52 E	5	CO <sub>2</sub>
Kyzylcha	Uzbekistan	KYZ240N00	40 52 N	66 09 E	340	CO <sub>2</sub>
Lulin	China	LLN223N00	23 28 N	120 52 E	2867	CH <sub>4</sub> , CO <sub>2</sub>
Memanbetsu	Japan	MMB243N00	43 55 N	144 11 E	32.9	N <sub>2</sub> O
Mikawa-Ichinomiya	Japan	MKW234N00	34 51 N	137 25 E	50	CO <sub>2</sub>
Minamitorishima	Japan	MNM224N00	24 16 N	153 58 E	8	CH <sub>4</sub> , CO, CO <sub>2</sub> , O <sub>3</sub>
Mt. Dodaira	Japan	DDR236N00	36 00 N	139 10 E	840	CO <sub>2</sub>
Mt. Waliguan	China	WLG236N00	36 16 N	100 54 E	3810	CH <sub>4</sub> , CO <sub>2</sub>
Mt. Waliguan	China	WLG236N00	36 16 N	100 54 E	3810	<sup>13</sup> CO <sub>2</sub> , C <sup>18</sup> O <sub>2</sub> , CH <sub>4</sub> , CO, CO <sub>2</sub> , H <sub>2</sub>
Nagoya	Japan	NGY235N00	35 08 N	136 58 E	35	N <sub>2</sub> O
Plateau Assy	Kazakhstan	KZM243N00	43 15 N	77 52 E	2519	<sup>13</sup> CO <sub>2</sub> , C <sup>18</sup> O <sub>2</sub> , CH <sub>4</sub> , CO, CO <sub>2</sub> , H <sub>2</sub>
Ryori	Japan	RYO239N00	39 01 N	141 49 E	260	CCl <sub>4</sub> , CFCs, CH <sub>3</sub> CCl <sub>3</sub> , CH <sub>4</sub> , CO, CO <sub>2</sub> , N <sub>2</sub> O, O <sub>3</sub>
Sary Taukum	Kazakhstan	KZD244N00	44 27 N	75 34 E	412	<sup>13</sup> CO <sub>2</sub> , C <sup>18</sup> O <sub>2</sub> , CH <sub>4</sub> , CO, CO <sub>2</sub> , H <sub>2</sub>
Ship between Ishigaki Island and Hateruma Island	Japan	SIH224N00	24 07 N	123 49 E	5	CO <sub>2</sub>
South China Sea (03N)	N/A	SCS903N00	3 00 N	105 00 E	15	<sup>13</sup> CO <sub>2</sub> , C <sup>18</sup> O <sub>2</sub> , CH <sub>4</sub> , CO, CO <sub>2</sub> , H <sub>2</sub>
South China Sea (06N)	N/A	SCS906N00	6 00 N	107 00 E	15	<sup>13</sup> CO <sub>2</sub> , C <sup>18</sup> O <sub>2</sub> , CH <sub>4</sub> , CO, CO <sub>2</sub> , H <sub>2</sub>

## LIST OF OBSERVING STATIONS (continued)

Station	Country/Territory	Index Number	Location		Altitude (m)	Parameter
			Latitude (°')	Longitude (°')		
South China Sea (09N)	N/A	SCS909N00	9 00 N	109 00 E	15	$^{13}\text{CO}_2$ , $\text{C}^{18}\text{O}_2$ , $\text{CH}_4$ , $\text{CO}$ , $\text{CO}_2$ , $\text{H}_2$
South China Sea (12N)	N/A	SCS912N00	12 00 N	111 00 E	15	$^{13}\text{CO}_2$ , $\text{C}^{18}\text{O}_2$ , $\text{CH}_4$ , $\text{CO}$ , $\text{CO}_2$ , $\text{H}_2$
South China Sea (15N)	N/A	SCS915N00	15 00 N	113 00 E	15	$^{13}\text{CO}_2$ , $\text{C}^{18}\text{O}_2$ , $\text{CH}_4$ , $\text{CO}$ , $\text{CO}_2$ , $\text{H}_2$
South China Sea (18N)	N/A	SCS918N00	18 00 N	113 00 E	15	$^{13}\text{CO}_2$ , $\text{C}^{18}\text{O}_2$ , $\text{CH}_4$ , $\text{CO}$ , $\text{CO}_2$ , $\text{H}_2$
South China Sea (21N)	N/A	SCS921N00	21 00 N	114 00 E	15	$^{13}\text{CO}_2$ , $\text{C}^{18}\text{O}_2$ , $\text{CH}_4$ , $\text{CO}$ , $\text{CO}_2$ , $\text{H}_2$
Suita	Japan	SUI234N00	34 49 N	135 31 E	63	$\text{CO}_2$
Tae-ahn Peninsula	Republic of Korea	TAP236N00	36 43 N	126 07 E	20	$^{13}\text{CO}_2$ , $\text{C}^{18}\text{O}_2$ , $\text{CH}_4$ , $\text{CO}$ , $\text{CO}_2$ , $\text{H}_2$
Takayama	Japan	TKY236N00	36 08 N	137 25 E	1420	$\text{CO}_2$
Tsukuba	Japan	TKB236N00	36 02 N	140 07 E	26	$\text{CH}_4$ , $\text{CO}_2$
Tsukuba	Japan	TKB236N10	36 02 N	140 07 E	25	$\text{O}_3$
Ulaan Uul	Mongolia	UUM244N00	44 27 N	111 04 E	914	$^{13}\text{CO}_2$ , $\text{C}^{18}\text{O}_2$ , $\text{CH}_4$ , $\text{CO}$ , $\text{CO}_2$ , $\text{H}_2$
Urawa	Japan	URW235N00	35 52 N	139 35 E	10	$\text{CO}_2$
Yonagunijima	Japan	YON224N00	24 28 N	123 01 E	30	$\text{CH}_4$ , $\text{CO}$ , $\text{CO}_2$ , $\text{O}_3$

### REGION III (South America)

Arembepe	Brazil	ABP312S00	12 46 S	38 10 W	0	$\text{CH}_4$ , $\text{CO}_2$
Arembepe	Brazil	ABP312S00	12 46 S	38 10 W	0	$\text{O}_3$
Bird Island	United Kingdom of Great Britain and Northern Ireland	SGI354S00	54 00 S	38 02 W	30	$\text{CH}_4$ , $\text{CO}_2$
Easter Island	Chile	EIC327S00	27 07 S	109 27 W	50	$^{13}\text{CO}_2$ , $\text{C}^{18}\text{O}_2$ , $\text{CH}_4$ , $\text{CO}$ , $\text{CO}_2$ , $\text{H}_2$
Huancayo	Peru	HUA312S00	12 04 S	75 31 W	3313	$\text{CO}_2$
Tierra del Fuego	Argentina	TDF354S00	54 52 S	68 28 W	20	$^{13}\text{CO}_2$ , $\text{C}^{18}\text{O}_2$ , $\text{CBrClF}_2$ , $\text{CFCs}$ , $\text{CH}_3\text{Br}$ , $\text{CH}_3\text{CCl}_3$ , $\text{CH}_4$ , $\text{CO}$ , $\text{CO}_2$ , $\text{H}_2$ , $\text{HCFCs}$ , $\text{HFCs}$
Ushuaia	Argentina	USH354S00	54 49 S	68 17 W	18	$\text{CO}$ , $\text{O}_3$

### REGION IV (North and Central America)

Alert	Canada	ALT482N00	82 27 N	62 31 W	210	$^{13}\text{CO}_2$ , $\text{C}^{18}\text{O}_2$ , $\text{C}_2\text{Cl}_4$ , $\text{CBrClF}_2$ , $\text{CBrF}_3$ , $\text{CCl}_4$ , $\text{CFCs}$ , $\text{CH}_2\text{Cl}_2$ , $\text{CH}_3\text{Br}$ , $\text{CH}_3\text{CCl}_3$ , $\text{CH}_4$ , $\text{CO}$ , $\text{CO}_2$ , $\text{H}_2$ , $\text{HCFCs}$ , $\text{HFCs}$ , $\text{N}_2\text{O}$ , $\text{SF}_6$
Alert	Canada	ALT482N00	82 27 N	62 31 W	210	$^{13}\text{CO}_2$ , $\text{CH}_4$ , $\text{CO}$ , $\text{CO}_2$ , $\text{H}_2$ , $\text{N}_2\text{O}$
Alert	Canada	ALT482N00	82 27 N	62 31 W	210	$\text{CH}_4$ , $\text{CO}$ , $\text{CO}_2$ , $\text{N}_2\text{O}$ , $\text{SF}_6$
Algoma	Canada	ALG447N00	47 01 N	84 22 W	411	$\text{O}_3$
Argyle	United States of America	AMT445N00	45 01 N	68 40 W	50	$^{13}\text{CO}_2$ , $\text{C}^{18}\text{O}_2$ , $\text{CH}_4$
Barrow	United States of America	BRW471N00	71 19 N	156 35 W	11	$^{13}\text{CH}_4$ , $^{13}\text{CO}_2$ , $\text{C}^{18}\text{O}_2$ , $\text{C}_2\text{Cl}_4$ , $\text{CBrClF}_2$ , $\text{CBrF}_3$ , $\text{CCl}_4$ , $\text{CFCs}$ , $\text{CH}_2\text{Cl}_2$ , $\text{CH}_3\text{Br}$ , $\text{CH}_3\text{CCl}_3$ , $\text{CH}_3\text{Cl}$ , $\text{CH}_4$ , $\text{CO}$ , $\text{CO}_2$ , $\text{H}_2$ , $\text{HCFCs}$ , $\text{HFCs}$ , $\text{N}_2\text{O}$ , $\text{O}_3$ , $\text{SF}_6$
Bratt's Lake	Canada	BRA450N00	50 12 N	104 42 W	595	$\text{O}_3$
Candle Lake	Canada	CDL453N00	53 52 N	104 39 W	489	$\text{CH}_4$ , $\text{CO}$ , $\text{CO}_2$
Cape Meares	United States of America	CMO445N00	45 28 N	123 58 W	30	$\text{CCl}_4$ , $\text{CFCs}$ , $\text{CH}_3\text{CCl}_3$ , $\text{CH}_4$ , $\text{N}_2\text{O}$
Cape Meares	United States of America	CMO445N00	45 28 N	123 58 W	30	$^{13}\text{CO}_2$ , $\text{C}^{18}\text{O}_2$ , $\text{CH}_4$ , $\text{CO}$ , $\text{CO}_2$ , $\text{H}_2$
Cape St. James	Canada	CSJ451N00	51 55 N	131 01 W	89	$\text{CO}_2$
Chalk River	Canada	CHA446N00	46 04 N	77 24 W	184	$\text{O}_3$
Chapais	Canada	CPS449N00	49 49 N	74 58 W	381	$\text{O}_3$
Chibougamau	Canada	CHM449N00	49 40 N	74 20 W	393	$\text{CH}_4$ , $\text{CO}$ , $\text{CO}_2$

## LIST OF OBSERVING STATIONS (continued)

Station	Country/Territory	Index Number	Location			Parameter
			Latitude (°')	Longitude (°')	Altitude (m)	
Cold Bay	United States of America	CBA455N00	55 12 N	162 43 W	25	$^{13}\text{CO}_2$ , $\text{C}^{18}\text{O}_2$ , $\text{CH}_4$ , $\text{CO}$ , $\text{CO}_2$ , $\text{H}_2$
East Trout Lake	Canada	ETL454N00	54 21 N	104 59 W	492	$\text{CH}_4$ , $\text{CO}$ , $\text{CO}_2$
Egbert	Canada	EGB444N00	44 13 N	79 46 W	253	$\text{O}_3$
Egbert	Canada	EGB444N01	44 13 N	79 46 W	253	$\text{CH}_4$ , $\text{CO}$ , $\text{CO}_2$
Estevan Point	Canada	ESP449N00	49 22 N	126 32 W	39	$^{13}\text{CO}_2$ , $\text{CH}_4$ , $\text{CO}$ , $\text{CO}_2$ , $\text{H}_2$ , $\text{N}_2\text{O}$
Estevan Point	Canada	ESP449N00	49 22 N	126 32 W	39	$\text{CH}_4$ , $\text{CO}_2$ , $\text{N}_2\text{O}$ , $\text{SF}_6$
Esther	Canada	EST451N00	51 40 N	110 12 W	707	$\text{O}_3$
Experimental Lakes Area	Canada	ELA449N00	49 40 N	93 43 W	369	$\text{O}_3$
Frasedale	Canada	FSD449N00	49 52 N	81 34 W	210	$\text{CH}_4$ , $\text{CO}$ , $\text{CO}_2$
Grifton	United States of America	ITN435N00	35 21 N	77 22 W	505	$^{13}\text{CO}_2$ , $\text{C}^{18}\text{O}_2$ , $\text{CCl}_4$ , $\text{CFCs}$ , $\text{CH}_4$ , $\text{CO}$ , $\text{CO}_2$ , $\text{H}_2$ , $\text{N}_2\text{O}$ , $\text{SF}_6$
Harvard Forest	United States of America	HFM442N00	42 53 N	72 17 W	340	$\text{CBrClF}_2$ , $\text{CCl}_4$ , $\text{CFCs}$ , $\text{CH}_3\text{Br}$ , $\text{CH}_3\text{CCl}_3$ , $\text{HCFCs}$ , $\text{HFCs}$ , $\text{N}_2\text{O}$ , $\text{SF}_6$
Kejimkujik	Canada	KEJ444N00	44 25 N	65 12 W	127	$\text{O}_3$
Key Biscayne	United States of America	KEY425N00	25 40 N	80 12 W	3	$^{13}\text{CO}_2$ , $\text{C}^{18}\text{O}_2$ , $\text{CH}_4$ , $\text{CO}$ , $\text{CO}_2$ , $\text{H}_2$
Kitt Peak	United States of America	KPA431N00	31 58 N	111 35 W	2083	$\text{CH}_4$
La Jolla	United States of America	SIO432N00	32 49 N	117 16 W	14	$\text{CH}_4$
La Palma	Cuba	PLM422N00	22 45 N	83 31 W	47	$\text{NO}_2$
Lac La Biche (Alberta)	Canada	LLB454N00	54 57 N	112 27 W	540	$\text{CH}_4$ , $\text{CO}_2$
Lac La Biche (Alberta)	Canada	LLB454N01	54 57 N	112 27 W	540	$\text{CH}_4$ , $\text{CO}$ , $\text{CO}_2$
Longwoods	Canada	LON442N00	42 52 N	81 28 W	239	$\text{O}_3$
Moody	United States of America	WKT431N00	31 19 N	97 19 W	708	$^{13}\text{CO}_2$ , $\text{C}^{18}\text{O}_2$ , $\text{CH}_4$
Mould Bay	Canada	MBC476N00	76 15 N	119 19 W	58	$^{13}\text{CO}_2$ , $\text{C}^{18}\text{O}_2$ , $\text{CH}_4$ , $\text{CO}$ , $\text{CO}_2$ , $\text{H}_2$
Niwot Ridge (C-1)	United States of America	NWR440N00	40 02 N	105 32 W	3021	$\text{C}_2\text{Cl}_4$ , $\text{CBrClF}_2$ , $\text{CBrF}_3$ , $\text{CCl}_4$ , $\text{CFCs}$ , $\text{CH}_2\text{Cl}_2$ , $\text{CH}_3\text{Br}$ , $\text{CH}_3\text{CCl}_3$ , $\text{CH}_3\text{Cl}$ , $\text{HCFCs}$ , $\text{HFCs}$ , $\text{N}_2\text{O}$ , $\text{O}_3$ , $\text{SF}_6$
Niwot Ridge (Saddle)	United States of America	NWR440N02	40 03 N	105 35 W	3528	$\text{O}_3$
Niwot Ridge (T-van)	United States of America	NWR440N01	40 03 N	105 35 W	3523	$^{13}\text{CH}_4$ , $^{13}\text{CO}_2$ , $\text{C}^{18}\text{O}_2$ , $\text{CH}_4$ , $\text{CO}$ , $\text{CO}_2$ , $\text{H}_2$
Olympic Peninsula	United States of America	OPW448N00	48 15 N	124 25 W	488	$\text{CH}_4$ , $\text{CO}_2$ , $\text{H}_2$
Pacific Ocean (15N)	N/A	POC915N00	15 00 N	145 00 W	10	$^{13}\text{CO}_2$ , $\text{C}^{18}\text{O}_2$ , $\text{CH}_4$ , $\text{CO}$ , $\text{CO}_2$ , $\text{H}_2$
Pacific Ocean (20N)	N/A	POC920N00	20 00 N	141 00 W	10	$^{13}\text{CO}_2$ , $\text{C}^{18}\text{O}_2$ , $\text{CH}_4$ , $\text{CO}$ , $\text{CO}_2$ , $\text{H}_2$
Pacific Ocean (25N)	N/A	POC925N00	25 00 N	139 00 W	10	$^{13}\text{CO}_2$ , $\text{C}^{18}\text{O}_2$ , $\text{CH}_4$ , $\text{CO}$ , $\text{CO}_2$ , $\text{H}_2$
Pacific Ocean (30N)	N/A	POC930N00	30 00 N	135 00 W	10	$^{13}\text{CO}_2$ , $\text{C}^{18}\text{O}_2$ , $\text{CH}_4$ , $\text{CO}$ , $\text{CO}_2$ , $\text{H}_2$
Pacific Ocean (35N)	N/A	POC935N00	35 00 N	137 00 W	10	$^{13}\text{CO}_2$ , $\text{C}^{18}\text{O}_2$ , $\text{CO}$ , $\text{H}_2$
Pacific Ocean (40N)	N/A	POC940N00	40 00 N	136 00 W	10	$^{13}\text{CO}_2$ , $\text{H}_2$
Pacific Ocean (45N)	N/A	POC945N00	45 00 N	131 00 W	10	$^{13}\text{CO}_2$ , $\text{H}_2$
Park Falls	United States of America	LEF445N00	45 55 N	90 16 W	868	$^{13}\text{CO}_2$ , $\text{C}^{18}\text{O}_2$ , $\text{CBrClF}_2$ , $\text{CCl}_4$ , $\text{CFCs}$ , $\text{CH}_3\text{Br}$ , $\text{CH}_3\text{CCl}_3$ , $\text{CH}_4$ , $\text{CO}$ , $\text{CO}_2$ , $\text{H}_2$ , $\text{HCFCs}$ , $\text{HFCs}$ , $\text{N}_2\text{O}$ , $\text{SF}_6$
Point Arena	United States of America	PTA438N00	38 57 N	123 43 W	17	$^{13}\text{CO}_2$ , $\text{C}^{18}\text{O}_2$ , $\text{CH}_4$ , $\text{CO}$ , $\text{CO}_2$

## LIST OF OBSERVING STATIONS (continued)

Station	Country/Territory	Index Number	Location			Parameter
			Latitude (°')	Longitude (°')	Altitude (m)	
Ragged Point	Barbados	RPB413N00	13 10 N	59 25 W	45	$^{13}\text{CO}_2$ , $\text{C}^{18}\text{O}_2$ , $\text{CH}_4$ , $\text{CO}$ , $\text{CO}_2$ , $\text{H}_2$ , $\text{O}_3$
Ragged Point	Barbados	RPB413N00	13 10 N	59 25 W	45	$\text{C}_2\text{Cl}_4$ , $\text{C}_2\text{HCl}_3$ , $\text{CBrClF}_2$ , $\text{CBrF}_3$ , $\text{CCl}_4$ , $\text{CFCs}$ , $\text{CH}_2\text{Cl}_2$ , $\text{CH}_3\text{Br}$ , $\text{CH}_3\text{CCl}_3$ , $\text{CH}_3\text{Cl}$ , $\text{CH}_4$ , $\text{CHCl}_3$ , $\text{HCFCs}$ , $\text{HFCs}$ , $\text{N}_2\text{O}$ , $\text{SF}_6$ , $\text{SO}_2\text{F}_2$
Sable Island	Canada	WSA443N00	43 55 N	60 01 W	5	$\text{CH}_4$ , $\text{CO}$ , $\text{CO}_2$ , $\text{N}_2\text{O}$ , $\text{SF}_6$
Saturna	Canada	SAT448N00	48 46 N	123 07 W	178	$\text{O}_3$
Shemya Island	United States of America	SHM452N00	52 43 N	174 04 E	40	$^{13}\text{CO}_2$ , $\text{C}^{18}\text{O}_2$ , $\text{CH}_4$ , $\text{CO}$ , $\text{CO}_2$ , $\text{H}_2$
Southern Great Plains	United States of America	SGP436N00	36 46 N	97 30 W	314	$^{13}\text{CO}_2$ , $\text{C}^{18}\text{O}_2$ , $\text{CH}_4$ , $\text{CO}$ , $\text{CO}_2$
St. Croix	United States of America	AVI417N00	17 45 N	64 45 W	3	$\text{CH}_4$ , $\text{CO}_2$
St. David's Head	United Kingdom of Great Britain and Northern Ireland	BME432N00	32 22 N	64 39 W	30	$^{13}\text{CO}_2$ , $\text{C}^{18}\text{O}_2$ , $\text{CH}_4$ , $\text{CO}$ , $\text{CO}_2$ , $\text{H}_2$
Sutton	Canada	SUT445N00	45 04 N	72 40 W	243	$\text{O}_3$
Toronto	Canada	TOT443N00	43 46 N	79 28 W	198	$\text{CH}_4$ , $\text{CO}$ , $\text{CO}_2$
Trinidad Head	United States of America	THD441N00	41 02 N	124 09 W	120	$\text{C}_2\text{Cl}_4$ , $\text{C}_2\text{HCl}_3$ , $\text{CBrClF}_2$ , $\text{CBrF}_3$ , $\text{CCl}_4$ , $\text{CFCs}$ , $\text{CH}_2\text{Cl}_2$ , $\text{CH}_3\text{Br}$ , $\text{CH}_3\text{CCl}_3$ , $\text{CH}_3\text{Cl}$ , $\text{CH}_4$ , $\text{CHCl}_3$ , $\text{HCFCs}$ , $\text{HFCs}$ , $\text{N}_2\text{O}$ , $\text{SF}_6$ , $\text{SO}_2\text{F}_2$
Trinidad Head	United States of America	THD441N00	41 02 N	124 09 W	120	$^{13}\text{CO}_2$ , $\text{C}^{18}\text{O}_2$ , $\text{CBrClF}_2$ , $\text{CCl}_4$ , $\text{CFCs}$ , $\text{CH}_3\text{Br}$ , $\text{CH}_3\text{CCl}_3$ , $\text{CH}_4$ , $\text{CO}$ , $\text{CO}_2$ , $\text{HCFCs}$ , $\text{HFCs}$ , $\text{N}_2\text{O}$ , $\text{O}_3$ , $\text{SF}_6$
Tudor Hill	United Kingdom of Great Britain and Northern Ireland	BMW432N00	32 16 N	64 52 W	30	$^{13}\text{CO}_2$ , $\text{C}^{18}\text{O}_2$ , $\text{CH}_4$ , $\text{CO}$ , $\text{CO}_2$ , $\text{H}_2$ , $\text{O}_3$
Wendover	United States of America	UTA439N00	39 52 N	113 43 W	1320	$^{13}\text{CO}_2$ , $\text{C}^{18}\text{O}_2$ , $\text{CH}_4$ , $\text{CO}$ , $\text{CO}_2$ , $\text{H}_2$

### REGION V (South-West Pacific)

Baring Head	New Zealand	BAR541S00	41 25 S	174 52 E	85	$\text{CH}_4$ , $\text{CO}_2$
Baring Head	New Zealand	BAR541S00	41 25 S	174 52 E	85	$^{13}\text{CH}_4$ , $^{14}\text{CO}_2$ , $\text{CH}_4$ , $\text{CO}$ , $\text{CO}_2$ , $\text{N}_2\text{O}$ , $\text{O}_3$ , VOCs
Bukit Koto Tabang	Indonesia	BKT500S00	0 12 S	100 19 E	864.5	$\text{NO}_2$ , $\text{SO}_2$
Bukit Koto Tabang	Indonesia	BKT500S00	0 12 S	100 19 E	864.5	$^{13}\text{CO}_2$ , $\text{C}^{18}\text{O}_2$ , $\text{CH}_4$ , $\text{CO}_2$
Bukit Koto Tabang	Indonesia	BKT500S00	0 12 S	100 19 E	864.5	$\text{CO}$ , $\text{O}_3$
Cape Ferguson	Australia	CFA519S00	19 16 S	147 03 E	2	$^{13}\text{CO}_2$ , $\text{CH}_4$ , $\text{CO}$ , $\text{CO}_2$ , $\text{H}_2$ , $\text{N}_2\text{O}$
Cape Grim	Australia	CGO540S00	40 40 S	144 40 E	94	$^{13}\text{CO}_2$ , $\text{CH}_4$ , $\text{CO}$ , $\text{CO}_2$ , $\text{H}_2$ , $\text{N}_2\text{O}$
Cape Grim	Australia	CGO540S00	40 40 S	144 40 E	94	$^{13}\text{CH}_4$ , $^{13}\text{CO}_2$ , $\text{C}^{18}\text{O}_2$ , $\text{C}_2\text{Cl}_4$ , $\text{CBrClF}_2$ , $\text{CBrF}_3$ , $\text{CCl}_4$ , $\text{CFCs}$ , $\text{CH}_2\text{Cl}_2$ , $\text{CH}_3\text{Br}$ , $\text{CH}_3\text{CCl}_3$ , $\text{CH}_4$ , $\text{CO}$ , $\text{CO}_2$ , $\text{H}_2$ , $\text{HCFCs}$ , $\text{HFCs}$ , $\text{N}_2\text{O}$ , $\text{SF}_6$ , $\text{N}_2\text{O}_2\text{F}_2$
Cape Grim	Australia	CGO540S00	40 40 S	144 40 E	94	$\text{C}_2\text{Cl}_4$ , $\text{C}_2\text{HCl}_3$ , $\text{CBrClF}_2$ , $\text{CBrF}_3$ , $\text{CCl}_4$ , $\text{CFCs}$ , $\text{CH}_2\text{Cl}_2$ , $\text{CH}_3\text{Br}$ , $\text{CH}_3\text{CCl}_3$ , $\text{CH}_4$ , $\text{CHCl}_3$ , $\text{CO}$ , $\text{H}_2$ , $\text{HCFCs}$ , $\text{HFCs}$ , $\text{N}_2\text{O}$ , $\text{SF}_6$ , $\text{SO}_2\text{F}_2$
Cape Grim	Australia	CGO540S00	40 40 S	144 40 E	94	$\text{CO}_2$ , $\text{O}_3$

## LIST OF OBSERVING STATIONS (continued)

Station	Country/Territory	Index Number	Location			Parameter
			Latitude (°')	Longitude (°')	Altitude (m)	
Cape Kumukahi	United States of America	KUM519N00	19 31 N	154 49 W	3	$^{13}\text{CO}_2$ , $\text{C}^{18}\text{O}_2$ , $\text{C}_2\text{Cl}_4$ , $\text{CBrClF}_2$ , $\text{CBrF}_3$ , $\text{CCl}_4$ , $\text{CFCs}$ , $\text{CH}_2\text{Cl}_2$ , $\text{CH}_3\text{Br}$ , $\text{CH}_3\text{CCl}_3$ , $\text{CH}_4$ , $\text{CO}$ , $\text{CO}_2$ , $\text{H}_2$ , $\text{HCFCs}$ , $\text{HFCs}$ , $\text{N}_2\text{O}$ , $\text{SF}_6$
Christmas Island	Kiribati	CHR501N00	1 42 N	157 10 W	3	$^{13}\text{CO}_2$ , $\text{C}^{18}\text{O}_2$ , $\text{CH}_4$ , $\text{CO}$ , $\text{CO}_2$ , $\text{H}_2$
Danum Valley GAW Baseline Station	Malaysia	DMV504N00	4 58 N	117 49 E	426	$\text{CO}_2$ , $\text{O}_3$
Guam	United States of America	GMI513N00	13 25 N	144 46 E	2	$^{13}\text{CO}_2$ , $\text{C}^{18}\text{O}_2$ , $\text{CH}_4$ , $\text{CO}$ , $\text{CO}_2$ , $\text{H}_2$
Jakarta	Indonesia	JKR506S00	6 10 S	106 49 E	7	$\text{NO}_2$ , $\text{SO}_2$
Kaitorete Spit	New Zealand	NZL543S00	43 49 S	172 37 E	3	$\text{CH}_4$
Lauder	New Zealand	LAU545S00	45 01 S	169 40 E	370	$\text{O}_3$
Macquarie Island	Australia	MQA554S00	54 28 S	158 58 E	12	$^{13}\text{CO}_2$ , $\text{CH}_4$ , $\text{CO}$ , $\text{CO}_2$ , $\text{H}_2$ , $\text{N}_2\text{O}$
Mauna Loa	United States of America	MLO519N00	19 32 N	155 34 W	3397	$^{13}\text{CO}_2$ , $\text{CH}_4$ , $\text{CO}$ , $\text{CO}_2$ , $\text{H}_2$ , $\text{N}_2\text{O}$
Mauna Loa	United States of America	MLO519N00	19 32 N	155 34 W	3397	$^{13}\text{CH}_4$ , $^{13}\text{CO}_2$ , $\text{C}^{18}\text{O}_2$ , $\text{C}_2\text{Cl}_4$ , $\text{CBrClF}_2$ , $\text{CBrF}_3$ , $\text{CCl}_4$ , $\text{CFCs}$ , $\text{CH}_2\text{Cl}_2$ , $\text{CH}_3\text{Br}$ , $\text{CH}_3\text{CCl}_3$ , $\text{CH}_3\text{Cl}$ , $\text{CH}_4$ , $\text{CO}$ , $\text{CO}_2$ , $\text{H}_2$ , $\text{HCFCs}$ , $\text{HFCs}$ , $\text{N}_2\text{O}$ , $\text{O}_3$ , $\text{SF}_6$
Pacific Ocean (00N)	N/A	POC900N00	0 00 N	155 00 W	10	$^{13}\text{CO}_2$ , $\text{C}^{18}\text{O}_2$ , $\text{CH}_4$ , $\text{CO}$ , $\text{CO}_2$ , $\text{H}_2$
Pacific Ocean (05N)	N/A	POC905N00	5 00 N	151 00 W	10	$^{13}\text{CO}_2$ , $\text{C}^{18}\text{O}_2$ , $\text{CH}_4$ , $\text{CO}$ , $\text{CO}_2$ , $\text{H}_2$
Pacific Ocean (05S)	N/A	POC905S00	5 00 S	159 00 W	10	$^{13}\text{CO}_2$ , $\text{C}^{18}\text{O}_2$ , $\text{CH}_4$ , $\text{CO}$ , $\text{CO}_2$ , $\text{H}_2$
Pacific Ocean (10N)	N/A	POC910N00	10 00 N	149 00 W	10	$^{13}\text{CO}_2$ , $\text{C}^{18}\text{O}_2$ , $\text{CH}_4$ , $\text{CO}$ , $\text{CO}_2$ , $\text{H}_2$
Pacific Ocean (10S)	N/A	POC910S00	10 00 S	161 00 W	10	$^{13}\text{CO}_2$ , $\text{C}^{18}\text{O}_2$ , $\text{CH}_4$ , $\text{CO}$ , $\text{CO}_2$ , $\text{H}_2$
Pacific Ocean (15S)	N/A	POC915S00	15 00 S	171 00 W	10	$^{13}\text{CO}_2$ , $\text{C}^{18}\text{O}_2$ , $\text{CH}_4$ , $\text{CO}$ , $\text{CO}_2$ , $\text{H}_2$
Pacific Ocean (20S)	N/A	POC920S00	20 00 S	174 00 W	10	$^{13}\text{CO}_2$ , $\text{C}^{18}\text{O}_2$ , $\text{CH}_4$ , $\text{CO}$ , $\text{CO}_2$ , $\text{H}_2$
Pacific Ocean (25S)	N/A	POC925S00	25 00 S	171 00 W	10	$^{13}\text{CO}_2$ , $\text{C}^{18}\text{O}_2$ , $\text{CH}_4$ , $\text{CO}$ , $\text{CO}_2$ , $\text{H}_2$
Pacific Ocean (30S)	N/A	POC930S00	30 00 S	176 00 W	10	$^{13}\text{CO}_2$ , $\text{C}^{18}\text{O}_2$ , $\text{CH}_4$ , $\text{CO}$ , $\text{CO}_2$ , $\text{H}_2$
Pacific Ocean (35S)	N/A	POC935S00	35 00 S	180 00 E	10	$^{13}\text{CO}_2$ , $\text{C}^{18}\text{O}_2$ , $\text{CH}_4$ , $\text{CO}$ , $\text{CO}_2$ , $\text{H}_2$
Sand Island	United States of America	MID528N00	28 11 N	177 22 W	7.7	$^{13}\text{CO}_2$ , $\text{C}^{18}\text{O}_2$ , $\text{CH}_4$ , $\text{CO}$ , $\text{CO}_2$ , $\text{H}_2$
Tanah Rata	Malaysia	TAR504N00	4 28 N	101 22 E	1545	$\text{O}_3$
Tutuila (Cape Matatula)	United States of America	SMO514S00	14 14 S	170 34 W	42	$^{13}\text{CH}_4$ , $^{13}\text{CO}_2$ , $\text{C}^{18}\text{O}_2$ , $\text{C}_2\text{Cl}_4$ , $\text{CBrClF}_2$ , $\text{CBrF}_3$ , $\text{CCl}_4$ , $\text{CFCs}$ , $\text{CH}_2\text{Cl}_2$ , $\text{CH}_3\text{Br}$ , $\text{CH}_3\text{CCl}_3$ , $\text{CH}_3\text{Cl}$ , $\text{CH}_4$ , $\text{CO}$ , $\text{CO}_2$ , $\text{H}_2$ , $\text{HCFCs}$ , $\text{HFCs}$ , $\text{N}_2\text{O}$ , $\text{O}_3$ , $\text{SF}_6$
Tutuila (Cape Matatula)	United States of America	SMO514S00	14 14 S	170 34 W	42	$\text{C}_2\text{Cl}_4$ , $\text{C}_2\text{HCl}_3$ , $\text{CBrClF}_2$ , $\text{CBrF}_3$ , $\text{CCl}_4$ , $\text{CFCs}$ , $\text{CH}_2\text{Cl}_2$ , $\text{CH}_3\text{Br}$ , $\text{CH}_3\text{CCl}_3$ , $\text{CH}_3\text{Cl}$ , $\text{CH}_4$ , $\text{CHCl}_3$ , $\text{HCFCs}$ , $\text{HFCs}$ , $\text{N}_2\text{O}$ , $\text{SF}_6$ , $\text{SO}_2\text{F}_2$

### REGION VI (Europe)

Adrigole	Ireland	ADR651N00	51 40 N	9 43 W	50	$\text{CCl}_4$ , $\text{CFCs}$ , $\text{CH}_3\text{CCl}_3$ , $\text{N}_2\text{O}$
Angra do Heroismo	Portugal	ANG638N00	38 40 N	27 13 W	74	$\text{O}_3$
Baltic Sea	Poland	BAL655N00	55 21 N	17 13 E	28	$^{13}\text{CO}_2$ , $\text{C}^{18}\text{O}_2$ , $\text{CH}_4$ , $\text{CO}$ , $\text{CO}_2$ , $\text{H}_2$
Begur	Spain	BGU641N00	41 58 N	3 13 E	13	$\text{CH}_4$ , $\text{CO}_2$
Beja	Portugal	BEJ638N00	38 01 N	7 52 W	246	$\text{O}_3$
Black Sea	Romania	BSC644N00	44 10 N	28 40 E	3	$^{13}\text{CO}_2$ , $\text{C}^{18}\text{O}_2$ , $\text{CH}_4$ , $\text{CO}$ , $\text{CO}_2$ , $\text{H}_2$
Bragança	Portugal	BRG641N00	41 47 N	6 43 W	690	$\text{SO}_2$
Brotjacklriegel	Germany	BRT648N00	48 49 N	13 13 E	1016	$\text{CO}_2$ , $\text{O}_3$
Brotjacklriegel	Germany	BRT648N00	48 49 N	13 13 E	1016	VOCs

## LIST OF OBSERVING STATIONS (continued)

Station	Country/Territory	Index Number	Latitude (°')	Longitude (°')	Location Altitude (m)	Parameter
Burgas	Bulgaria	BUR642N00	42 28 N	27 28 E	16	NO <sub>2</sub> , SO <sub>2</sub>
Campisabalos	Spain	CAM641N00	41 16 N	3 08 W	1360	VOCs
Castelo Branco	Portugal	CAS639N00	39 49 N	7 28 W	386	O <sub>3</sub>
Danki	Russian Federation	DAK654N00	54 53 N	37 47 E	140	O <sub>3</sub>
Deuselbach	Germany	DEU649N00	49 46 N	7 02 E	480	CH <sub>4</sub> , CO <sub>2</sub> , O <sub>3</sub>
Dobele	Latvia	DBL656N00	56 22 N	23 11 E	42	O <sub>3</sub>
Donon	France	DNN648N00	48 30 N	7 07 E	775	VOCs
Doñana	Spain	DON637N00	37 02 N	6 32 W	5	NO <sub>2</sub> , O <sub>3</sub> , SO <sub>2</sub>
Dwejra Point	Malta	GOZ636N00	36 02 N	14 10 E	30	<sup>13</sup> CO <sub>2</sub> , C <sup>18</sup> O <sub>2</sub> , CH <sub>4</sub> , CO, CO <sub>2</sub> , H <sub>2</sub>
Eskdalemuir	United Kingdom of Great Britain and Northern Ireland	EDM655N00	55 19 N	3 12 W	242	O <sub>3</sub>
Fundata	Romania	FDT645N00	45 28 N	25 18 E	1383.5	CO <sub>2</sub> , NO <sub>2</sub> , O <sub>3</sub>
Fundata	Romania	FDT645N00	45 28 N	25 18 E	1383.5	NO <sub>2</sub> , SO <sub>2</sub>
Giordan Lighthouse	Malta	GLH636N00	36 04 N	14 13 E	167	CO, O <sub>3</sub>
Hegyhatsal	Hungary	HUN646N00	46 57 N	16 38 E	248	<sup>13</sup> CO <sub>2</sub> , C <sup>18</sup> O <sub>2</sub> , CH <sub>4</sub> , CO, CO <sub>2</sub> , H <sub>2</sub>
Hegyhatsal	Hungary	HUN646N00	46 57 N	16 38 E	248	CO <sub>2</sub>
Heimaey	Iceland	ICE663N00	63 23 N	20 16 W	100	<sup>13</sup> CO <sub>2</sub> , C <sup>18</sup> O <sub>2</sub> , CH <sub>4</sub> , CO, CO <sub>2</sub> , H <sub>2</sub> , O <sub>3</sub>
Hohe Warte	Austria	HHE648N00	48 15 N	16 22 E	202	NO, NO <sub>2</sub> , SO <sub>2</sub>
Hohe Warte	Austria	HHE648N00	48 15 N	16 22 E	202	NO, NO <sub>2</sub> , SO <sub>2</sub>
Hohenpeissenberg	Germany	HPB647N00	47 47 N	11 01 E	985	CH <sub>4</sub> , CO <sub>2</sub>
Hohenpeissenberg	Germany	HPB647N00	47 47 N	11 01 E	985	<sup>222</sup> Rn, CO, H <sub>2</sub> O <sub>2</sub> , NO, NO <sub>2</sub> , NO <sub>x</sub> , NO <sub>y</sub> , O <sub>3</sub> , PAN, ROOH, SO <sub>2</sub> , VOCs
Ille Grande	France	LPO648N00	48 48 N	3 35 W	10	CH <sub>4</sub> , CO <sub>2</sub>
Iskrba	Slovenia	IRB645N00	45 34 N	14 52 E	520	NO <sub>2</sub> , O <sub>3</sub> , SO <sub>2</sub>
Ivan Sedlo	Bosnia and Herzegovina	IVN643N00	43 46 N	18 01 E	970	NO <sub>2</sub> , SO <sub>2</sub>
Jarczew	Poland	JCZ651N00	51 49 N	21 58 E	180	NO <sub>2</sub> , SO <sub>2</sub>
Jungfraujoch	Switzerland	JFJ646N00	46 32 N	7 59 E	3580	CH <sub>4</sub> , CO, N <sub>2</sub> O, NO, NO <sub>2</sub> , NO <sub>x</sub> , O <sub>3</sub> , SF <sub>6</sub> , SO <sub>2</sub>
K-puszta	Hungary	KPS646N00	46 58 N	19 33 E	125	CO <sub>2</sub> , NO <sub>2</sub> , O <sub>3</sub> , SO <sub>2</sub>
Kamenicki Vis	Serbia	KAM643N00	43 23 N	21 56 E	813	NO <sub>2</sub> , SO <sub>2</sub>
Kloosterburen	Netherlands (the)	KTB653N00	53 23 N	6 25 E	0	CO, NO, NO <sub>2</sub> , NO <sub>x</sub> , SO <sub>2</sub>
Kollumerwaard	Netherlands (the)	KMW653N00	53 19 N	6 16 E	0	CH <sub>4</sub> , CO, CO <sub>2</sub> , NO, NO <sub>2</sub> , NO <sub>x</sub> , O <sub>3</sub> , SO <sub>2</sub>
Kosetice	Czech Republic	KOS649N00	49 34 N	15 04 E	534	VOCs
Kosetice	Czech Republic	KOS649N00	49 34 N	15 04 E	534	CH <sub>4</sub> , CO, NO, NO <sub>2</sub> , O <sub>3</sub> , SO <sub>2</sub>
Kovk	Slovenia	KVK646N00	46 07 N	15 05 E	600	O <sub>3</sub>
Krvavec	Slovenia	KVV646N00	46 17 N	14 31 E	1720	CO, O <sub>3</sub>
La Cartuja	Spain	CAR637N00	37 12 N	3 36 W	720	NO <sub>2</sub> , SO <sub>2</sub>
La Tardiere	France	LAT646N00	46 38 N	0 45 W	133	VOCs
Lampedusa	Italy	LMP635N00	35 31 N	12 37 E	45	CH <sub>4</sub> , CO <sub>2</sub>
Lampedusa	Italy	LMP635N00	35 31 N	12 37 E	45	CBrClF <sub>2</sub> , CBrF <sub>3</sub> , CCl <sub>4</sub> , CFCs, CH <sub>2</sub> Br <sub>2</sub> , CH <sub>2</sub> Cl <sub>2</sub> , CH <sub>3</sub> Br, CH <sub>3</sub> CCl <sub>3</sub> , CH <sub>3</sub> Cl, CH <sub>3</sub> I, CH <sub>4</sub> , CHCl <sub>3</sub> , CO <sub>2</sub> , HCFCs, HFCs, N <sub>2</sub> O, SF <sub>6</sub>
Lazaropole	The former Yugoslav Republic of Macedonia	LZP641N00	41 31 N	20 41 E	1320	NO <sub>2</sub> , SO <sub>2</sub>
Leba	Poland	LEB654N00	54 45 N	17 31 E	2	NO <sub>2</sub> , SO <sub>2</sub>
Lisboa / Gago Coutinho	Portugal	LIS638N00	38 46 N	9 07 W	105	O <sub>3</sub>
Logroño	Spain	LOG642N00	42 27 N	2 30 W	370	NO <sub>2</sub> , SO <sub>2</sub>
Mace Head	Ireland	MHD653N00	53 19 N	9 54 W	25	O <sub>3</sub>

## LIST OF OBSERVING STATIONS (continued)

Station	Country/Territory	Index Number	Latitude (°')	Longitude (°')	Location	Altitude (m)	Parameter
Mace Head	Ireland	MHD653N00	53 19 N	9 54 W	25	13CO <sub>2</sub> , C <sup>18</sup> O <sub>2</sub> , CBrClF <sub>2</sub> , CBrF <sub>3</sub> , CCl <sub>4</sub> , CFCs, CH <sub>3</sub> Br, CH <sub>3</sub> CCl <sub>3</sub> , CH <sub>4</sub> , CO, CO <sub>2</sub> , H <sub>2</sub> , HCFCs, HFCs, N <sub>2</sub> O, SF <sub>6</sub>	
Mace Head	Ireland	MHD653N00	53 19 N	9 54 W	25	C <sub>2</sub> Cl <sub>4</sub> , C <sub>2</sub> HCl <sub>3</sub> , CBrClF <sub>2</sub> , CBrF <sub>3</sub> , CCl <sub>4</sub> , CFCs, CH <sub>2</sub> Cl <sub>2</sub> , CH <sub>3</sub> Br, CH <sub>3</sub> CCl <sub>3</sub> , CH <sub>4</sub> , CO, HCFCs, HFCs, N <sub>2</sub> O, SF <sub>6</sub> , SO <sub>2</sub> F <sub>2</sub>	
Mace Head	Ireland	MHD653N00	53 19 N	9 54 W	25	CO <sub>2</sub>	
Mahón	Spain	MHN639N00	39 52 N	4 19 E	78	NO <sub>2</sub> , O <sub>3</sub> , SO <sub>2</sub>	
Monte Cimone	Italy	CMN644N00	44 10 N	10 41 E	2165	O <sub>3</sub>	
Monte Cimone	Italy	CMN644N00	44 10 N	10 41 E	2165	CO <sub>2</sub>	
Monte Velho	Portugal	MVH638N00	38 04 N	8 48 W	43	O <sub>3</sub>	
Neuglobsow	Germany	NGL653N00	53 10 N	13 01 E	65	CH <sub>4</sub> , CO, CO <sub>2</sub> , O <sub>3</sub>	
Noia	Spain	NIA642N00	42 43 N	8 55 W	685	NO <sub>2</sub> , O <sub>3</sub> , SO <sub>2</sub>	
Ocean Station "M"	Norway	STM666N00	66 00 N	2 00 E	5	13CO <sub>2</sub> , C <sup>18</sup> O <sub>2</sub> , CH <sub>4</sub> , CO, CO <sub>2</sub> , H <sub>2</sub>	
Ocean Station Charlie	Russian Federation	STC652N00	52 45 N	35 30 W	5	CO <sub>2</sub>	
Ocean Station Charlie	United States of America	STC654N00	54 00 N	35 00 W	6	CO <sub>2</sub>	
Ochsenkopf	Germany	OXK650N00	50 01 N	11 48 E	1185	CH <sub>4</sub>	
Oulanka	Finland	OUL666N00	66 19 N	29 23 E	310	NO <sub>2</sub> , O <sub>3</sub> , SO <sub>2</sub>	
Pallas-Sammaltunturi	Finland	PAL667N00	67 58 N	24 07 E	560	VOCs	
Pallas-Sammaltunturi	Finland	PAL667N00	67 58 N	24 07 E	560	CO <sub>2</sub> , O <sub>3</sub>	
Pallas-Sammaltunturi	Finland	PAL667N00	67 58 N	24 07 E	560	13CO <sub>2</sub> , C <sup>18</sup> O <sub>2</sub> , CBrF <sub>3</sub> , CH <sub>4</sub> , CO, CO <sub>2</sub>	
Payerne	Switzerland	PAY646N00	46 49 N	6 57 E	490	CO, NO, NO <sub>2</sub> , NO <sub>x</sub> , O <sub>3</sub> , SO <sub>2</sub>	
Penhas Douradas	Portugal	PEN640N00	40 25 N	7 32 W	1380	O <sub>3</sub>	
Peyrusse Vieille	France	PVI643N00	43 37 N	0 10 E	200	VOCs	
Pic du Midi	France	PDM642N00	42 56 N	0 08 E	2877	CH <sub>4</sub> , CO <sub>2</sub>	
Plateau Rosa	Italy	PRS645N00	45 55 N	7 42 E	3480	CH <sub>4</sub> , CO <sub>2</sub> , O <sub>3</sub>	
Pleven	Bulgaria	PLV643N00	43 25 N	24 36 E	64	NO <sub>2</sub> , SO <sub>2</sub>	
Plovdiv	Bulgaria	PLD642N00	42 07 N	24 45 E	179	NO <sub>2</sub> , SO <sub>2</sub>	
Puszcza Borecka/Diabla Gora	Poland	DIG654N00	54 08 N	22 04 E	157	CO <sub>2</sub> , NO <sub>2</sub> , O <sub>3</sub> , SO <sub>2</sub>	
Puy de Dome Rigi	France Switzerland	PUY645N00 RIG646N00	45 46 N 46 04 N	2 57 E 8 26 E	1465 1031	CH <sub>4</sub> , CO <sub>2</sub> CO, NO, NO <sub>2</sub> , NO <sub>x</sub> , O <sub>3</sub> , SO <sub>2</sub> , VOCs	
Roquetes	Spain	ROQ640N00	40 49 N	0 28 E	50	NO <sub>2</sub> , O <sub>3</sub> , SO <sub>2</sub>	
Rucava	Latvia	RCV656N00	56 06 N	21 06 E	18	NO <sub>2</sub> , O <sub>3</sub> , SO <sub>2</sub>	
San Pablo de los Montes	Spain	SPM639N00	39 32 N	4 20 W	917	NO <sub>2</sub> , O <sub>3</sub> , SO <sub>2</sub>	
Schauinsland	Germany	SSL647N00	47 55 N	7 55 E	1205	CH <sub>4</sub> , CO, CO <sub>2</sub> , N <sub>2</sub> O, NO, NO <sub>2</sub> , O <sub>3</sub> , SF <sub>6</sub>	
Schmuecke	Germany	SCH650N00	50 38 N	10 46 E	937	VOCs	
Sede Boker	Israel	WIS631N00	31 07 N	34 52 E	400	13CO <sub>2</sub> , C <sup>18</sup> O <sub>2</sub> , CH <sub>4</sub> , CO, CO <sub>2</sub> , H <sub>2</sub>	
Semenic	Romania	SEM645N00	45 07 N	21 58 E	1432	NO <sub>2</sub> , SO <sub>2</sub>	
Shepeleva	Russian Federation	SHP659N00	59 58 N	29 07 E	4	O <sub>3</sub>	
Shetland	United Kingdom of Great Britain and Northern Ireland	SIS660N00	60 04 N	1 15 W	30	13CO <sub>2</sub> , CH <sub>4</sub> , CO, CO <sub>2</sub> , H <sub>2</sub> , N <sub>2</sub> O	
Site J	Denmark	GRL666N00	66 30 N	46 12 W	2030	CH <sub>4</sub>	
Sniezka	Poland	SNZ650N00	50 43 N	15 43 E	1603	NO <sub>2</sub> , SO <sub>2</sub>	
Sofia	Bulgaria	SOF642N00	42 38 N	23 22 E	586	NO <sub>2</sub> , SO <sub>2</sub>	
Sonnblick	Austria	SNB647N00	47 02 N	12 56 E	3106	CO, CO <sub>2</sub> , NO, NO <sub>y</sub> , O <sub>3</sub>	

## LIST OF OBSERVING STATIONS (continued)

Station	Country/Territory	Index Number	Latitude (°')	Longitude (°')	Altitude (m)	Location Parameter
Starina	Slovakia	STA649N00	49 02 N	22 16 E	345	VOCs
Stephansplatz	Austria	STP648N00	48 13 N	16 22 E	171	NO, NO <sub>2</sub> , SO <sub>2</sub>
Stephansplatz	Austria	STP648N00	48 13 N	16 22 E	171	NO, NO <sub>2</sub> , SO <sub>2</sub>
Stîna de Vale	Romania	STN646N00	46 40 N	22 37 E	1116	NO <sub>2</sub> , SO <sub>2</sub>
Summit	Denmark	SUM672N00	72 34 N	38 28 W	3238	<sup>13</sup> CO <sub>2</sub> , C <sup>18</sup> O <sub>2</sub> , CBrClF <sub>2</sub> , CCl <sub>4</sub> , CFCs, CH <sub>3</sub> Br, CH <sub>3</sub> CCl <sub>3</sub> , CH <sub>4</sub> , CO <sub>2</sub> , HCFCs, HFCs, N <sub>2</sub> O, O <sub>3</sub> , SF <sub>6</sub>
Suwalki	Poland	SWL654N00	54 07 N	22 56 E	184	NO <sub>2</sub> , SO <sub>2</sub>
Terceira Island	Portugal	AZR638N00	38 46 N	27 22 W	40	<sup>13</sup> CO <sub>2</sub> , C <sup>18</sup> O <sub>2</sub> , CH <sub>4</sub> , CO, CO <sub>2</sub> , H <sub>2</sub>
Teriberka	Russian Federation	TER669N00	69 12 N	35 06 E	40	CH <sub>4</sub> , CO <sub>2</sub>
Utö	Finland	UTO659N00	59 46 N	21 22 E	7	VOCs
Utö	Finland	UTO659N00	59 46 N	21 22 E	7	NO <sub>2</sub> , O <sub>3</sub> , SO <sub>2</sub>
Varna	Bulgaria	VRN643N00	43 12 N	27 55 E	41	NO <sub>2</sub> , SO <sub>2</sub>
Viana do Castelo	Portugal	VDC641N00	41 42 N	8 48 W	16	SO <sub>2</sub>
Vindeln	Sweden	VDL664N00	64 15 N	19 46 E	271	O <sub>3</sub>
Virolahti	Finland	VIR660N00	60 31 N	27 40 E	4	NO <sub>2</sub> , O <sub>3</sub> , SO <sub>2</sub>
Waldhof	Germany	LGB652N00	52 47 N	10 46 E	74	VOCs
Waldhof	Germany	LGB652N00	52 47 N	10 46 E	74	CO <sub>2</sub> , O <sub>3</sub>
Wank Peak	Germany	WNK647N00	47 31 N	11 09 E	1780	CO <sub>2</sub> , NOx, SO <sub>2</sub>
Westerland	Germany	WES654N00	54 55 N	8 19 E	12	CO <sub>2</sub> , O <sub>3</sub>
Zabljak	Montenegro	ZBL643N00	43 08 N	19 07 E	1450	NO <sub>2</sub> , SO <sub>2</sub>
Zavodnje	Slovenia	ZRN646N00	46 25 N	15 00 E	770	O <sub>3</sub>
Zeppelinfjellet (Ny-Alesund)	Norway	ZEP678N00	78 54 N	11 52 E	475	CCl <sub>4</sub> , CFCs, CH <sub>3</sub> CCl <sub>3</sub> , N <sub>2</sub> O, O <sub>3</sub> , SO <sub>2</sub>
Zeppelinfjellet (Ny-Alesund)	Norway	ZEP678N00	78 54 N	11 52 E	475	CO <sub>2</sub>
Zeppelinfjellet (Ny-Alesund)	Norway	ZEP678N00	78 54 N	11 52 E	475	<sup>13</sup> CO <sub>2</sub> , C <sup>18</sup> O <sub>2</sub> , CH <sub>4</sub> , CO, CO <sub>2</sub> , H <sub>2</sub>
Zingst	Germany	ZGT654N00	54 25 N	12 43 E	1	VOCs
Zingst	Germany	ZGT654N00	54 25 N	12 43 E	1	CH <sub>4</sub> , CO <sub>2</sub> , O <sub>3</sub>
Zosenei	Latvia	ZSN657N00	57 04 N	25 32 E	182	NO <sub>2</sub> , O <sub>3</sub> , SO <sub>2</sub>
Zugspitze	Germany	ZUG647N00	47 25 N	10 58 E	2960	CH <sub>4</sub> , CO, CO <sub>2</sub> , NO, NOx, NOy, O <sub>3</sub>
Zugspitze	Germany	ZUG647N00	47 25 N	10 58 E	2960	CO <sub>2</sub>
Zugspitze / Schneefernerhaus	Germany	ZSF647N00	47 25 N	10 58 E	2656	SO <sub>2</sub>
Zugspitze / Schneefernerhaus	Germany	ZSF647N00	47 25 N	10 58 E	2656	CH <sub>4</sub> , CO, CO <sub>2</sub> , N <sub>2</sub> O, NO, NO <sub>2</sub> , NOy, O <sub>3</sub> , SF <sub>6</sub>
Ähtäri	Finland	AHT662N00	62 34 N	24 11 E	180	NO <sub>2</sub> , O <sub>3</sub> , SO <sub>2</sub>
<b>ANTARCTICA</b>						
Arrival Heights	New Zealand	ARH777S00	77 47 S	166 40 E	184	<sup>13</sup> CH <sub>4</sub> , CH <sub>4</sub> , CO, N <sub>2</sub> O
Casey Station	Australia	CYA766S00	66 16 S	110 31 E	60	<sup>13</sup> CO <sub>2</sub> , CH <sub>4</sub> , CO, CO <sub>2</sub> , H <sub>2</sub> , N <sub>2</sub> O
Halley Bay	United Kingdom of Great Britain and Northern Ireland	HBA775S00	75 34 S	26 30 W	33	<sup>13</sup> CO <sub>2</sub> , C <sup>18</sup> O <sub>2</sub> , CH <sub>4</sub> , CO, CO <sub>2</sub> , H <sub>2</sub>
Jubany	Argentina	JBN762S00	62 13 S	58 40 W	15	CO <sub>2</sub>
Mawson	Australia	MAA767S00	67 37 S	62 52 E	32	<sup>13</sup> CO <sub>2</sub> , CH <sub>4</sub> , CO, CO <sub>2</sub> , H <sub>2</sub> , N <sub>2</sub> O
McMurdo Station	United States of America	MCM777S00	77 49 S	166 34 E	11	CH <sub>4</sub> , O <sub>3</sub>
Mizuho	Japan	MZH770S00	70 42 S	44 17 E	2230	CH <sub>4</sub>
Neumayer	Germany	NMY770S00	70 39 S	8 15 W	42	O <sub>3</sub>

## LIST OF OBSERVING STATIONS (continued)

Station	Country/Territory	Index Number	Location		Altitude	Parameter
			Latitude (°')	Longitude (°')	(m)	
Palmer Station	United States of America	PSA764S00	64 55 S	64 00 W	10	$^{13}\text{CO}_2$ , $\text{C}^{18}\text{O}_2$ , $\text{CBrClF}_2$ , $\text{CCl}_4$ , CFCs, $\text{CH}_3\text{Br}$ , $\text{CH}_3\text{CCl}_3$ , $\text{CH}_4$ , $\text{CO}$ , $\text{CO}_2$ , $\text{H}_2$ , HCFCs, HFCs, $\text{N}_2\text{O}$ , $\text{SF}_6$
South Pole	United States of America	SPO789S00	89 58 S	24 48 W	2810	$^{13}\text{CO}_2$ , $\text{CH}_4$ , $\text{CO}$ , $\text{CO}_2$ , $\text{H}_2$ , $\text{N}_2\text{O}$
South Pole	United States of America	SPO789S00	89 58 S	24 48 W	2810	$^{13}\text{CH}_4$ , $^{13}\text{CO}_2$ , $\text{C}^{18}\text{O}_2$ , $\text{C}_2\text{Cl}_4$ , $\text{CBrClF}_2$ , $\text{CBrF}_3$ , $\text{CCl}_4$ , CFCs, $\text{CH}_2\text{Cl}_2$ , $\text{CH}_3\text{Br}$ , $\text{CH}_3\text{CCl}_3$ , $\text{CH}_3\text{Cl}$ , $\text{CH}_4$ , $\text{CO}$ , $\text{CO}_2$ , $\text{H}_2$ , HCFCs, HFCs, $\text{N}_2\text{O}$ , $\text{O}_3$ , $\text{SF}_6$
Syowa Station	Japan	SYO769S00	69 00 S	39 34 E	16	$\text{O}_3$
Syowa Station	Japan	SYO769S00	69 00 S	39 34 E	16	$^{13}\text{CO}_2$ , $\text{C}^{18}\text{O}_2$ , $\text{CH}_4$ , $\text{CO}$ , $\text{CO}_2$ , $\text{H}_2$
Syowa Station	Japan	SYO769S00	69 00 S	39 34 E	16	$\text{CO}_2$

### MOBILE STATION

Aircraft (over Bass Strait and Cape Grim)	Australia	AIA999900				$^{13}\text{CO}_2$ , $\text{CH}_4$ , $\text{CO}$ , $\text{CO}_2$ , $\text{H}_2$ , $\text{N}_2\text{O}$
Aircraft: Orleans	France	ORL999900			150	$\text{CH}_4$ , $\text{CO}_2$
Akademik Korolev, R/V	United States of America	AKD999900				$\text{CH}_4$
Alligator liberty, M/V	Japan	ALG999900				$\text{CO}_2$
Atlantic Ocean	United States of America	AOC9XXX00			10	$\text{CH}_4$ , $\text{CO}_2$
BACPAC 99	United States of America	BAC999900				$\text{CCl}_4$ , CFCs, $\text{CH}_3\text{Br}$ , $\text{CH}_3\text{CCl}_3$ , $\text{CH}_3\text{Cl}$ , HCFCs
BLAST1	United States of America	BLA999900				$\text{CCl}_4$ , CFCs, $\text{CH}_3\text{Br}$ , $\text{CH}_3\text{CCl}_3$ , $\text{CH}_3\text{Cl}$ , HCFCs
BLAST2	United States of America	BLA999901				$\text{CCl}_4$ , CFCs, $\text{CH}_3\text{Br}$ , $\text{CH}_3\text{CCl}_3$ , $\text{CH}_3\text{Cl}$ , HCFCs
BLAST3	United States of America	BLA999902				$\text{CCl}_4$ , CFCs, $\text{CH}_3\text{Br}$ , $\text{CH}_3\text{CCl}_3$ , $\text{CH}_3\text{Cl}$ , HCFCs
CLIVAR 01	United States of America	CLI999900				$\text{CCl}_4$ , CFCs, $\text{CH}_3\text{Br}$ , $\text{CH}_3\text{CCl}_3$ , $\text{CH}_3\text{Cl}$ , HCFCs
Comprehensive Observation Network for TRace gases by AIrLiner (CONTRAIL)	Japan	EOM999900				$\text{CH}_4$ , $\text{CO}_2$
Discoverer 1983 & 1984, R/V	United States of America	DIS999900				$\text{CH}_4$
Discoverer 1985, R/V	United States of America	DSC999900				$\text{CH}_4$
Drake Passage	United States of America	DRP999900				$\text{CH}_4$ , $\text{CO}_2$
Gas Change Experiment	United States of America	GAS999900				$\text{CCl}_4$ , CFCs, $\text{CH}_3\text{Br}$ , $\text{CH}_3\text{CCl}_3$ , $\text{CH}_3\text{Cl}$ , HCFCs
HATS Ocean Projects	United States of America	HOP999900				HFCs
INSTAC-I (International Strato/Tropospheric Air Chemistry Project)	Japan	INS999900				$^{13}\text{CO}_2$ , $\text{CH}_4$ , $\text{CO}_2$
John Biscoe, R/V	United States of America	JBS999900				$\text{CH}_4$

## LIST OF OBSERVING STATIONS (continued)

Station	Country/Territory	Index Number	Location			Parameter
			Latitude (°')	Longitude (°')	Altitude (m)	
Keifu Maru, R/V	Japan	KEF999900				CO <sub>2</sub>
Kofu Maru, R/V	Japan	KOF999900				CO <sub>2</sub>
Korolev, R/V	United States of America	KOR999900				CH <sub>4</sub>
Long Lines Expedition, R/V	United States of America	LLE999900				CH <sub>4</sub>
MRI Research, 1978-1986, R/V	Japan	MRI999900				CH <sub>4</sub>
MRI Research, Hakuko Maru, R/V	Japan	HKH999900				CO <sub>2</sub>
MRI Research, Kaiyo Maru, R/V	Japan	KIY999900				CO <sub>2</sub>
MRI Research, Mirai, R/V	Japan	MMR999900				CO <sub>2</sub>
MRI Research, Natushima, R/V	Japan	NTU999900				CO <sub>2</sub>
MRI Research, Ryofu Maru, R/V	Japan	RFM999900				CO <sub>2</sub>
MRI Research, Wellington Maru, R/V	Japan	WLT999900				CO <sub>2</sub>
Mexico Naval H-02, R/V	United States of America	MXN999900				CH <sub>4</sub>
NOPACCS - Hakurei Maru - Oceanographer, R/V	Japan	HAK999900				TIC
PHASE I-04	United States of America	PHA999900				CCl <sub>4</sub> , CFCs, CH <sub>3</sub> Br, CH <sub>3</sub> CCl <sub>3</sub> , CH <sub>3</sub> Cl, HCFCs
Pacific Ocean	United States of America	POC9XXX00				10 <sup>13</sup> CO <sub>2</sub> , C <sup>18</sup> O <sub>2</sub> , CH <sub>4</sub> , CO, CO <sub>2</sub> , H <sub>2</sub>
Pacific-Atlantic Ocean	United States of America	PAO999900				CH <sub>4</sub>
Polar Star, R/V	United States of America	PLS999900				CH <sub>4</sub>
Ryofu Maru, R/V	Japan	RYF999900				CFCs, CH <sub>4</sub> , CO <sub>2</sub> , N <sub>2</sub> O, TIC
South China Sea	United States of America	SCS9XXX00				15 <sup>13</sup> CO <sub>2</sub> , C <sup>18</sup> O <sub>2</sub> , CH <sub>4</sub> , CO, CO <sub>2</sub> , H <sub>2</sub>
Soyo Maru, R/V	Japan	SOY999900				CO <sub>2</sub>
Surveyor, R/V	United States of America	SUR999900				CH <sub>4</sub>
The Observation of Atmospheric Methane Over Japan	Japan	OAM999900				CH <sub>4</sub>
The Observation of Atmospheric Sulfur Hexafluoride Over Japan	Japan	OAS999900				SF <sub>6</sub>
WEST COSMIC - Hakurei Maru No.2 - Wakataka-Maru	Japan	HAK999901				TIC
Western Pacific	United States of America	WAK999900				CO <sub>2</sub>
northern and western Pacific	Japan	WPC9XXX00				10 CH <sub>4</sub> , CO <sub>2</sub>
		NWP999900				N <sub>2</sub> O

## LIST OF CONTRIBUTORS

Station Country/Territory	Name	Address
------------------------------	------	---------

### REGION I (Africa)

Izaña (Tenerife) (Spain)	Angel J. Gomez-Pelaez Carlos Marrero	Izana Atmospheric Research Center, Meteorological State Agency of Spain (AEMET) C/ La Marina, 20, Planta 6. Apartado 880. 38071 Santa Cruz de Tenerife, Spain
Cape Point (South Africa)	Ernst Günther Brunke	South African Weather Service (Climate Division) SAWS, c/o CSIR (Environmentek), P.O. Box 320, Stellenbosch 7599, South Africa
Amsterdam Island (France)	Jean Sciare Michel Ramonet	LSCE (Laboratoire des Sciences du Climat et de l'Environnement) UMR CEA-CNRS LSCE - CEA Saclay - Orme des Merisiers - Bat.701 91191 Gif-sur-Yvette, France
Mt. Kenya (Kenya)	Josiah Kariuki Murageh Jörg Klausen Stephan Henne	KMD, Kenyan Meteorological Department Kenya Meteorological Department Dagoretti Corner P.O. Box 30259 00100 Nairobi, Kenya
Cape Verde Observatory (Cape Verde)	Katie Read	Department of Chemistry, University of York Department of Chemistry, University of York, Heslington, York, Y010 5DD, United Kingdom
Funchal (Portugal)	Maria Amelia V.Lopes	Instituto de Meteorologia,I.P. Rua C-Aeroporto de Lisboa 1749-077 Lisboa Portugal
Assekrem (Algeria)	Mimouni Mohamed	Office National de la Meteorologie POBox 31 Tamanrasset 11000, Algeria

### REGION II (Asia)

Nagoya (Japan)	A. Matsunami	Research Center for Advanced Energy Conversion, Nagoya University Furo-cho, Chikusaku, Nagoya 464-8603, Japan
Cape Ochi-ishii Hateruma (Japan)	Hitoshi MUKAI	Center for Global Environmental Research, National Institute for Environmental Studies 16-2, Onogawa, Tsukuba-shi, Ibaraki 305-8506, Japan
Gosan (Republic of Korea)	Jaebum Lee Okjung Ju Sang-Kyun Kim	Researcher of Global Environment Research Center Environmental Research Complex, Gyeongseo-dong, Seo-gu, Incheon, 404-708, Republic of Korea

## LIST OF CONTRIBUTORS (continued)

Station Country/Territory	Name	Address
Anmyeon-do (Republic of Korea)	Jeong-Sik Kim Youngmoon YOUNG Ki-Jun Park	National Institute of Meteorological Research, Global Atmosphere Watch Center, Korea Meteorology Administration 1764-6, Seungen-Ri, Anmyeon-Eup, Taean-Kun, ChungNam, 357-961, Republic of Korea
Hok Tsui (Hong Kong, China)	Ka Se Lam	Department of Civil and Structural Engineering, Hong Kong Polytechnic University Hung Hom, Kowloon, Hong Kong
Mikawa-Ichinomiya (Japan)	Koji Ohno	Aichi Air Environment Division 1-2 Sannomaru-3chome, Naka-ku, Nagoya, Aichi 460-8501, Japan
Mt. Walinguan (China)	Lingxi ZHOU	PI for Greenhouse Gases & Related Tracers Chinese Academy of Meteorological Sciences (CAMS) China Meteorological Administration (CMA) 46 Zhongguancun Nandajie Beijing 100081, China
Memanbetsu (Japan)	Michio Hirota	Geochemical Research Department, Meteorological Research Institute 1-1, Nagamine, Tsukuba, Ibaraki 305-0052, Japan
Tsukuba (Japan)	Michio Hirota Yousuke Sawa	Geochemical Research Department, Meteorological Research Institute 1-1, Nagamine, Tsukuba, Ibaraki 305-0052, Japan
Hamamatsu (Japan)	Mitsuo TODA	Shizuoka University 3-5-1 Jyohoku, Hamamatsu 432-8561, Japan
Bering Island Kotelny Island (Russian Federation)	Nina Paramonova	Main Geophysical Observatory (MGO) Karbyshev Street 7, St. Petersburg, 194021, Russian Federation
Kyzylcha (Uzbekistan)		
Everest - Pyramid (Nepal)	Paolo Cristofanelli Paolo Bonasoni	ISAC-CNR ISAC-CNR, VIA Gobetti 101 - 40129 Bologna -Italy
Takayama (Japan)	Shohei Murayama	Research Institute for Environmental Management Technology, National Institute of Advanced Industrial Science and Technology (AIST) AIST Tsukuba West, 16-1 Onogawa, Tsukuba, Ibaraki 305-8569, Japan
Gosan (Republic of Korea)	So-young Bang	Applied Meteorology Research Laboratory, Meteorological Research Institute (METRI), Korea Meteorological Administration (KMA) 460-18, Shindaebang-dong, Dongjak-gu, Seoul 156-720, Rep. of Korea

## LIST OF CONTRIBUTORS (continued)

Station Country/Territory	Name	Address
Ship between Ishigaki Island and Hateruma Island (Japan)	Takakiyo Nakazawa Shuji Aoki	Center for Atmospheric and Oceanic Studies, Graduate School of Science, Tohoku University Aoba, Sendai 980-8578, Japan
Suita (Japan)	Tomohiro Oda	Division of Sustainable Energy and Environmental Engineering, Graduate School of Engineering, Osaka University, Japan Green Engineering Lab Division of Sustainable Energy and Environmental Engineering 2-1 Yamadaoka, Suita, Osaka 565-0871 Japan
Tsukuba (Japan)	Tosiro Kimura	Lower Aerological Observations Division, Aerological Observatory, Japan Meteorological Agency (JMA) Lower Aerological Observations Division, Aerological Observatory 1-2 Nagamine, Tsukuba, Ibaraki, 305-0052, Japan
Issyk-Kul (Kyrgyzstan)	V. Sinyakov	Laboratory of Geophysics, Institute of Fundamental sciences at the Kyrgyz National University Manas Street 101, Bishkek, 720033, Kyrgyz Republic
Mt. Dodaira Kisai Urawa (Japan)	Yosuke MUTO	Center for Environmental Science in Saitama 914 Kamitanadare, Kisai-machi, Kita-Saitama-gun, Saitama 347-0115, Japan
Minamitorishima Ryori Yonagunijima (Japan)	Yuji ESAKI	Atmospheric Environment Division, Global Environment and Marine Department, Japan Meteorological Agency (JMA) 1-3-4 Otemachi, Chiyoda-ku, Tokyo 100-8122, Japan

### REGION III (South America)

Arembepe (Brazil)	Joelmo Oliveira	
Huancayo (Peru)	Mutsumi Ishitsuka	Observatorio de Huancayo, Instituto Geofisico del Peru Apartado 46, Huancayo, Peru
Ushuaia (Argentina)	Sergio Lupo	Servicio Meteorológico Nacional - Gobierno de Tierra del Fuego Estación VAG Ushuaia Subsecretaría de Ciencia y Tecnología, Ministerio de Educación, Cultura, Ciencia y Tecnología Gobierno de Tierra del Fuego 9410 Ushuaia, Tierra del Fuego, Argentina

## LIST OF CONTRIBUTORS (continued)

Station Country/Territory	Name	Address
------------------------------	------	---------

### REGION IV (North and Central America)

Alert	Doug Worthy	Environment Canada (EC) 4905 Dufferin Street, Toronto, Ontario, Canada, M3H 5T4
Candle Lake		
Chibougamau		
Cape St. James		
Egbert		
Estevan Point		
East Trout Lake		
Frasedale		
Lac La Biche (Alberta)		
Toronto		
Sable Island		
(Canada)		
Algoma	Mike Shaw	Environment Canada/Meteorological Service of Canada Air Quality Research Branch 4905 Dufferin Street, Toronto, Ontario CANADA M3H 5T4
Bratt's Lake		
Chalk River		
Chapais		
Egbert		
Experimental Lakes Area		
Esther		
Kejimkujik		
Longwoods		
Saturna		
Sutton		
(Canada)		
La Palma	Osvaldo Cuesta Santos	Institute of Meteorology, Atmospheric Environment Research Center Aptdo. 17032, Postal Code 11700, Havana 17, Cuba
(Cuba)		

### REGION V (South-West Pacific)

Baring Head (New Zealand)	Antony Gomez Sylvia Nichol Gordon Brailsford	National Institute of Water & Atmospheric Research Ltd. 301 Evans Bay Parade, Greta Point Private Bag 14-901, Kilbirnie, Wellington, New Zealand
Cape Grim (Australia)	Bruce Forgan Ian Galbally	Commonwealth Bureau of Meteorology 700 Collins St, Docklands GPO Box 1289K, Melbourne, Victoria 3001, Australia
Tanah Rata (Malaysia)	Lim Sze Fook	Environmental Studies Division Malaysian Meteorological Department Jalan Sultan, 46667 Petaling Jaya, Selangor, Malaysia

## LIST OF CONTRIBUTORS (continued)

Station Country/Territory	Name	Address
Danum Valley GAW Baseline Station (Malaysia)	Lim Sze Fook Maznorizan Mohamad	Environmental Studies Division Malaysian Meteorological Department Jalan Sultan, 46667 Petaling Jaya, Selangor, Malaysia
Bukit Koto Tabang Jakarta (Indonesia)	Nurhayati	Bureau of Meteorology and Geophysics Jalan Angkasa 1 No.2 Jakarta 10720, Indonesia
Bukit Koto Tabang (Indonesia)	Nurhayati Ilahi, Asep Firman Jörg Klausen	Bureau of Meteorology and Geophysics Jalan Angkasa 1 No.2 Jakarta 10720, Indonesia

### REGION VI (Europe)

Puszcza Borecka/Diabla Gora (Poland)	Anna Degorska	Institute of Environmental Protection Kolektorska 4 01-692 Warsaw, Poland
Kollumerwaard Kloosterburen (Netherlands (the))	Arien Stolk Hans Berkhout	RIVM - Laboratory for Environmental Measurements (LVM) P.O. Box 1, 3720 BA Bilthoven, The Netherlands
Hohe Warte Stephansplatz (Austria)	August Kaiser	Department for Environmental Meteorology Central Institute for Meteorology and Geodynamics Postfach 342, Hohe Warte 38, A-1191 Wien, Austria
Iskrba Krvavec (Slovenia)	Brigita Jesenovec Marijana Murovec	Ministry of Environment and Spatial Planning - Environmental Agency of the Republic of Slovenia (EARS) Vojkova 1/b, SI-1000 Ljubljana, Slovenia
Jungfraujoch Payerne Rigi (Switzerland)	Brigitte Buchmann Thomas Seitz	Empa, Swiss Federal Laboratories for Materials Testing and Research, Air Pollution / Environmental Technology Überlandstrasse 129, CH-8600 Dübendorf, Switzerland
Fundata Semenic Stîna de Vale (Romania)	Daniela ZISU	National Research and Development Institute for Environmental Protection Splaiul Independentei nr. 294, sector 6, 77703 Bucuresti, Romania
Kamenicki Vis (Serbia)	Dragan Djordjevic	Republic Hydrometeorological Service, Environmental Control Department Kneza Viseslava 66, 11030 Belgrade, Serbia

## LIST OF CONTRIBUTORS (continued)

Station Country/Territory	Name	Address
Burgas Plovdiv Pleven Sofia Varna (Bulgaria)	Ekaterina Batchvarova	National Institute of Meteorology and Hydrology 66 Tzarigradsko chaussee, 1784 Sofia, Bulgaria
Jarczew Leba Suwalki (Poland)	Eugeniusz Brejnak	Institute of Meteorology and Water Management; Laboratory for Research and Monitoring of Air Pollution 61 Podlesna Street, 01-673 Warszawa, Poland
Sniezka (Poland)	Eugeniusz Brejnak Krzaczkowski Piotr, MSc	Institute of Meteorology and Water Management; Laboratory for Research and Monitoring of Air Pollution 61 Podlesna Street, 01-673 Warszawa, Poland
Monte Cimone (Italy)	Fabio Malaspina Riccardo Santaguida	Italian Air Force Meteorological Service C.A.M.M. Mt. CIMONE, Via delle Ville 40, 41029-Sestola (MO), Italy
Fundata (Romania)	Florin Nicodim	National Meteorological Administration Sos. Bucuresti-Ploiesti nr. 97, 71552 Bucharest, Romania
Lampedusa (Italy)	Florinda Artuso Salvatore Chiavarini Salvatore Piacentino Alcide di Sarra	Italian National Agency for New Technology, Energy and the Environment (ENEA) ENEA ACS-CLIMOSS, Via Anguillarese 301, 00060 S.Maria di Galeria, Rome, Italy
Plateau Rosa (Italy)	Francesco Apadula Daniela Heltai Andrea Lanza	ERSE (former CESI RICERCA) Environment and Sustainable Development Department via Rubattino 54, 20134 Milano, Italy
Site J (Denmark)	Gen Hashida Shinji Morimoto Shuji Aoki	National Institute of Polar Research Kaga 1-9-10, Itabashi-ku, Tokyo 173-8515, Japan
Mace Head (Ireland)	Gerard Spain	National University of Ireland, Galway (NUI) Mace Head Research Station Carna, Co. Galway
Hohe Warte Stephansplatz (Austria)	Guenther Schermann	Municipal Department 22 - Environmental Protection Air quality subdepartment, City of Vienna Ebendorferstrasse 4, A-1082 Vienna, Austria
Vindeln (Sweden)	Hakan Blomgren	IVL Swedish Environmental Research Institute P.O.Box 5302 S-400 14 Goteborg, Sweden
Wank Peak Zugspitze (Germany)	Hans-Eckhart Scheel	Fraunhofer-Institute for Atmospheric Environmental Research, since 1.1.2002: Forschungszentrum Karlsruhe, IMK-IFU D-82467 Garmisch-Partenkirchen, Germany

## LIST OF CONTRIBUTORS (continued)

Station Country/Territory	Name	Address
Danki Shepeleva (Russian Federation)	Irina Brouskina	
La Cartuja Doñana Logroño Mahón Noia Roquetes San Pablo de los Montes (Spain)	J.M. Saenz	Servicio de Desarrollos Medioambientales, Instituto Nacional de Meteorología, Ministerio de Medio Ambiente Leonardo Prieto Castro, 8, 28071 Madrid, Spain
Zeppelinfjellet (Ny-Alesund) (Norway)	Johan Strom	Department of Applied Environmental Science (ITM), Stockholm University SE-106 91 Stockholm, Sweden
Pallas-Sammaltunturi (Finland)	Juha Hatakka Timo Salmi	Finnish Meteorological Institute P.O.Box 503, FI-00101 Helsinki, Finland
Brotjacklriegel Deuselbach Waldhof Neuglobsow Schauinsland Westerland Zingst Zugspitze / Schneefernerhaus Zugspitze (Germany)	Karin Uhse	Umweltbundesamt (UBA, Federal Environmental Agency) Air Monitoring Network Paul-Ehrlich-Strasse 29, D-63225 Langen, Germany
Hegyhatsal K-puszta (Hungary)	Laszlo Haszpra	Hungarian Meteorological Service P.O. Box 39, H-1675 Budapest, Hungary
Angra do Heroísmo Beja Bragança Castelo Branco Lisboa / Gago Coutinho Monte Velho Penhas Douradas Viana do Castelo (Portugal)	Maria Amelia V.Lopes	Instituto de Meteorologia,I.P. Rua C-Aeroporto de Lisboa 1749-077 Lisboa Portugal
Kovk Zavodnje (Slovenia)	Marijana Murovec	Environmental Agency of Republic of Slovenia Environment Office Sektor za kakovost zraka / Air Quality Division Vojkova 1b, 1001 Ljubljana, p.p. 2608, Slovenia

## LIST OF CONTRIBUTORS (continued)

Station Country/Territory	Name	Address
Dobele Rucava Zoseni (Latvia)	Marina Frolova	Observation Network Department, Latvian Environment, Geology and Meteorology Centre, Ministry of Environmental 165 Maskavas str. LV-1019, Riga, Latvia
Sonnblick (Austria)	Marina Fröhlich Wolfgang Spangl Elisabeth Friedbacher	Federal Environment Agency Austria Spittelauer Lände 5, A-1090 Wien, Austria
Ivan Sedlo (Bosnia and Herzegovina)	Martin Tais	Meteoroloski zavod Bosne i Hercegovine Bardakcije 12, 71000 Sarajevo, Bosnia and Herzegovina
Ille Grande Pic du Midi Puy de Dome (France)	Michel Ramonet	LSCE (Laboratoire des Sciences du Climat et de l'Environnement) UMR CEA-CNRS LSCE - CEA Saclay - Orme des Merisiers - Bat.701 91191 Gif-sur-Yvette, France
Mace Head (Ireland)		
Begur (Spain)		
Kosetice (Czech Republic)	Milan Vana	Czech Hydrometeorological Institute, Kosetice Observatory Na Sabatce 17, 143 06 Praha 4 - Komorany, Czech Republic
Ocean Station Charlie Teriberka (Russian Federation)	Nina Paramonova	Main Geophysical Observatory (MGO) Karbshev Street 7, St. Petersburg, 194021, Russian Federation
Zeppelinfjellet (Ny-Alesund) (Norway)	Ove Hermansen	Norwegian Institute for Air Research (NILU) P. O. Box 100 Instituttveien 18, N-2027 Kjeller, Norway
Monte Cimone (Italy)	Paolo Bonasoni	ISAC-CNR ISAC-CNR, VIA Gobetti 101 - 40129 Bologna -Italy
Eskdalemuir (United Kingdom of Great Britain and Northern Ireland)	Peter Kuria	Air and Environment Quality Division, DEFRA 4/F15, Ashdown House 123 Victoria Street, London, SW1E 3DE, United Kingdom
Giordan Lighthouse (Malta)	Raymond Ellul	Atmospheric Research Unit / Physics Department /University of Malta Msida MSD 06, Malta
Zugspitze / Schneefernerhaus (Germany)	Stefan Gilge Christian Plass-Duelmer Wolfgang Fricke	Deutscher Wetterdienst (DWD, German Meteorological Service) Meteorologisches Observatorium Hohenpeissenberg Albin-Schwaiger-Weg 10, D-82383 Hohenpeissenberg, Germany

## LIST OF CONTRIBUTORS (continued)

Station Country/Territory	Name	Address
Hohenpeissenberg (Germany)	Stefan Gilge Wolfgang Fricke Christian Plass-Duelmer	Deutscher Wetterdienst (DWD, German Meteorological Service) Meteorologisches Observatorium Hohenpeissenberg Albin-Schwaiger-Weg 10, D-82383 Hohenpeissenberg, Germany
Lazaropole (The Former Yugoslav Republic of Macedonia)	Suzana Alcinova Monevska	Hydrometeorological Service Skupi bb, 1000 Skopie, The former Yugoslav Republic of Macedonia
Kosetice (Czech Republic)	Sverre Solberg	Norwegian Institute for Air Research P.O.Box 100, NO-2027 Kjeller, Norway
Pallas-Sammaltunturi Utö (Finland)		
Donon La Tardiere Peyrusse Vieille (France)		
Brotjacklriegel Waldhof Schmuecke Zingst (Germany)		
Starina (Slovakia)		
Campisabalos (Spain)		
Ähtäri Oulanka Utö Virolahti (Finland)	Timo Salmi	Finnish Meteorological Institute Erik Palmenin aukio 1, P.O.Box 503, FIN-00101 Helsinki, Finland
<b>ANTARCTICA</b>		
Arrival Heights (New Zealand)	Antony Gomez Sylvia Nichol Gordon Brailsford	National Institute of Water & Atmospheric Research Ltd. 301 Evans Bay Parade, Greta Point Private Bag 14-901, Kilbirnie, Wellington, New Zealand
Jubany (Italy)	Luigi Ciattaglia	ICES (Int.l Center for Earth Sciences) c/o CNR-Istituto di Acustica- Area della Ricerca di Roma Tor Vergata, via Fosso del Cavaliere 100, 00133 Rome, Italy

## LIST OF CONTRIBUTORS (continued)

Station Country/Territory	Name	Address
Neumayer (Germany)	Rolf Weller	Alfred Wegener Institute Am Handelshafen 12, 27570 Bremerhaven, Germany
Mizuho (Japan)	Takakiyo Nakazawa	Center for Atmospheric and Oceanic Studies, Graduate School of Science, Tohoku University Aoba, Sendai 980-8578, Japan
Syowa Station (Japan)	Takakiyo Nakazawa Gen Hashida Shinji Morimoto	Center for Atmospheric and Oceanic Studies, Graduate School of Science, Tohoku University Aoba, Sendai 980-8578, Japan
Syowa Station (Japan)	Terumasa Tashiro Yasuo Shudou	Office of Antarctic Observations, Japan Meteorological Agency (JMA) 1-3-4 Otemachi, Chiyoda-ku, Tokyo 100-8122, Japan

### MOBILE STATION

NOPACCS - Hakurei Maru -	General Environmental Texhnos	The General Environmental Technos Co., Ltd. (Old: Kansai Environmental Engineering Center, Co., Ltd.) 1-3-5, Azuchi machi, Chuo-ku, Osaka 541-0052, Japan
WEST COSMIC - Hakurei Maru No.2 - (Japan)		
INSTAC-I (International Strato/Tropospheric Air Chemistry Project) (Japan)	Hidekazu Matsueda	Geochemical Research Department, Meteorological Research Institute Nagamine 1-1, Tsukuba, Ibaraki 305-0052, Japan
Comprehensive Observation Network for TRace gases by AIRLiner (CONTRAIL) (Japan)	Hidekazu Matsueda Toshinobu Machida	Geochemical Research Department, Meteorological Research Institute Nagamine 1-1, Tsukuba, Ibaraki 305-0052, Japan
MRI Research, Mirai, R/V (Japan)	Hisayuki Yoshikawa-Inoue	Laboratory of Marine and Atmospheric Geochemistry Graduate School of Environmental Earth Science, Hokkaido University N10W5, Kita-ku, Sapporo 060-0810, Japan
MRI Research, Hakuho Maru, R/V MRI Research, Kaiyo Maru, R/V MRI Research, 1978-1986, R/V MRI Research, Natushima, R/V MRI Research, Ryofu Maru, R/V MRI Research, Wellington Maru, R/V (Japan)	Masao Ishii	Geochemical Research Department, Meteorological Research Institute Nagamine 1-1, Tsukuba, Ibaraki 305-0052, Japan

## LIST OF CONTRIBUTORS (continued)

Station Country/Territory	Name	Address
Aircraft: Orleans (France)	Michel Ramonet	LSCE (Laboratoire des Sciences du Climat et de l'Environnement) UMR CEA-CNRS LSCE - CEA Saclay - Orme des Merisiers - Bat.701 91191 Gif-sur-Yvette, France
The Observation of Atmospheric Methane Over Japan	Michio Hirota	Geochemical Research Department, Meteorological Research Institute 1-1, Nagamine, Tsukuba, Ibaraki 305-0052, Japan
The Observation of Atmospheric Sulfur Hexafluoride Over Japan (Japan)		
northern and western Pacific (Japan)	Takakiyo Nakazawa Shuji Aoki Kentaro Ishijima	Center for Atmospheric and Oceanic Studies, Graduate School of Science, Tohoku University Aoba, Sendai 980-8578, Japan
Alligator liberty, M/V Keifu Maru, R/V Kofu Maru, R/V Ryofu Maru, R/V (Japan)	Takashi Miyao	Pollutants Chemical Analysis Center, Marine Division, Climate and Marine Department, Japan Meteorological Agency (JMA) 1-3-4 Otemachi, Chiyoda-ku, Tokyo 100-8122, Japan
Soyo Maru, R/V Wakataka-Maru (Japan)	Tsuneo Ono	Hokkaido National Fisheries Research Institute 116 Katsurakoi, Kushiro 085-0802, Japan

## LIST OF CONTRIBUTORS (continued)

Station Country/Territory	Name	Address
<b>NOAA/CMDL Flask Network</b>		
Assekrem (Algeria)	Bruce Vaughn** James White** ( $^{13}\text{CH}_4$ , $^{13}\text{CO}_2$ and $\text{C}^{18}\text{O}_2$ )	(*)NOAA/ESRL Global Monitoring Division 325 Broadway R/GMD1 Boulder, CO 80305-3328, U.S.A.
Tierra del Fuego (Argentina)	Edward J. Dlugokencky* ( $\text{CH}_4$ )	(**)Institute of Arctic and Alpine Research (INSTAAR) Campus box 450, University of Colorado, Boulder, CO 80309-0450, U.S.A.
Cape Grim (Australia)	Paul C. Novelli* (CO and $\text{H}_2$ )	
Ragged Point (Barbados)	Thomas J. Conway* ( $\text{CO}_2$ )	
Arembepe (Brazil)		
Alert Lac La Biche Mould Bay (Canada)		
Easter Island (Chile)		
Lulin Mt. Waliguan (China)		
Summit (Denmark)		
Pallas-Sammaltunturi (Finland)		
Amsterdam Island Crozet (France)		
Hohenpeissenberg Ochsenkopf (Germany)		
Hegyhatsal (Hungary)		
Heimaey (Iceland)		
Bukit Koto Tabang (Indonesia)		

## LIST OF CONTRIBUTORS (continued)

Station Country/Territory	Name	Address
Mace Head (Ireland)		
Sede Boker (Israel)		
Lampedusa (Italy)		
Syowa Station (Japan)		
Sary Taukum Plateau Assy (Kazakhstan)		
Mt. Kenya (Kenya)		
Christmas Island (Kiribati)		
Kaashidhoo (Maldives)		
Dwejra Point (Malta)		
Ulaan Uul (Mongolia)		
Gobabeb (Namibia)		
Baring Head Lauder Kaitorete Spit (New Zealand)		
Ocean Station "M" Zeppelinfjellet (Ny-Alesund) (Norway)		
Baltic Sea (Poland)		
Terceira Island (Portugal)		
Tae-ahn Peninsula (Republic of Korea)		

## LIST OF CONTRIBUTORS (continued)

Station Country/Territory	Name	Address
Black Sea (Romania)		
Mahe Island (Seychelles)		
Izaña (Tenerife) (Spain)		
Ascension Island St. David's Head Tudor Hill Halley Bay Bird Island (United Kingdom of Great Britain and Northern Ireland)		
Akademik Korolev, R/V Argyle Atlantic Ocean St. Croix Barrow Cold Bay Cape Meares Discoverer 1983 & 1984, R/V Drake Passage Discoverer 1985, R/V Guam Grifton John Biscoe, R/V Key Biscayne Korolev, R/V Kitt Peak Cape Kumukahi Park Falls Long Lines Expedition, R/V McMurdo Station Sand Island Mauna Loa Mexico Naval H-02, R/V Niwot Ridge (T-van) Niwot Ridge (Saddle) Oceanographer, R/V Olympic Peninsula Pacific-Atlantic Ocean Polar Star, R/V Pacific Ocean Palmer Station Point Arena South China Sea		

## LIST OF CONTRIBUTORS (continued)

Station Country/Territory	Name	Address
Southern Great Plains		
Shemya Island		
La Jolla		
Tutuila (Cape Matatula)		
South Pole		
Ocean Station Charlie		
Surveyor, R/V		
Trinidad Head		
Wendover		
Moody		
Western Pacific		
(United States of America)		

### NOAA/CMDL/HATS Network

Tierra del Fuego (Argentina)	Geoffrey S. Dutton James W. Elkins Stephen A. Montzka	Halocarbons and Other Atmosphere Trace Species Group (HATS)/NOAA/ESRL Global Monitoring Division 325 Broadway R/GMD1 Boulder, CO 80305-3328, U.S.A.
Cape Grim (Australia)		
Alert (Canada)		
Summit (Denmark)		
Mace Head (Ireland)		
BACPAC 99		
BLAST1		
BLAST2		
BLAST3		
Barrow		
CLIVAR 01		
Gas Change Experiment		
Harvard Forest		
HATS Ocean Projects		
Grifton		
Cape Kumukahi		
Park Falls		
Mauna Loa		
Niwot Ridge (C-1)		
PHASE I-04		
Palmer Station		
Tutuila (Cape Matatula)		
South Pole		
Trinidad Head		
(United States of America)		

## LIST OF CONTRIBUTORS (continued)

Station Country/Territory	Name	Address
------------------------------	------	---------

### **NOAA/CMDL Surface Ozone Network**

Ragged Point (Barbados)	Sam Oltmans	NOAA/ESRL Global Monitoring Division 325 Broadway R/GMD1 Boulder, CO 80305-3328, U.S.A.
Summit (Denmark)		
Heimaey (Iceland)		
Lauder (New Zealand)		
Tudor Hill (United Kingdom of Great Britain and Northern Ireland)		
Barrow McMurdo Station Mauna Loa Niwot Ridge (C-1) Niwot Ridge (Saddle) Tutuila (Cape Matatula) South Pole Trinidad Head (United States of America)		

## LIST OF CONTRIBUTORS (continued)

Station Country/Territory	Name	Address
------------------------------	------	---------

### CSIRO Flask Network

Aircraft (over Bass Strait and Cape Grim)	Ray Langenfelds	Commonwealth Scientific and Industrial Research Organisation (CSIRO)
Cape Ferguson	Paul Krummel	CSIRO Marine and Atmospheric Research
Cape Grim	Paul Steele	Private Bag 1
Casey Station	Colin Allison	Aspendale, Vic 3195, Australia
Mawson		
Macquarie Island (Australia)		
Alert		
Estevan Point (Canada)		
Cape Rama (India)		
Shetland (United Kingdom of Great Britain and Northern Ireland)		
Mauna Loa South Pole (United States of America)		

### ALE/GAGE/AGAGE Network

Cape Grim (Australia)	Ray Wang	School of Earth and Atmospheric Sciences, Georgia Institute of Technology 311 Ferst Drive
Ragged Point (Barbados)		School of Earth and Atmospheric Sciences Georgia Institute of Technology Atlanta, GA 30332-0340, U.S.A.
Adrigole Mace Head (Ireland)		
Cape Meares Tutuila (Cape Matatula) Trinidad Head (United States of America)		



# GLOSSARY

## AGENCIES AND PROGRAMMES:

<b>AEMET</b>	Agencia Estatal de Meteorología (Spain)
<b>AES</b>	Atmospheric Environment Service (Canada, presently MSC)
<b>AGAGE</b>	Advanced Global Atmospheric Gases Experiment
<b>Aichi</b>	Aichi Prefecture (Japan)
<b>AIST</b>	National Institute of Advanced Industrial Science and Technology (Japan)
<b>AQRB</b>	Air Quality Research Branch, Meteorological Service of Canada (Canada)
<b>ALE</b>	Atmospheric Lifetime Experiment
<b>AWI</b>	Alfred Wegener Institute (Germany)
<b>BMG</b>	Bureau of Meteorology and Geophysics (Indonesia)
<b>BoM</b>	Commonwealth Bureau of Meteorology (Australia)
<b>CAMS</b>	Chinese Academy of Meteorological Sciences (China)
<b>CESI</b>	Italian Electrical Experimental Center (Italy)
<b>CFR</b>	Centre des Faibles Radioactivites (France)
<b>CHMI</b>	Czech Hydrometeorological Institute (Czech Republic)
<b>CMA</b>	China Meteorological Administration (China)
<b>CMDL</b>	Climate Monitoring and Diagnostics Laboratory (NOAA, USA, presently ESRL/GMD)
<b>CNRS</b>	Centre National de la Recherche Scientifique (France)
<b>CNR-ICES</b>	International Center for Earth Sciences, Consiglio Nazionale delle Ricerche (Italy)
<b>CSIRO</b>	Commonwealth Scientific and Industrial Research Organisation (Australia)
<b>DEFRA</b>	Department for Environment, Food and Rural Affairs (United Kingdom)
<b>DNA-IAA</b>	Dirección Nacional del Antártico-Instituto Antártico Argentino (Argentina)
<b>DWD</b>	Deutscher Wetterdienst (German Meteorological Service, Germany)
<b>EARS</b>	Environmental Agency of the Republic of Slovenia
<b>EC</b>	Environment Canada (Canada)
<b>EMPA</b>	Swiss Federal Laboratories for Material Testing and Research (Switzerland)
<b>ENEA</b>	Italian National Agency for New Technology, Energy and the Environment (Italy)
<b>ERSE S.p.A.</b>	ENEA – Ricerca sul Sistema Elettrico, Società per Azioni (Italy)
<b>FMI</b>	Finnish Meteorological Institute
<b>GAGE</b>	Global Atmospheric Gases Experiment
<b>GAW</b>	Global Atmosphere Watch (WMO)
<b>GERC</b>	Global Environment Research Center of NIER (Republic of Korea)
<b>HATS</b>	Halocarbons and other Atmospheric Trace Species
<b>HMS</b>	Hungarian Meteorological Service (Hungary)
<b>IAFMS</b>	Italian Air Force Meteorological Service (Italy)
<b>IGP</b>	Instituto Geofísico del Perú (Peru)
<b>IM</b>	Instituto de Meteorología (Portugal)
<b>IMK-IFU</b>	Institut für Meteorologie und Klimatologie, Atmosphärische Umweltforschung, Forschungszentrum Karlsruhe (Germany)
<b>INM</b>	Instituto Nacional de Meteorología (Spain)
<b>INMET</b>	Instituto Nacional de Meteorología (Brazil)
<b>INMH</b>	National Meteorological Administration (Romania)
<b>IOEP</b>	Institute of Environmental Protection (Poland)
<b>ISAC</b>	Istituto di Scienze dell'Atmosfera e del Clima, Consiglio Nazionale delle Ricerche (Italy)
<b>DNA-IAA</b>	Dirección Nacional del Antártico - Instituto Antártico Argentino (Argentina)

<b>ITM</b>	Department of Applied Environmental Science, Stockholm University, (Sweden)
<b>IVL</b>	Swedish Environmental Research Institute, Göteborg (Sweden)
<b>JMA</b>	Japan Meteorological Agency (Japan)
<b>JMA/AO</b>	Aerological Observatory, Japan Meteorological Agency, Tsukuba, Japan
<b>KMA</b>	Korea Meteorological Administration (Republic of Korea)
<b>KMD</b>	Kenya Meteorological Department (Kenya)
<b>KSNU</b>	Kyrgyz State National University (Kyrgyzstan)
<b>LEGMA</b>	Latvian Environment, Geology and Meteorology Agency (Latvia)
<b>LSCE</b>	Laboratoire des Sciences du Climat et de l'Environnement (France)
<b>METRI</b>	Meteorological Research Institute (KMA, Republic of Korea)
<b>MGO</b>	Main Geophysical Observatory (Russian Federation)
<b>MMD</b>	Malaysian Meteorological Department
<b>MISU</b>	Department of Meteorology, Stockholm University (Sweden)
<b>MRI</b>	Meteorological Research Institute (Japan/JMA)
<b>MSC</b>	Meteorological Service of Canada (Canada, formerly AES)
<b>Nagoya Univ.</b>	Nagoya University (Japan)
<b>NCEP</b>	National Centers for Environmental Prediction (USA/NOAA)
<b>NIES</b>	National Institute for Environmental Studies (Japan)
<b>NILU</b>	Norwegian Institute for Air Research (Norway)
<b>NIMH</b>	Institutul National de Meteorologie, Hidrologie si Gospodarirea Apelor (Romania)
<b>NIPR</b>	National Institute of Polar Research (Japan)
<b>NIRE</b>	National Institute for Resources and Environment (Japan)
<b>NIST</b>	National Institute of Standards and Technology (USA)
<b>NIWA</b>	National Institute of Water & Atmospheric Research (New Zealand)
<b>NOAA/GMD</b>	Earth System Research Laboratory, Global Monitoring Division (NOAA, USA, formerly CMDL)
<b>NUI</b>	National University of Ireland, Galway (Ireland)
<b>ONM</b>	Office National de la Météorologie (Algeria)
<b>Osaka Univ.</b>	Osaka University (Japan)
<b>PolyU</b>	Hong Kong Polytechnik University, Hong Kong (China)
<b>RIVM</b>	National Institute for Health and Environment (Netherlands)
<b>Roshydromet</b>	Russian Hydrometeorological Service
<b>Saitama</b>	Saitama Prefecture (Japan)
<b>SAWS</b>	South African Weather Service (South Africa)
<b>Shizuoka</b>	Shizuoka University (Japan)
<b>SIO</b>	Scripps Institution of Oceanography, University of California at San Diego (USA)
<b>SMN</b>	Servicio Meteorológico Nacional (Argentina)
<b>SNU</b>	Seoul National University (Republic of Korea)
<b>Tohoku Univ.</b>	Tohoku University (Japan)
<b>UBA</b>	Umweltbundesamt (Germany)
<b>UBA Austria</b>	Umweltbundesamt (Federal Environmental Agency), Austria
<b>UHEI-IUP</b>	Institut für Umweltphysik, Universität Heidelberg (Germany)
<b>UM</b>	University of Malta (Malta)
<b>UY</b>	University of York (United Kingdom of Great Britain and Northern Ireland)
<b>WDCGG</b>	World Data Centre for Greenhouse Gases, operated by JMA, Japan (WMO)
<b>WMO</b>	World Meteorological Organization
<b>ZAMG</b>	Zentralanstalt für Meteorologie und Geodynamik (Austria)

## ATMOSPHERIC SPECIES:

<b>CCl<sub>4</sub></b>	tetrachloromethane (carbon tetrachloride)
<b>CFC-11</b>	chlorofluorocarbon-11 (trichlorofluoromethane, CCl <sub>3</sub> F)
<b>CFC-12</b>	chlorofluorocarbon-12 (dichlorodifluoromethane, CCl <sub>2</sub> F <sub>2</sub> )
<b>CFC-113</b>	chlorofluorocarbon-113 (1,1,2-trichlorotrifluoroethane, CCl <sub>2</sub> FCClF <sub>2</sub> )
<b>CFCs</b>	chlorofluorocarbons
<b>CH<sub>2</sub>Cl<sub>2</sub></b>	dichloromethane (methylene chloride)
<b>CH<sub>3</sub>Cl</b>	chloromethane (methyl chloride)
<b>CH<sub>3</sub>Br</b>	bromomethane (methyl bromide)
<b>Halon-1211</b>	chlorodifluorobromomethane (CBrClF <sub>2</sub> )
<b>Halon-1301</b>	bromotrifluoromethane (CBrF <sub>3</sub> )
<b>HCFC-141b</b>	hydrochlorofluorocarbon-141b (1,1-dichloro-1-fluoroethane, CH <sub>3</sub> CCl <sub>2</sub> F)
<b>HCFC-142b</b>	hydrochlorofluorocarbon-142b (1,1-difluoro-1-chloroethane, CH <sub>3</sub> CClF <sub>2</sub> )
<b>HCFC-22</b>	hydrochlorofluorocarbon-22 (chlorodifluoromethane, CHClF <sub>2</sub> )
<b>HCFCs</b>	hydrochlorofluorocarbons
<b>HFC-134a</b>	hydrofluorocarbon-134a (1,1,1,2-tetrafluoroethane, CH <sub>2</sub> FCF <sub>3</sub> )
<b>HFC-152a</b>	hydrofluorocarbon -152a (1,1-difluoroethane, CHF <sub>2</sub> CH <sub>3</sub> )
<b>HFCs</b>	hydrofluorocarbons
<b>CH<sub>4</sub></b>	methane
<b>CH<sub>3</sub>CCl<sub>3</sub></b>	trichloroethane (methyl chloroform)
<b>CO</b>	carbon monoxide
<b>CO<sub>2</sub></b>	carbon dioxide
<b>N<sub>2</sub>O</b>	nitrous oxide
<b>NO</b>	nitrogen monoxide
<b>NO<sub>2</sub></b>	nitrogen dioxide
<b>NO<sub>x</sub></b>	nitrogen oxides
<b>O<sub>3</sub></b>	ozone
<b>SF<sub>6</sub></b>	sulphur hexafluoride
<b>SO<sub>2</sub></b>	sulphur dioxide

## UNITS:

<b>ppb</b>	parts per billion
<b>ppm</b>	parts per million
<b>ppt</b>	parts per trillion

## Others:

<b>ENSO</b>	El Niño-Southern Oscillation
<b>M/V</b>	merchant vessel
<b>R/V</b>	research vessel
<b>SOI</b>	Southern Oscillation Index
<b>SST</b>	Sea Surface Temperature

# LIST OF WMO WDCGG PUBLICATIONS

## DATA REPORTING MANUAL:

WDCGG No. 1      January      1991

## WMO WDCGG DATA REPORT:

			(period of data accepted)				
WDCGG No. 2 Part A	October	1992	October	1990	~	August	1992
WDCGG No. 2 Part B	October	1992	October	1990	~	August	1992
WDCGG No. 3	October	1993	September	1992	~	March	1993
WDCGG No. 5	March	1994	April	1993	~	September	1993
WDCGG No. 6	September	1994	September	1993	~	March	1994
WDCGG No. 7	March	1995	April	1994	~	December	1994
WDCGG No. 9	September	1995	January	1995	~	June	1995
WDCGG No.10	March	1996	July	1995	~	December	1995
WDCGG No.11	September	1996	January	1996	~	June	1996
WDCGG No.12	March	1997	July	1996	~	November	1996
WDCGG No.14	September	1997	December	1996	~	June	1997
WDCGG No.16	March	1998	July	1997	~	December	1997
WDCGG No.17	September	1998	January	1998	~	June	1998
WDCGG No.18	March	1999	July	1998	~	December	1998
WDCGG No.20	September	1999	January	1999	~	June	1999
WDCGG No.21	March	2000	July	1999	~	December	1999
WDCGG No.23	September	2000	January	2000	~	June	2000
WDCGG No.25	March	2001	July	2000	~	December	2000

## WMO WDCGG DATA CATALOGUE:

WDCGG No. 4	December	1993
WDCGG No.13	March	1997
WDCGG No.19	March	1999
WDCGG No.24	March	2001

## WMO WDCGG DATA SUMMARY:

WDCGG No. 8	October	1995
WDCGG No.15	March	1998
WDCGG No.22	March	2000
WDCGG No.26	March	2002
WDCGG No.27	March	2003
WDCGG No.28	March	2004
WDCGG No.29	March	2005
WDCGG No.30	March	2006
WDCGG No.31	March	2007
WDCGG No.32	March	2008
WDCGG No.33	March	2009

## WMO WDCGG CD-ROM:

			(period of data accepted)				
CD-ROM No. 1	March	1995	October	1990	~	December	1994
CD-ROM No. 2	March	1996	October	1990	~	June	1995
CD-ROM No. 3	March	1997	October	1990	~	June	1996
CD-ROM No. 4	March	1998	October	1990	~	December	1997
CD-ROM No. 5	March	1999	October	1990	~	December	1998
CD-ROM No. 6	March	2000	October	1990	~	December	1999
CD-ROM No. 7	March	2001	October	1990	~	December	2000
CD-ROM No. 8	March	2002	October	1990	~	January	2002
CD-ROM No. 9	March	2003	October	1990	~	December	2002
CD-ROM No.10	March	2004	October	1990	~	December	2003
CD-ROM No.11	March	2005	October	1990	~	December	2004

CD-ROM No.12	March	2006	October	1990	~	December	2005
CD-ROM No.13	March	2007	October	1990	~	November	2006
CD-ROM No.14	March	2008	October	1990	~	November	2007

**WMO WDCCG DVD:**

(period of data accepted)

DVD No. 1	March	2009	October	1990	~	November	2008
DVD No. 2	March	2010	October	1990	~	November	2009